Characterizing the role of BPIFB proteins during positive strand RNA virus infection

by

Azia Starr Evans

BS, San Diego State University, 2013

MS, San Jose State University, 2016

Submitted to the Graduate Faculty of the

School of Medicine in partial fulfillment

of the requirements for the degree of

Doctor of Philosophy

University of Pittsburgh

2020

UNIVERSITY OF PITTSBURGH

SCHOOL OF MEDICINE

This dissertation was presented

by

Azia Starr Evans

It was defended on

August 28, 2020

and approved by

Jennifer M. Bomberger, PhD, Associate Professor, Department Microbiology and Molecular Genetics

Seema S. Lakdawala, PhD, Assistant Professor, Department Microbiology and Molecular Genetics

Jeffery L. Brodsky, PhD, Professor, Department of Biological Sciences

Terence S. Dermody, MD, Professor, Department of Pediatrics

Dissertation Director: Carolyn B. Coyne, PhD, Professor, Department of Pediatrics

Characterizing the role of BPIFB proteins during positive strand RNA virus infection

Azia Starr Evans, PhD

University of Pittsburgh, 2020

The lifecycle of positive strand RNA viruses occurs in close association to host intracellular membranes as a mechanism to isolate viral replication from cellular restriction factors and innate immune detection. Distinct virus families rely on different membrane sources, each employing unique strategies to manipulate host membranes for their own advantage. One major source of these membranes is the endoplasmic reticulum (ER), which functions at the center of many cellular processes, including secretory pathway and autophagy vesicle trafficking. We have identified Bactericidal/permeability-increasing protein (BPI) fold-containing family B3 (BPIFB3) as a host endoplasmic reticulum (ER) localized protein that differentially controls the replication of two distinct virus families, enteroviruses and flaviviruses, through a non-canonical autophagy pathway. BPIFB3 belongs to the BPIFB protein family which have predicted lipid binding and transfer abilities. This family of proteins has been largely uncharacterized, and their intracellular function has remained to be elucidated. Here we expand on our previous work and address the cellular function of BPIFB3 in two parts. First, we focus on the effects of BPIFB3 induced autophagy on the replication of two flaviviruses, dengue virus (DENV) and Zika virus (ZIKV), and determine that the reticulophagy mediated turnover of ER membranes during BPIFB3 depletion inhibits DENV and ZIKV replication. Second, we identify two unique BPIFB3 binding partners, ADP Ribosylation Factor GTPase Activating Protein 1 (ARFGAP1) and Transmembrane emp24 domain-containing protein 9 (TMED9), that are required for the induction of BPIFB3si mediated non-canonical autophagy. Lastly, we expand on the work presented here in the context

of what is known about non-canonical autophagy regulation and present a novel model for BPIFB3 function. We further discuss the downstream effects of BPIFB3 depletion on autophagy regulation and positive strand RNA virus replication. This work defines BPIFB3 as a novel regulator of flavivirus replication and provides meaningful insights into the mechanisms of non-canonical autophagy regulation and their impact on positive strand RNA virus replication.

Table of Contents

List of Figures

1.0 Introduction

Positive strand RNA viruses, including flaviviruses and enteroviruses, rely on host intracellular membranes for multiple stages of their replicative lifecycle. In addition to relying on host membranes for entry and egress, these viruses also usurp membranes for the formation of viral replication organelles (RO) which are essential to the replication and assembly of progeny virions. Our work has been largely focused on understanding the host factors that are required for the viral manipulation of host membranes, allowing for RO formation. Research from our laboratory has identified the host proteins BPIFB3 and BPIFB6 as regulators of enterovirus replication (1, 2). However, prior to this work, members of the BPIFB protein family were not extensively studied. Early reports on BPIFB proteins focused on characterizing their expression pattern in human tissues and analysis of their predicted gene function based on sequence homology to existing lipid binding proteins (3–5). These initial studies identified BPIFB proteins and the related BPIFA proteins as secreted proteins that are highly expressed in the lung, palate, and nasal epithelium (6). Both BPIFB and BPIFA proteins were initially predicted to have a similar function to BPI as secreted antimicrobial or surfactant proteins in the human airway (5). However, our work has defined an intracellular role for two members of the BPIFB protein family irrespective of tissue localization. BPIFB3 and BPIFB6 are endoplasmic reticulum (ER) localized proteins that have clear roles in regulating vesicle trafficking from the ER. Our previous work defined a role for BPIFB6 in secretory pathway trafficking (2), while the work presented here in combination with previously published work extensively characterizes the role of BPIFB3 in the regulation of non-canonical autophagy and RNA virus replication (1, 7, 8).

1.1 Positive strand RNA viruses

Positive sense single stranded RNA viruses comprise a group of virus families that are classified by the structure of their genetic material and share a number of key commonalities in their replication cycles. Viruses within this group encompass a diverse array of human pathogens that have distinct structural and pathological differences. Including many pathogens that are known to cause moderate to severe disease in humans, such as poliovirus, dengue virus, Zika virus, and members of the coronavirus family.

Following internalization and uncoating of the virion, the genome of all positive strand RNA viruses serves as mRNA and is directly translated by the host ribosome. This allows these viruses to not package their own replication machinery within the capsid given that the RNA-dependent RNA polymerase that is required for viral replication can be produced immediately following entry of the virus (9). After the first wave of protein translation, the virally encoded replication machinery copies the positive sense genome to produce the compliment negative strand. This compliment strand is then used as a template for the production of more viral RNA (vRNA) genomes that can be used for the translation of additional viral proteins or packaged to produce progeny virions (10).

One common theme that all positive strand RNA viruses share is the enclosure of their replication machinery within host derived membrane compartments, termed replication organelles (**Figure 1**) (11–14). The formation of ROs is an essential stage of the viral life cycle that serves to enclose the viral genetic material and the double stranded RNA replication intermediate from detection by innate immune receptors that would trigger activation of a host antiviral response. For viruses within the picornavirus, flavivirus, and coronavirus families RO formation requires extensive remodeling of the host endomembrane system. For both flaviviruses and coronaviruses,

ROs are formed on membranes of the ER where viral replication and assembly of new virus particles occurs (**Figure 1B and 1D**) (11, 15, 16). The location of RO formation is important for these viruses as they are both enveloped virions that bud into the ER lumen and acquire their envelop from ER derived membranes. In contrast, enteroviruses within the picornavirus family establish cytoplasmic ROs on membranes derived from the ER, Golgi, autophagosome, and lysosomal membranes (**Figure 1A**) (17). This distinction in the origin of ROs between flaviviruses and enteroviruses is an important feature that contributes to the sensitivity of each virus family to distinct cellular autophagy pathways (18).

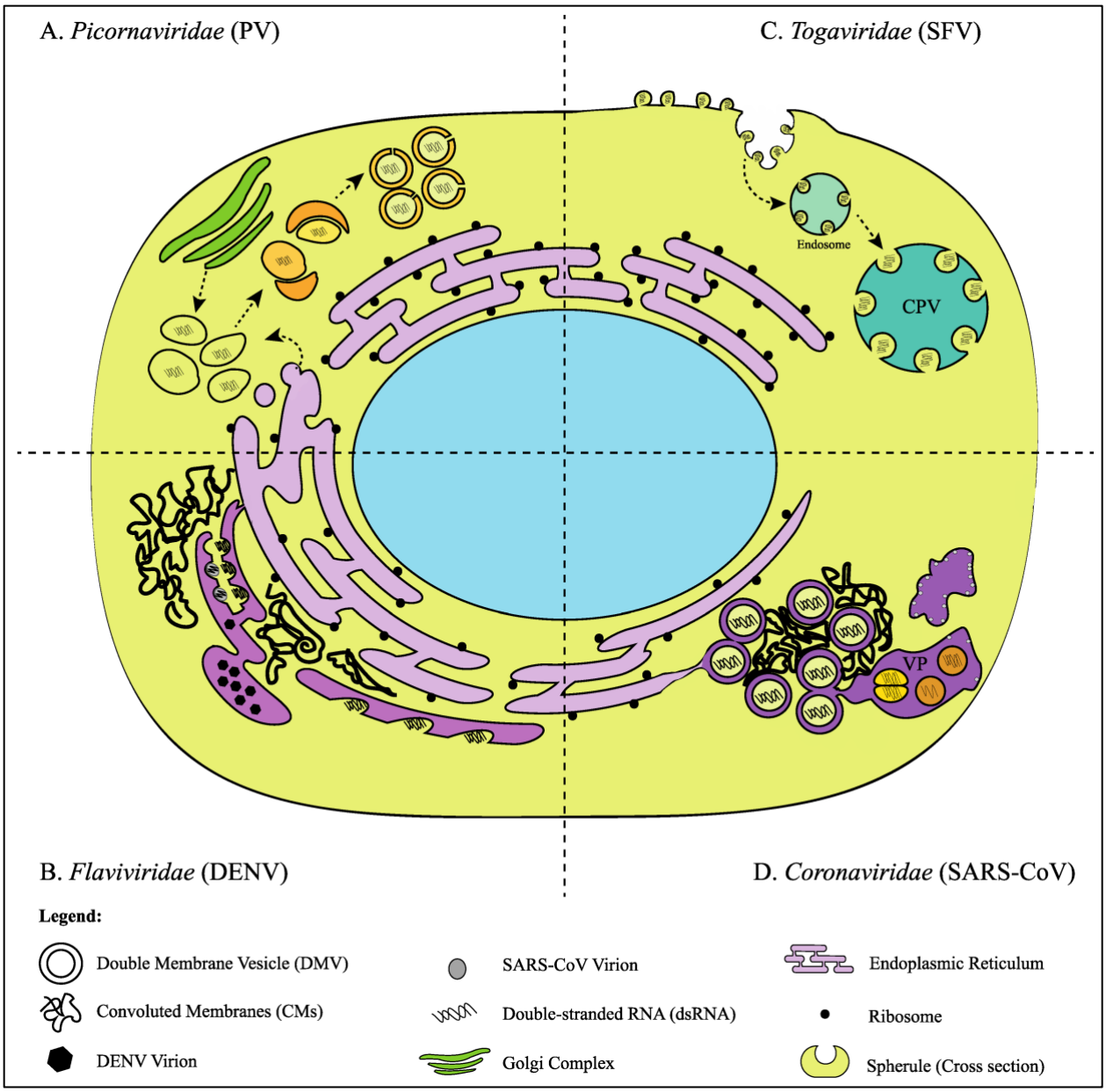

Figure 1 Positive strand RNA virus replication organelles

Positive sense RNA viruses commonly form ROs within the cellular endomembrane system. These ROs serve as a site of vRNA replication and virion assembly. Membrane sources for the biogenesis of viral ROs originate from Golgi and autophagosome derived vesicles **(A)**, existing and newly synthesized ER **(B and D)**, and plasma membrane and endosomal membranes **(C)**. The virus examples shown here, including poliovirus (PV), dengue virus (DENV), Severe acute respiratory syndrome (SARS) coronavirus, and Semliki Forest virus (SFV), represent four major strategies used in RO formation. Figure adapted from Reid et al. Viruses 2015 (14).

1.1.1 Enteroviruses

Viruses within the *enterovirus* genus belong to the *picornaviridae* family and are comprised of a small positive sense single stranded RNA genome, that is encapsulated in a 30 nm non-enveloped virion. Broadly, the picornavirus family predominantly consists of vertebrate viruses and includes enteroviruses, rhinoviruses, hepatoviruses, cardioviruses, and aphthoviruses (9). Enteroviruses are specifically named due to their enteric transmission route, despite the fact that many of these viruses disperse to alternate sites in the body to manifest symptoms (19). Enterovirus transmission occurs through the fecal-oral route, where the viral particles encounter their target receptor on unique cells within the intestinal epithelium. Infection of the intestinal epithelium induces a primary stage of viremia that allows for spread of the virus to secondary target tissues (19). Most enteroviruses induce mild disease symptoms, however dissemination to secondary tissues has been associated with severe complications. These severe complications are dependent on the secondary tissue tropism, and include the nervous system (poliovirus), heart (coxsackievirus B), liver (echoviruses), or pancreas (coxsackievirus B) (20).

1.1.1.1 Enterovirus lifecycle

Enterovirus infection (outlined in **Figure 2**) is initiated following binding of the virion to a receptor on the target cell surface that then induces receptor mediated endocytosis. Release of the genome happens in response to conformational changes in the virion that are induced either following engagement with the receptor or by the decreasing pH of the endosome following internalization and differs depending on the specific virus. Following delivery of the genome to the cytosol, the positive sense vRNA can be directly translated by host ribosomes through an internal ribosome entry site (IRES), producing a single polypeptide. This polypeptide is then co-

and post-translationally processed by the viral proteases, 2A, 3C, and 3CD, to produce ten distinct viral proteins (21). Following the initial round of viral protein production, the genome is replicated to produce more positive sense copies for both additional protein translation and virion packaging. Enterovirus genome replication, like most positive strand RNA viruses, occurs tightly associated with intracellular membranes, directly allowing for the concentration of viral replication factors and protection from innate immune pattern recognition receptors (PRRs) (22). Enteroviruses rely on cytoplasmic vesicles that originate from the ER, Golgi, or autophagosomes to establish their replication machinery and form ROs. Establishment of ROs requires both host and viral proteins, including enterovirus proteins 2BC and 3A which are membrane associated (23, 24). Of the host proteins that are required for RO formation, many of them are specifically related to lipid modifying proteins including phosphatidylinositol 4- kinase- β (PI4KB) and oxysterol- binding protein (OSBP) (12, 25). These host proteins play an essential role in controlling membrane lipid and cholesterol content and establishing membrane contact sites between ROs, the ER, and other membranes.

Once the genome has been replicated, de novo genomes serve as templates for additional viral protein production, producing more viral structural proteins for virion assembly and non-structural proteins that play key roles in immune evasion. Assembly of progeny virions occurs in the cytoplasm of cells and requires the viral structural proteins VP0, VP1, and VP3 which assemble around the positive sense genome to form the immature virion. VP0 is then proteolytically processed in to VP2 and VP4 to form a fully mature virus particle (21). Given that enteroviruses are nonenveloped viruses, viral release occurs by cell death and lyses. However, a number of studies have identified instances of nonlytic enteroviruses release through the association of viral particles with the cellular autophagy pathway.

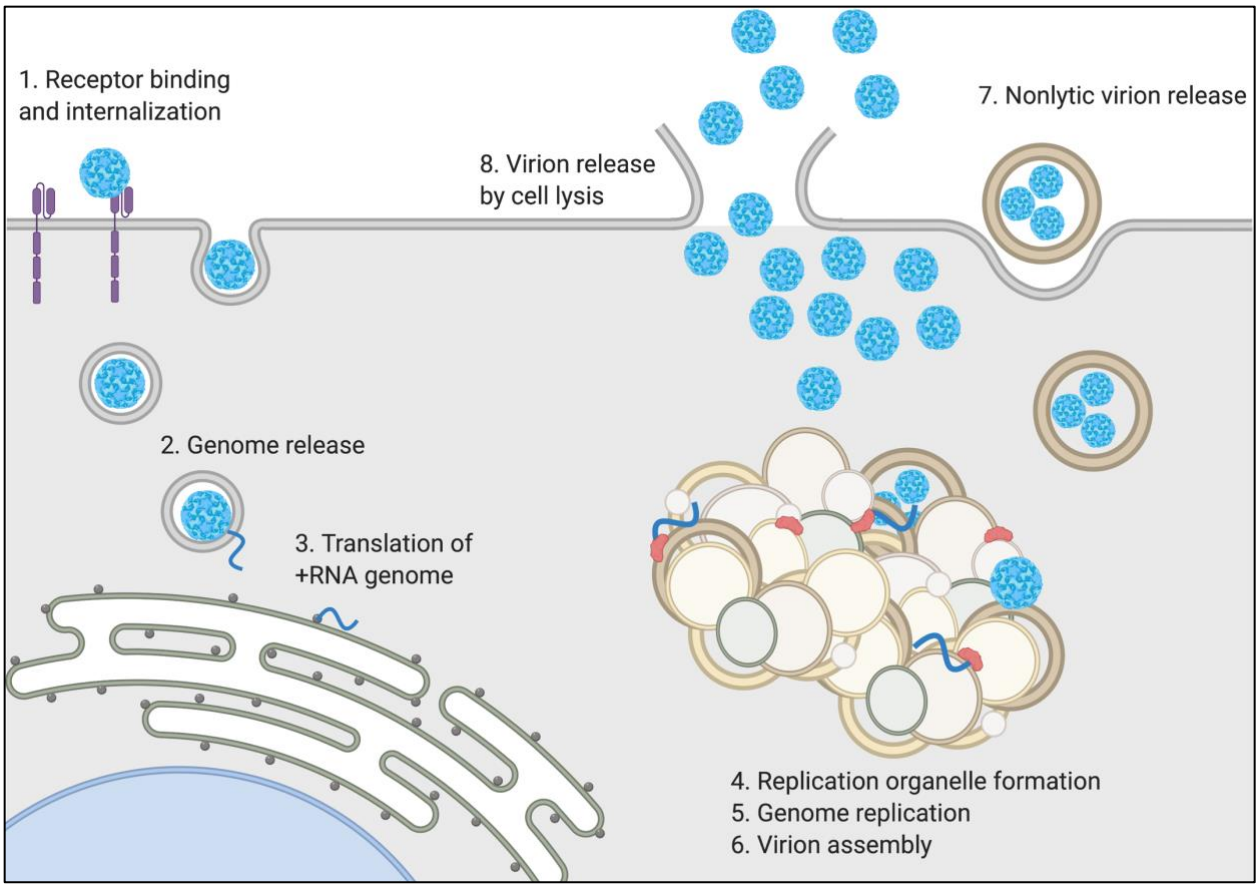

Figure 2 Enterovirus lifecycle

The enterovirus lifecycle can be broken down in to eight distinct stages. Starting with receptor binding and entry of the virus particle the virus is internalized where conformational changes in the capsid are induced by the late endosome and allow for genome release. The genome is immediately translated, where the production of viral proteins initiates the formation of viral ROs derived from vesicles originating from the ER, Golgi, and autophagosomes. Within the ROs the viral genome is replicated and packaging of progeny virions occurs. Virions can then be released from the cell by two mechanisms, through nonlytic release of by cell lysis. Created with BioRender.com

1.1.2 Flaviviruses

Viruses belonging to the *flavivirus* genus are enveloped, positive strand RNA viruses approximately 50 nm in diameter (9). Flaviviruses are a member the *flaviviradae* family of viruses,

which more broadly encompasses *pestivirus* and *hepacivirus*, however flaviviruses are unique in that they include many emerging pathogens due their arthropod vector transmission. All viruses within the *flavivirus* genus are transmitted through arthropod vectors to humans, including many mosquito-borne viruses (DENV, ZIKV, yellow fever virus, Japanese encephalitis virus, and West Nile virus) and tick-borne pathogens (tick-borne encephalitis virus and Kyansunar forest virus) (26). In recent years, the increased circulation of ZIKV in the population has caused an escalation in concern regarding the pervasiveness of viral vectors transmitting these viruses, specifically the *Aedes aegypti* and *Aedes albopictus* mosquitos. However, *Aedes* species mosquitos are not only responsible for ZIKV transmission but are also the primary insect vector for dengue virus (DENV) and yellow fever virus (YFV), which have been circulating in the Americas long before the emergence of ZIKV in 2015 (27).

Within the flavivirus genus, DENV and ZIKV have many similarities at the molecular level, however the tissue tropism and severe clinical manifestations are highly varied between these two viruses. Dengue virus predominantly infects circulating immune cells, including monocytes, macrophages, and dendritic cells, however there have also been reports of infection within hepatocytes and endothelial cells (28). A primary infection with DENV induces mild to moderate dengue fever symptoms, including joint and muscle pain, headache, vomiting, or rash. Following clearance, this primary infection confers prolonged immunity to the specific DENV serotype, however severe complications arise when a secondary infection with a different viral serotype occurs. Secondary DENV infection is characterized by hemorrhagic and capillary leak, which is termed dengue hemorrhagic fever and dengue shock syndrome. Onset of these severe complications is caused by the incomplete neutralization of pre-existing DENV antibodies circulating in the patient that lead to antibody dependent enhancement (ADE) and increased

infection (28, 29). In contrast, Zika virus has been shown to infect a wide array of cellular targets, including multiple cells types within the brain, eye, placenta, testis, and female reproductive tract (30–34). Most cases of infection with ZIKV show mild symptoms that include fever, rash, joint pain, or headache. However, in a small percentage of cases, ZIKV infection can induce severe neurological complications, including Guillain-Barre´ syndrome. Furthermore, the 2015 emergence of ZIKV demonstrated cases of vertical transmission between the mother and fetus that lead to severe developmental defects including cases of microcephaly (35). Despite, the clear distinction between DENV and ZIKV pathogenesis, these viruses demonstrate clear similarities in replication strategies employed within their target cells.

1.1.2.1 Flavivirus lifecycle

Flavivirus infection is initiated when a virus particle encounters its cognate receptor on a target cell (**Figure 3**). Receptor engagement induces endocytosis of the viral particle and allows for pH dependent fusion between the viral envelop and endosome membrane (36). Fusion with the endosome membrane is mediated by the viral envelop (E) protein and allows for the release of viral genomic RNA to the cytoplasm (37). Similar to enteroviruses, the viral genomic RNA can be directly translated by host ribosomes, producing a single polypeptide that is proteolytically processed by viral and host proteases to make ten distinct viral proteins. Unique to flaviviruses, this viral polyprotein is directly embedded in the ER following translation and allows for extensive ER remodeling and the production of viral ROs (38). These membrane enclosed compartments are essential for the viral life cycle, providing replication factories with high concentrations of viral proteins where viral RNA can be produced and virions can be assembled (15, 16). This step is also essential to protect viral replication components from PRR detection. Of the seven non-structural (NS) proteins, NS1, NS4A, and NS4B have been implicated in membrane rearrangement during

flavivirus infection (39–41). However, the mechanism by which membrane remodeling occurs remains largely unknown.

Following translation and the formation of viral ROs the positive strand RNA genome is replicated, allowing for the production of increasing amounts of viral structural and non-structural proteins and the switch to virion assembly. Virion assembly occurs within the membrane bound ROs where it is thought that the inner capsid is assembled around the RNA genome prior to budding into the ER lumen where the virus acquires the viral envelope (15, 42). Immature virions are then retained in the ER as packets of virus particles prior to trafficking and release from the cell surface. These immature virions are trafficked through the classical secretory pathway where they are proteolytically processed by host proteases in the trans Golgi to form mature virions (43). Mature virions are then non-lytically released from the host by exocytosis.

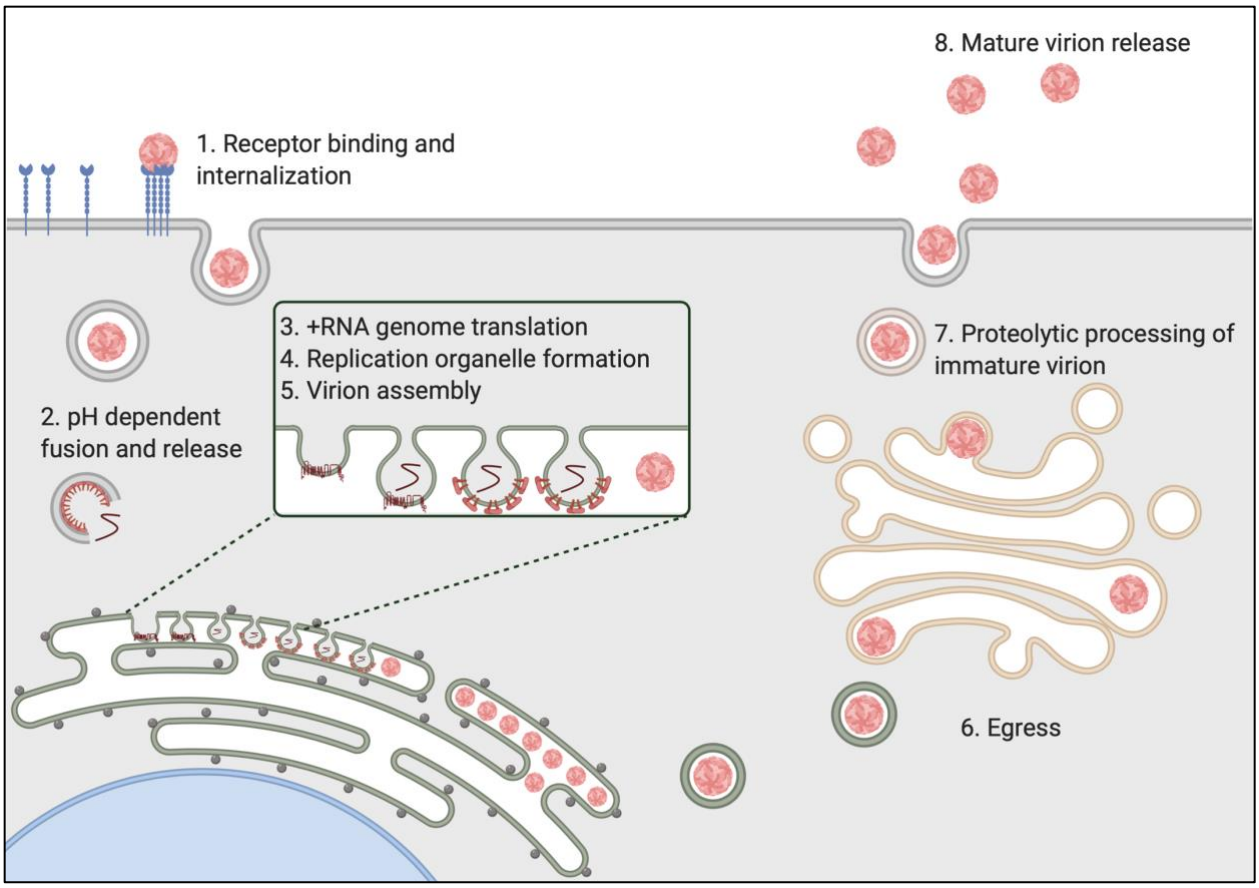

Figure 3 Flavivirus lifecycle

The flavivirus lifecycle can be broken down in to eight distinct stages. Starting with receptor binding and entry of the virus particle the virus is internalized where it undergoes pH dependent fusion with the late endosome in order to release the RNA genome. The genome is then translated, where the production of viral proteins initiates the formation of viral ROs. Within the ROs the viral genome is replicated, where it is packaged in to de novo virus particles. Virions then bud into the ER lumen, acquiring their viral envelop before they traffick through the Golgi for maturation and release. Created with BioRender.com.

1.2 Tubular lipid-binding (TULIP) superfamily

The BPIFB protein family exists within a much broader family of proteins that are characterized by their lipid binding and lipid transfer properties. BPIFB proteins belong to the BPI-

like protein family, which is one of three protein families within the larger tubular lipid-binding (TULIP) superfamily (44). Beyond the BPI-like family, TULIP proteins encompass two other distinct families of lipid transfer proteins (LTP) including the SMP-like and TAKEOUT-like families. LTPs within this TULIP superfamily are characterized by their tube-like structure that directly allows for the binding and transport of lipids within the inner cavity of the protein (45). The proteins within this family that have been functionally characterized as important components of membrane contact sites between the ER and other organelles, where they provide a direct method of lipid transport independent from vesicle trafficking (46). SMP-like proteins have been found to be highly prevalent at ER-mitochondria contact sites (MCS) (47), while TAKEOUT-like proteins have been more extensively classified in arthropods and suggested to play an important role in hormone transport rather than lipid transport (44). In contrast, the BPI-like family broadly encompasses proteins that function directly in the innate immune response (BPI and LBP), as well as proteins that function in lipid transport between plasma lipoproteins and tissues (cholesteryl transfer protein (CETP) and phospholipid transfer protein (PLTP)) (44).

1.2.1 BPI-like protein family

Proteins within the BPI-like family are characterized by their protein structure and contain one or more BPI folds (48). These BPI folds have a characteristic alpha-helix wrapped in a curved β-sheet structure that creates a central cavity proposed to be crucial for the lipid transport activity (44). The proteins that founded the initial classification of this protein family can be divided in to two distinct categories based on their protein function. First, BPI and LPS binding protein (LBP) are characterized for their roles in antibacterial signaling, where they both function as secreted factors that bind and neutralize lipopolysaccharide (LPS) to modulate the downstream signaling

response in macrophages or other innate immune cells (49). Second, CETP and PLTP encompass a separate branch of the protein family that is characterized by their lipid transfer properties. CETP and PLTP both function as circulating proteins that play an essential role in lipid exchange with plasma lipoproteins (50, 51). Following the initial classification of this protein, it has since grown to include the BPIF protein family which includes all BPIFA and BPIFB proteins.

1.2.2 BPIF/ PLUNC protein family

BPIFB proteins (previously referred to as LPLUNC) exits within the larger BPIF family of proteins that are classified by containing one or more BPI folds (48). Proteins within the BPIF superfamily were initially characterized based on their tissue expression profile and were named the PLUNC (palate, lung, and nasal epithelium clone) family of proteins (3). Once it was realized that more than one PLUNC gene existed, the nomenclature was changed to sPLUNC and LPLUNC, differentiated by the existence of one or two BPI domains respectively. This nomenclature was later reformed to what we now refer to as the BPIF (bactericidal/permeability-increasing protein fold) superfamily, which contains BPIFA and BPIFB in humans, previously sPLUNC and LPLUNC respectively (48).

Within the BPIF superfamily, BPIFA (sPLUNC) proteins have been studied to a higher degree than BPIFB proteins. However, these studies have been almost exclusively restricted to the function of BPIFA1 within the oral cavity and respiratory tract (52–54). Most studies have focused on the role of these proteins in relation to their predicted innate immunological functions similar to that of BPI. Within the lung and palate, BPIFA proteins are primarily secreted where they function as surfactants as well as anti-microbial factors specific to bacterial infection (54, 55). While high levels of expression within the lung and oral cavity has suggested an exclusive role of

both BPIFA and BPIFB protein function within these tissues, results from our laboratory suggest high expression is not required to elicit their intracellular function. Previous data from studies of both BPIFB3 and BPIFB6 suggest that these proteins play essential functions in cellular physiology even at extremely low expression levels (1, 2).

1.2.3 BPIFB family of proteins

The BPIFB protein family has seven distinct family members that have been identified in humans, including BPIFB1 through BPIFB6 and BPIFB9 (48). The initial identification of these proteins predicted them to play important roles in host defense similar to the function of BPI within the mouth, nose, and upper airways where their expression was initially identified (56). However, our work has identified a clear role for two of these proteins, BPIFB3 and BPIFB6, in host cellular defenses beyond the respiratory tract (1, 2). Of the BPIFB protein family, we have previously characterized the localization of BPIFB2, BPIFB3, BPIFB4, and BPIFB6 and found that unlike BPI, which elicits its molecular function as a secreted protein, BPIFB2, BPIFB3, and BPIFB6 are retained within the ER in multiple cell lines (2). In contrast, BPIFB4 localizes to the nucleus (2). These data were in agreement with previous sequence analysis that demonstrated BPIFB2, BPIFB3, and BPIFB6 all contain a signal sequence responsible for ER targeting that BPIFB4 specifically lacks (3). In humans, BPIFB9 has only been identified as a pseudogene and its expression pattern or predicted function have not been characterized to date (57). Structural data for any of the BPIFB proteins has yet to be resolved, however predictive hierarchical algorithms based on sequence homology map the predicted protein structure of BPIFB3 to CETP and BPIFB6 to BPI (**Figure 4**) (58–60). This taken together with the intracellular localization of BPIFB3 and

BPIFB6 suggests a possible function in facilitating lipid transport intracellularly between membrane contact sites, either within the endomembrane system or between other organelles.

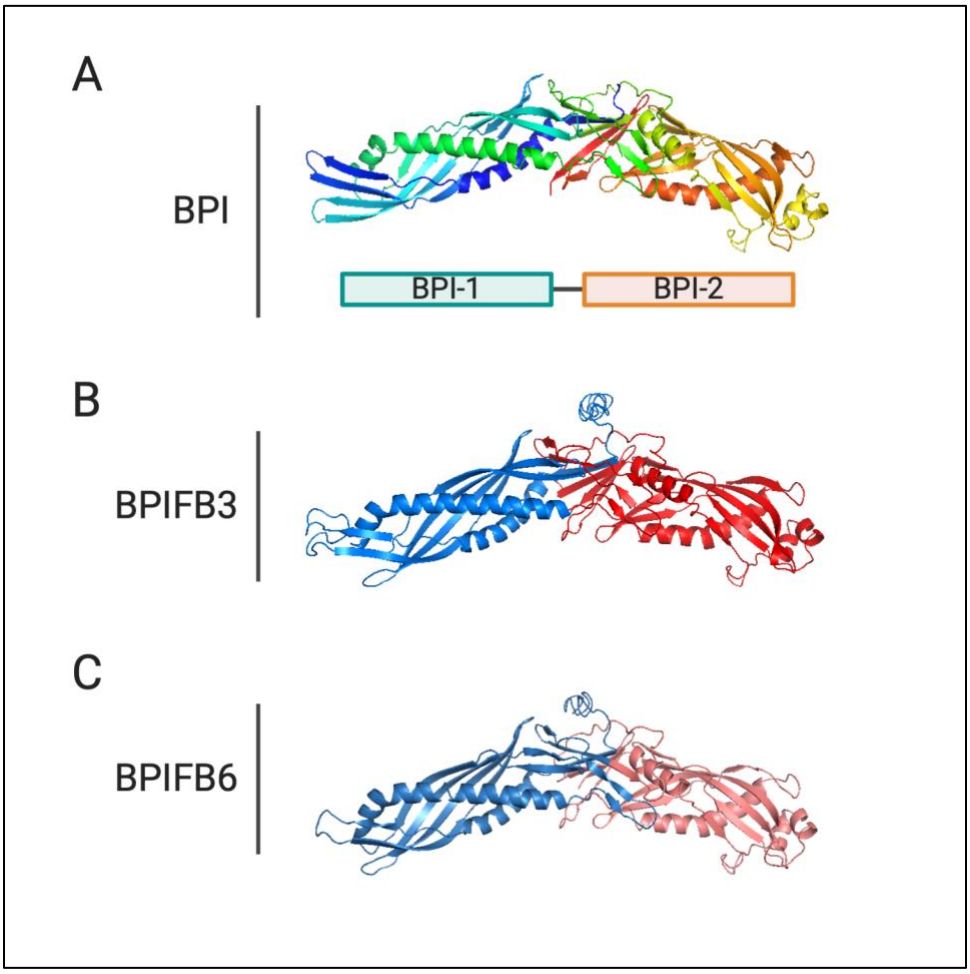

Figure 4 Predicted protein structure of BPIFB3 and BPIFB6

The predicted protein structure of BPIFB3 and BPIFB6 show a high degree of similarity to the structure of human BPI. **(A)** The structure of BPI (adapted from PDB: 1BP1) is composed of two BPI domains, one n-terminal and one c-terminal fold. **(B)** The predicted structure of BPIFB3 generated using the hierarchical protein structure prediction software, I-TASSER. The sequence of BPIFB3 maps to the structure of BPI-like family protein CETP. **(C)** The predicted protein structure of BPIFB6 generated using I-TASSER maps to the structure of human BPI.

Within the BPIFB protein family, we have most extensively characterized the roles of BPIFB3 and BPIFB6. While both of these proteins localize to the endoplasmic reticulum (ER)

they elicit distinct functions related to vesicle trafficking. BPIFB3 expression directly impacts the formation and trafficking of autophagosomes within the autophagy pathway, while BPIFB6 plays a role trafficking between the ER and Golgi (1, 2). Despite the functions attributed to other proteins within the larger TULIP protein family, including LPS binding, lipid transfer, and surfactant activity, there has not been direct evidence that BPIFB proteins have similar functions. Despite this limited evidence for a direct role in lipid transport, BPIFB3 and BPIFB6 bind lipids in an *in vitro* lipid dot blot experiment (2). Testing of the individual BPI domains, demonstrated that BPI-2 of BPIFB3 was able to bind a variety of lipids, including PA, PS, PE, PI(4)P, cardiolipin, and sulfatide (2). While both BPI domains of BPIFB6 showed lipid binding properties for a number of lipids, including PA, PS, PE, PI(4)P, PI(4,5)P2, PI(3,4,5)P3, cardiolipin, and sulfatide (2). Beyond this evidence in lipid binding capacity, our work demonstrating a role of BPIFB3 and BPIFB6 in regulating cellular trafficking events provides limited support for a role in direct lipid transport.

1.2.3.1 BPIFB3 functions to regulate non-canonical autophagy

BPIFB3 is an ER localized protein that predominantly localizes to the perinuclear sheet-like ER domains. Studies of BPIFB3 function by RNAi mediated depletion revealed that BPIFB3 plays an important role in the regulation of a non-canonical autophagy pathway (1). Silencing of BPIFB3 leads to an explicit increase in the number of autophagosomes and lysosomes within the cytoplasm, while the overexpression of BPIFB3 inhibits autophagy. Our previous work, as well as work presented in section 3 of this dissertation, has determined that BPIFB3 depletion-induced autophagy functions independent of the core macroautophagy machinery (1, 7). Data suggests a role for BPIFB3 in autophagy regulation independent from what is currently understood. This enhancement in autophagy that occurs during BPIFB3 depletion directly increases the replication of coxsackievirus B3 (CVB); an enterovirus that replicates on autophagosome derived membranes

within the cytoplasm of host cells. Depletion of BPIFB3 by RNAi results in a 10-fold enhancement of CVB replication and infectious virus production. This is directly tied to the upregulation of autophagy that occurs during BPIFB3 depletion, as the increased number of autophagosomes within the cytoplasm allows for an increase in CVB replication capacity (1).

1.2.3.2 BPIFB6 is important for Golgi maintenance and trafficking

In contrast to the role of BPIFB3 in regulating non-canonical autophagy, our previous work with BPIFB6 has determined that it plays an essential role in maintaining Golgi morphology. The RNAi mediated depletion of BPIFB6 results in Golgi fragmentation and a disruption of trafficking through the secretory pathway but has no effect on autophagy levels or ER morphology (2). Localization studies of BPIFB6 determined that it exclusively localizes to the ER; highly co-localizing with the ER sheet marker Climp63 and in close proximity to Atlastin3 (ATL3) at membrane junctions within the ER. In contrast to the role of BPIFB3 in CVB infection, BPIFB6 depletion results in a decrease in viral replication and infectious particle production (2). This data suggests that the expression or presence of BPIFB6 is required for efficient CVB replication or trafficking.

1.3 Autophagy

Autophagy is the catabolic cellular process by which excess proteins, lipids, and organelles are targeted for degradation by the lysosome. The most widely characterized form of autophagy is macroautophagy, which functions both as a bulk clearance and selective autophagy pathway that relies on the formation of a double membrane vesicle to traffic and degrade its contents by fusing

with the lysosome (**Figure 5A**) (61). Macroautophagy, both bulk and selective pathways, function under nutrient deprivation to induce the degradation of unnecessary cytoplasmic contents. However, in recent years, studies in both yeast and mammalian cells have broadened our understanding of the specific regulation of organelle turnover by autophagy that functions under broader stress signals than nutrient deprivation (62–64). Organelle specific autophagy encompasses the targeted degradation of membrane bound cellular organelles by autophagy receptors unique to each organelle. The mammalian organelle pathways studied to date include reticulophagy (ER), mitophagy (mitochondria), pexophagy (peroxisomes), and nucleophagy (nucleus) (65). Of these organelle maintenance pathways, most studies have characterized them as a specific subset of macroautophagy due to the reliance on many of the same key autophagy proteins and characteristic double membrane vesicles.

Beyond macroautophagy, two other forms of autophagy have been characterized that function independent of the core autophagy machinery, including microautophagy and chaperone-mediated autophagy (**Figure 5B and 5C**). Microautophagy refers to the direct engulfment of material by the lysosome or vacuole and has been almost exclusively studied in yeast (66). Chaperone-mediated autophagy (CMA) was the first pathway to suggest that autophagy could function to selectively degrade cargo, however, it has since been understood that other autophagy pathways can function in s selective manner also. CMA itself is the specific degradation of content by the lysosome and does not fall under the classification of macroautophagy because it does not rely on the formation of the double membrane autophagosome (67). Because macroautophagy is the most highly characterized of these pathways, it is frequently referred to as canonical autophagy, however there have been numerous reports demonstrating that autophagy can function outside the control of canonical macroautophagy machinery.

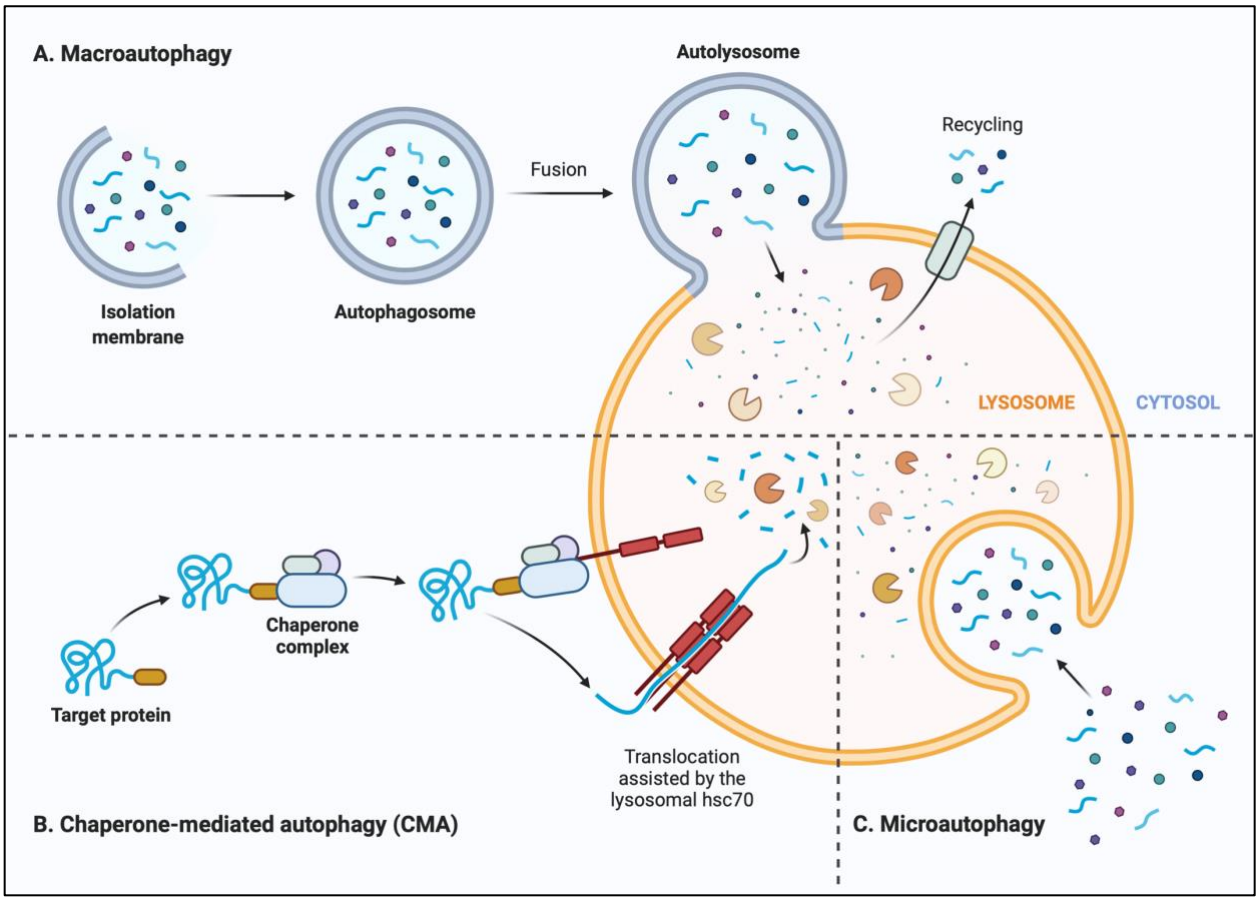

Figure 5 Three major autophagy pathways

The three major autophagy pathways that have been identified in mammalian cells and yeast include macroautophagy, chaperone-mediated autophagy, and microautophagy. **(A)** Macroautophagy can be broken in to three key phases, first the formation of the isolation membrane is responsible for the sequestration of target cargo, next the autophagosome is released from the membrane source and matures, until the final stage where it fuses with the lysosome to form the autolysosome degrade the contents of the vesicle. **(B)** Chaperone-mediated autophagy relies on the binding and trafficking of ubiquitinated target material by HSC-70 directly to the membrane of the lysosome, where it interacts with lysosomal proteins to translocate the target protein to the lysosome for degradation. **(C)** microautophagy refers to the direct engulfment of cargo through a non-specific pathway by the lysosome or vacoule in yeast. Created with BioRender.com

1.3.1 Macroautophagy

Bulk clearance and selective macroautophagy broadly function in response to cellular stress signals. Bulk autophagy and some forms of specific autophagy are initiated downstream of cellular nutrient sensors, such as mammalian target of rapamycin complex 1 (mTORC1) and AMP-activated protein kinase (AMPK) to degrade unnecessary cytoplasmic contents by targeting to the lysosome (61). The initiation of macroautophagy can be broken down in to four key stages, autophagosome nucleation, formation of the isolation membrane, LC3 processing, and vesicle release. First, following activation from upstream signals, the initiation of autophagosome nucleation is controlled by the Unc-51 Like Autophagy Activating Kinase 1 (ULK1) complex, which is directly activated downstream of mTORC1 inhibition and AMPK activation (68). ULK1 activation allows for the recruitment and assembly of the ULK1 protein complex components, including ATG101, FIP200, and ATG13 (69, 70). This complex is responsible for the recruitment and activation of the phosphoinositide 3-kinase (PI3K) complex which is required to trigger formation of the isolation membrane (71–73). Isolation membrane formation occurs on membranous organelles of the secretory pathway and has been directly linked to membranes of the ER, Golgi, and ER-Golgi intermediate compartment (ERGIC) (71, 74, 75). The PI3K complex consists of essential canonical autophagy machinery, including Beclin-1 (BECN1), UVRAG, and the catalytic subunit of the PI3K complex, PI3KC3 (also known as VPS34). This complex directly phosphorylates membrane lipids, resulting in increased phosphatidylinositol 3-phosphate (PI(3)P) lipid content on the isolation membrane (76). The early stages of autophagosome formation, including the isolation membrane, omegasome, and autophagosome are all marked by an increase in PI(3)P content (76, 77). Activity of the PI3K complex and the change in lipid composition is

further responsible for the recruitment of PI(3)P binding proteins, including DFCP1 and WIPI2, as the isolation membrane continues to expand to form the omegasome (78, 79).

The third stage of macroautophagy initiation is marked by the processing and conjugation of LC3 and ATG5-ATG12. In order for successful targeting of cargo and maturation of the autophagosome, LC3 must be processed and covalently attached to the membrane lipid, phosphatidylethanolamine (PE) (80). Likewise, the covalent conjugation of ATG5 to ATG12 is required for the successful targeting of lipidated LC3 (LC3-II) to the autophagosome membrane (81). The macroautophagy initiation machinery consists of two ubiquitin like conjugation systems that are responsible for the covalent modifications of LC3 and ATG5-ATG12. LC3 lipidation relies on ATG7 and ATG3, which serve as the E1 (ubiquitin-activating) and E2 (ubiquitin-conjugating) like enzymes required for PE attachment (78, 80, 82–84). Simultaneous to LC3 processing, the second conjugation system functions to form the ATG5-ATG12 complex, which is required for LC3 membrane association. ATG5-ATG12 association relies on ATG7 and ATG10 as the E1- and E2-like enzymes. The ATG5-ATG12 complex recruits ATG16L1, which together acts as the E3-like ligase that is responsible for targeting LC3-II to the omegasome (78, 81, 85–87). It is important to note that LC3-II remains stably associated with the autophagosome throughout the maturation process, which makes it one of the most useful markers to monitor the level of autophagy induction. Following the association of ATG5-ATG12-ATG16L1 and LC3-II with the omegasome, the membrane continues to elongate until the final stage of autophagosome formation, vesicle fusion and release. The mechanisms controlling the fusion and release of the autophagosome are not well understood. Inhibiting LC3 lipidation causes the phagophore to elongate but remain associated with the ER, suggesting the LC3-II interaction is essential for autophagosome release (88). Calcium signaling through SERCA is required for release of the

autophagosome, as treatment with thapsigargin, a specific inhibitor of SERCA, prevents autophagosome release (89, 90). Upon release from the ER the autophagosome matures until eventual fusion with the lysosome, forming the autolysosome, in a process termed autophagic flux that leads to degradation of cargo. During autophagosome maturation, vesicles can fuse with other compartments such as endosomes, forming an amphisome, prior to their fusion with the lysosome (61, 71).

Macroautophagy can function as both a bulk clearance pathway and a selective pathway. For instances of bulk cellular maintenance, the autophagosome directly engulfs cellular debris indiscriminately at the site of vesicle formation. However, the specificity of selective macroautophagy originates from the targeted sequestration of material through the specific interaction with p62. In macroautophagy, p62 functions as a cargo adapter protein where it can interact with target material through ubiquitin signals and LC3 on the autophagosome through its LC3 interacting region (LIR) (91).

1.3.2 Organelle specific autophagy

The turnover and maintenance of organelles via autophagy are classified as selective macroautophagy pathways due to the reliance on key components of the macroautophagy machinery and hallmark double membrane vesicle. Each organelle is targeted to the autophagosome through unique receptors that interact with LC3 to facilitate organelle turnover. In mammalian cells, reticulophagy and mitophagy are the two most defined organelle maintenance pathways, however research in yeast and some evidence from mammalian studies demonstrates that pexophagy (peroxisomes) and nucleophagy (nucleus) are also important maintenance pathways that function through similar canonical autophagy machinery (65, 92–96). Unlike

macroautophagy which is largely understood to respond during states of nutrient deprivation, each organelle specific pathway can be induced by activation signals unique to the individual pathway. While certain reticulophagy pathways do function in response to nutrient stress (97–100), additional pathways have been identified to play an important role in membrane clearance following ER stress and the unfolded protein response (UPR) (63, 101). In contrast, activation of mitophagy can uniquely occur via cell fate decision signals that balance cell survival with apoptosis (102, 103), while pexophagy activation has been linked to reactive oxygen species (ROS) levels (104).

1.3.2.1 Reticulophagy

The first reports of autophagy dependent ER degradation were identified in yeast, through the direct engulfment of ER membranes by the vacuole (105, 106). This pathway was coined "ER-phagy" and is more characteristic of a microautophagy pathway, as it functions independent of the hallmark macroautophagy double membrane vesicle. Later reports identified the receptor mediated degradation of ER membranes through macroautophagy machinery in both yeast and mammalian cells, terming this targeted degradation pathway as reticulophagy in order to differentiate it from the originally termed ER-phagy pathway (94, 100). In the years since, numerous reticulophagy receptors have been characterized, each mediating the turnover of specific ER domains in response to unique signals. Each receptor functions through the interaction of its LIR domain that binds LC3 to directly target ER membranes as cargo for the autophagosome.

Multiple mammalian reticulophagy receptors have been identified that induce ER turnover in response to cellular and nutrient stress cues, these receptors include reticulophagy regulator 1 (RETREG1), reticulon 3 (RTN3), atlastin 3 (ATL3), and TEX264 (99, 100, 107–109). Each of these reticulophagy receptors comprises its own expression pattern that contributes toward its

functionality. RETREG1 and TEX264 are perinuclear ER sheet localized proteins that specifically regulate the turnover of this ER domain in response starvation signals (100, 109). Similarly, RTN3 and ATL3 localize to the tubular ER network and play an important role in the specific degradation of ER tubules (107, 108). In contrast to the starvation induced activation signals that have been characterized for these four pathways, two unique receptors have been identified that function in response to ER stress. CCPG1 has been characterized as an ER localized protein that functions in response to UPR activation, playing an important role in the clearance of luminal misfolded proteins (101). Furthermore, the translocon component, Sec62, functions as an autophagy mediated recovery pathway following UPR activation and ER stress (63). While the activation cues for these pathways vary, reliance on the canonical autophagy machinery for many of them has been validated. However, emerging evidence suggests there is more variability in these pathways than originally identified. Specifically, our work presented in chapter 2 here suggests that RETREG1 clearance can also function independent of the canonical macroautophagy machinery (7).

1.3.3 Microautophagy

Microautophagy refers to the direct engulfment of cargo by the vacuole or lysosome membrane and has been characterized in yeast to a significantly higher degree than mammalian cells (66, 105, 106). While there have been very limited reports of its occurrence in mammalian cells, some studies have related mammalian microautophagy to endosomal sorting as a method to deliver cargo to the late endosome/ multivesicular body (110–112). In contrast, studies in yeast have described this as both a mechanism to regulate proteasome turnover and organelle maintenance. Organelle turnover that has been linked to microautophagy in yeast includes

degradation of the ER, nucleus, mitochondria, and peroxisomes (105, 113). However, there is still a lot of uncertainty around the role of microautophagy in yeast versus mammalian cells, including whether the described functions of these two pathways are related (110). While there has been some study of microautophagy in yeast, there is still a high degree of characterization that needs to be done to determine if there is a parallel pathway that functions in mammalian cells. This uncertainty is made even more complex by the limited resources available to study this pathway, given that no conserved pathway marker has been identified. Current studies of microautophagy have exclusively relied on electron microscopy to directly visualize cargo engulfment in the absence of macroautophagy machinery (66, 114).

1.3.4 Chaperone mediated autophagy

Unlike microautophagy and macroautophagy, CMA has been exclusively identified in mammalian cells and functions to specifically degrade proteins by direct targeting to the lysosome (67). Proteins are targeted for degradation by CMA through a consensus motif (KFERQ) that flags it for recognition by the HSC70 chaperone (115, 116). HSC70 can then interact with the lysosomal membrane protein, LAMP2A to directly target proteins for lysosomal degradation (117). The precise role of CMA in mammalian cell has yet to be fully elucidated. However, CMA has been found to occur at basal levels in most cells and is also upregulated in cellular stress responses, including nutrient deprivation, DNA damage, hypoxia, and oxidative stress (118, 119). Therefore, it has been associated as a general protein homeostasis pathway. The primary signaling pathway identified in the control of CMA is the mTORC2-AKT1 signaling axis. Similar to mTORC1 signaling in macroautophagy, mTORC2 activity functions to suppress CMA while the inhibition of mTORC2 and AKT1 increases CMA activity (120). While this pathway plays an important role

as a protein control pathway, it serves a very distinct function from macroautophagy and microautophagy and can be more similarly compared to the proteasome pathway in terms of cellular maintenance.

1.3.5 Non-canonical autophagy

The term non-canonical autophagy is used to describe all forms of autophagy that function outside of our understanding of canonical macroautophagy. While this also applies to microautophagy and CMA, the use of it in this document refers to specific cases of autophagy that rely on double membrane vesicle formation outside the control of what has been established as the canonical macroautophagy regulatory machinery. There have been multiple reports of non-canonical autophagy to date, however there has yet to be a consensus pathway identified that contributes to its activation (101, 121–123). One study in particular linked control of non-canonical autophagy to unsaturated fatty acid exposure. Finding that human osteosarcoma cells that were exposed to oleate, a monounsaturated fatty acid, and a panel of other unsaturated fatty acids (UFA) induced autophagy independent from canonical autophagy regulators ULK1, BECN1, or PI3KC3 (123). This UFA specific autophagy pathway functioned independent of pharmacological autophagy inhibitors, including 3-methyladenine and wortmannin. This UFA regulated non-canonical autophagy pathway draws a number of parallels from the non-canonical autophagy pathway that is induced during BPIFB3 depletion. As we previously found that BPIFB3si induced autophagy functions independent of BECN1 and other canonical autophagy machinery (1, 7). This understanding of non-canonical autophagy also relates to the predicted lipid binding capacity for BPIFB3 and may provide insight into the mechanism of BPIFB3-mediated control of non-canonical autophagy.

1.3.6 The relationship between enterovirus replication and autophagy

One major link between enterovirus replication and the autophagy pathway is the origin of membranes for RO formation (124). Enterovirus ROs have autophagy specific markers, including the autophagy adapter protein LC3, in addition to ER and Golgi specific markers (125, 126). Studies of both poliovirus (PV) and CVB have demonstrated that viral replication is linked to the induction of autophagy, as inhibition of the pathway by pharmacological inhibitors restricts replication. While infection in the presence of chemical inducers of autophagy, such as rapamycin, enhance the level of viral replication (127, 128). In support of this phenomenon, our previous work focused on understanding the role of BPIFB3-depletion induced autophagy during CVB infection, demonstrated that an increase in autophagy is directly linked to an increase in viral replication (1). Despite the reports that clearly link CVB replication to autophagy levels, CVB blocks the autophagy pathway prior to fusion with the lysosome (17). Therefore, CVB benefits from the early upregulation of the pathway, but prevents the later degradative stages of autophagy. This is in stark contrast to PV infection, which has been linked to vesicles containing markers for both autophagosomes and lysosomes, as PV is able to remain stable in the acidic environment of the lysosome (129). It has also been suggested that regulation of the autophagy pathway by enteroviruses serves as a mechanism to initiate membrane lipid remodeling required for RO formation (22, 130, 131). The regulation of autophagy is tightly linked to membrane lipid content, as the PI3K complex is required to generate an increase in the PI(3)P during isolation membrane formation and an increase in PI(4)P levels has also been linked to an increase in autophagy (73, 78, 132). Importantly, PI(4)P lipid levels have also been associated with enterovirus replication organelles, as PI4KB is a required host protein in the formation of viral ROs (133).

Beyond the role of autophagosome membranes during enterovirus RO formation, studies have reported that trafficking of viral particles through an autophagy related pathway plays an important role in the non-lytic release of CVB (126, 127, 134). Enlarged autophagosome like structures, termed megaphagosomes, secreted from cells were found to contain multiple CVB particles. This data suggests that the autophagy pathway may be subverted to allow for CVB egress prior to the destruction of cellular integrity. This is similar to a phenomenon that was identified in PV replication, termed autophagosome-mediated exit without lysis (AWOL) (135, 136). However, in contrast to CVB releaser in megaphagosomes, PV AWOL release has only been characterized in neurons. Non-CVB or PV enterovirus replication has also been linked to up regulation of the autophagy pathway, including during rhinovirus, echovirus 7, and enterovirus 71 infection (137–140).

1.3.7 The relationship between the flavivirus lifecycle and autophagy

The impact of various autophagy pathways on flavivirus infection has been a highly studied field as it has become clear both DENV and ZIKV are differentially affected by distinct autophagy pathways. Early reports studying the effects of macroautophagy during DENV infection found it to have pro-viral effects on viral entry, replication, and egress (37, 141, 142). While other reports suggested autophagy played an antiviral role in flavivirus replication (141, 143, 144). However, a more recent study characterized the individual components of the macroautophagy machinery by individual CRISPR knockouts and found that deletion of certain proteins restricted the ability of DENV to replicate while other macroautophagy regulators showed no effect (145). This is in agreement with reports from other viruses that suggest not all autophagy components are required

for viral manipulation of the pathway and represents a more complex understanding of the impact autophagy plays during flavivirus replication.

Beyond the role of canonical macroautophagy, studies have begun to look at the role of individual organelle specific autophagy pathways on flavivirus replication (146–148). These studies provide a more comprehensive understanding of the effects of specific organelle turnover during viral infection. Importantly, these studies point towards a more complex view of the relationship between flavivirus replication and autophagy rather than the traditional generalization that autophagy broadly benefits flavivirus infection. The first organelle specific autophagy pathway to be characterized during DENV infection was the degradation of lipid droplets in a pathway termed lipophagy. The autophagy mediated degradation of lipid droplets during DENV infection provides an important source for increased lipid metabolism and ATP generation to promote DENV replication (147). DENV infection specifically upregulates this pathway through the activation of AMPK and inhibition of mTORC1 (148). In contrast to the pro-viral role of lipophagy during DENV infection, reports from our laboratory determined that the RETREG1 dependent degradation of ER membranes is anti-viral to DENV and ZIKV replication (146); demonstrating that the turnover of specific cellular compartments differentially impacts flavivirus infection.

1.4 Conclusions

BPIFB proteins are an uncharacterized family of mammalian proteins that were identified in the human airway where they were suggested to play a role in extracellular innate immune defense. However, our previous work has identified an important intracellular role for BPIFB3 and

BPIFB6 in the regulation of vesicle trafficking that has important implications in controlling positive strand RNA virus replication. The work presented here expands on the role of BPIFB3 in three parts. First, we focus on the effects of BPIFB3 induced autophagy on the replication of two flaviviruses, DENV and ZIKV, and determine that the reticulophagy mediated turnover of ER membranes during BPIFB3 depletion inhibits DENV and ZIKV replication. Second, we identify two unique BPIFB3 binding partners, ARFGAP1 and Transmembrane emp24 domain-containing protein 9 TMED9, that are required for the induction of BPIFB3si mediated non-canonical autophagy. We further demonstrate that ARFGAP1 and TMED9 are required for the BPIFB3 depletion induced effects on RNA virus infection. Lastly, we expand on the work presented here on BPIFB3 in the context of what is known in regard to non-canonical autophagy and present a novel model for BPIFB3 function and its downstream effects on autophagy regulation and positive strand RNA virus replication.

2.0 BPIFB3 regulates ER morphology to promote flavivirus replication

Flaviviruses, including DENV) and ZIKV, rely heavily on the availability of ER membranes throughout their lifecycle and degradation of ER membranes restricts flavivirus replication. Accordingly, DENV and ZIKV restrict ER turnover by protease-mediated cleavage of RETREG1, also known as FAM134B, an autophagy receptor responsible for targeted ER sheet degradation. Given that the induction of autophagy may play an important role in flavivirus replication, the antiviral role of RETREG1 suggests specialized autophagic pathways may have differential effects on the flavivirus lifecycle. We previously identified BPIFB3 as a regulator of autophagy that negatively controls enterovirus replication. Here, we show that in contrast to enteroviruses, BPIFB3 functions as a positive regulator of DENV and ZIKV infection and that its RNAi-mediated silencing inhibits the formation of viral replication organelles. Mechanistically, we show that depletion of BPIFB3 enhances RETREG1-dependent reticulophagy leading to enhanced ER turnover and the suppression of viral replication. Consistent with this, the antiviral effects of BPIFB3 depletion can be reversed by RETREG1 silencing, suggesting a specific role for BPIFB3 in regulating ER turnover. These studies define BPIFB3 as a required host factor for both DENV and ZIKV replication and further contribute to our understanding of the requirements for autophagy during flavivirus infection. The data presented here have been previously published in Evans AS, Lennemann NJ, Coyne CB. 2020. BPIFB3 Regulates Endoplasmic Reticulum Morphology to Facillitate Flavivirus Replication. J Virol 94:1–13.

2.1 Introduction

Flaviviruses, which include DENV and ZIKV, are enveloped, positive-sense RNA viruses that replicate exclusively in association with ER membranes of infected cells (15, 16). Viral ER localized ROs function to sequester replication machinery within membrane bound compartments and thus provide a high concentration of host and viral replication factors, while isolating replication intermediates from clearance by the innate immune system (13, 42). Autophagy is an intrinsic cellular pathway that not only functions in cellular maintenance, but also plays an important role in the clearance of intracellular pathogens (151, 152). Autophagy can target many aspects of flavivirus infection, including direct clearance of viral particles or clearance of viral replication factories within the ER (62, 146, 153). However, the full relationship between flaviviruses and autophagy remains unclear.

We previously identified BPIFB3 as a regulator of CVB infection, a positive-sense RNA virus belonging to the *Enterovirus* genus, through its negative regulation of a non-canonical form of autophagy (1). Similar to flaviviruses, CVB relies on the availability of intracellular membranes to establish replication compartments; however, the source of these cellular membranes is variable (127). In this study, we determined whether BPIFB3 was more broadly involved in regulating RNA virus replication, specifically focusing on flaviviruses given their close association with the ER. Here we show that in contrast to CVB, BPIFB3 expression is required for the replication of two flaviviruses, DENV and ZIKV. Moreover, we show that BPIFB3 regulates ER membrane morphology and that loss of BPIFB3 prevents the establishment of ER-localized flavivirus ROs. Our data provide evidence that BPIFB3 silencing increases the level of ER turnover through RETREG1-dependent reticulophagy and that inhibition of this pathway by silencing of RETREG1 expression restores flavivirus infection. Our study thus demonstrates the differential control of

flavivirus and enterovirus replication by BPIFB3 and further suggests that reticulophagy is anti-flaviviral. These data also define a more specific role for BPIFB3 in regulating reticulophagy and provides insights into the cellular function of this protein.

2.2 Results

2.2.1 BPIFB3 is required for efficient flavivirus infection

We previously identified BPIFB3 as a negative regulator of coxsackievirus B (CVB) replication through the restriction of autophagy (1). To determine if BPIFB3 functions more broadly to regulate the replication of other RNA viruses, we assessed the impact of BPIFB3 silencing on flavivirus replication. For these studies we utilized human brain microvascular endothelial cells (HBMEC), an immortalized cell line model of the blood-brain barrier microvasculature (156). HBMEC were transfected with a siRNA targeting BPIFB3 (BPIFB3si) or a scrambled control siRNA (CONsi) and infected with DENV or ZIKV at a multiplicity of infection (MOI) of 1 for 48 hours, or with CVB for 16 hours. Infection was quantified by RT-qPCR for DENV, ZIKV, and CVB viral RNA (vRNA) (**Figure 6A**) or by fluorescent focus unit assays (FFU) for DENV and ZIKV (**Figure 6B**). In contrast to CVB, BPIFB3 silencing significantly restricted both DENV and ZIKV infection, resulting in an approximately 90% reduction in vRNA and a 100-fold decrease in infectious particle production (**Figures 6A-B**). Consistent with this, we observed a stark decrease in double stranded vRNA staining, a replication intermediate of DENV and ZIKV, in BPIFB3si transfected cells infected with DENV and ZIKV compared to CONsi (**Figure 6C**).

To determine whether other members of the BPIFB family are also required for flavivirus replication, we tested the effects of RNAi mediated silencing of the other ER localized BPIFB proteins, including BPIFB2 and BPIFB6. We have shown previously that in contrast to BPIFB3, BPIFB6 is a proviral host factor for CVB, and other enterovirus, replication (2). Unlike BPIFB3, we found that silencing of BPIFB2 did not significantly impact DENV and ZIKV, while silencing of BPIFB6 restricted ZIKV replication and infectious particle production while having no significant effect on DENV (**Figures 6D-E**). Given that we previously showed that BPIFB6 regulates Golgi morphology, this discrepancy between the effects of BPIFB6 silencing on DENV and ZIKV may be indicative of distinct trafficking pathways utilized by these viruses (2). In all studies, knockdown efficiency was confirmed by RT-qPCR (**Figure 6A and 6D**). These data point to a specific role for BPIFB3 in flavivirus replication.

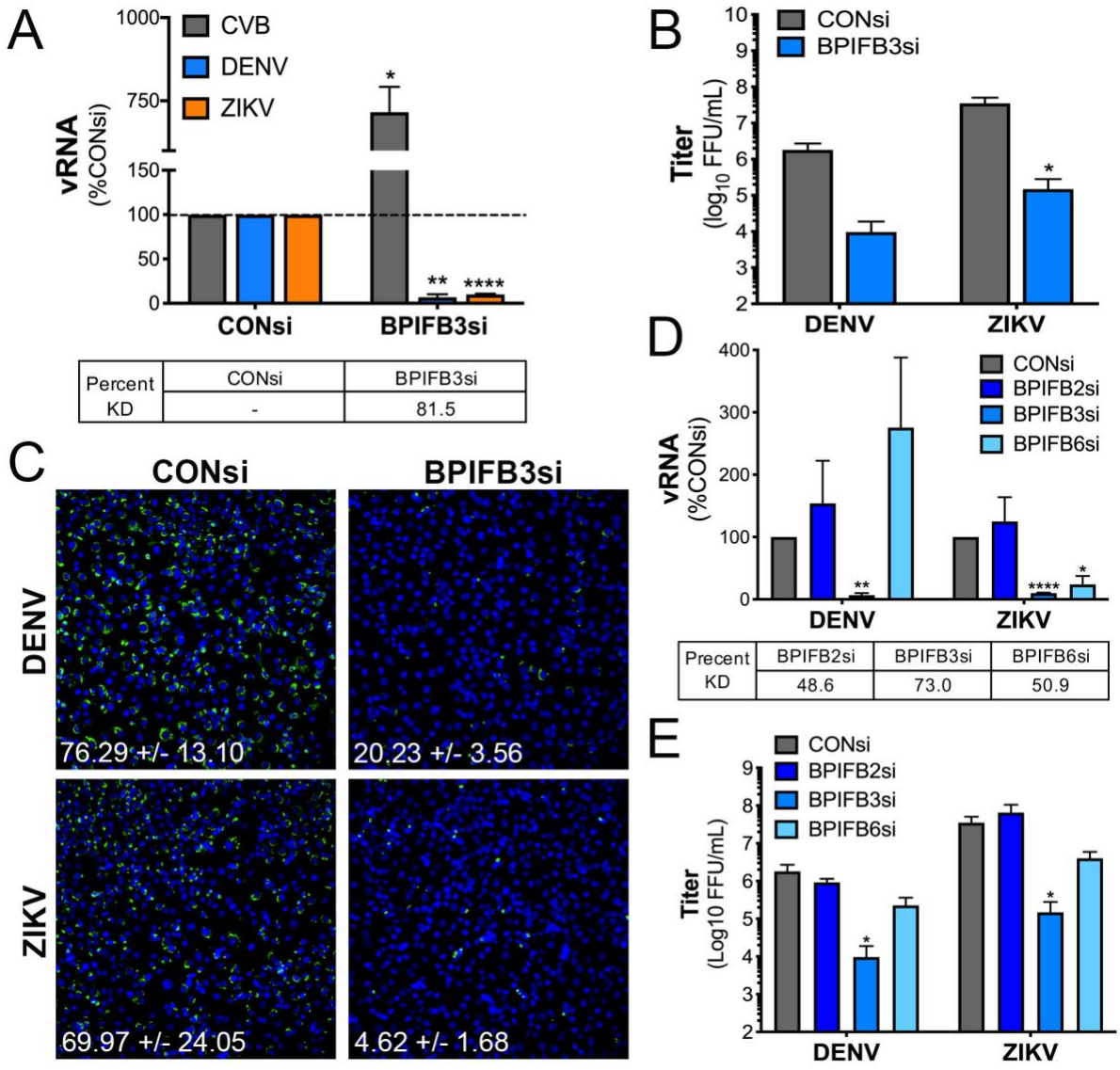

Figure 6 BPIFB3 is specifically required for both DENV and ZIKV infection

(A) Infection levels of CVB, DENV, and ZIKV determined by RT-qPCR. Data are presented as a percent fold change from CONsi-transfected cells. KD efficiency for BPIFB3 was determined by RT-qPCR is shown as percent KD compared to CONsi. **(B)** Titration (by fluorescence focus unit assay) of DENV and ZIKV infectious particle production from HBMEC from panel A. **(C)** Immunofluorescence microscopy for dsRNA (green), a replication intermediate, in CONsi or BPIFB3si transfected HBMEC. Average percent infected cells plus and minus the standard deviation is listed below each image. Scale bar is 50 μm. **(D)** RT-qPCR for vRNA infection levels of DENV and ZIKV in cells depleted of BPIFB2, BPIFB3, or BPIFB6. Percent KD compared to CONsi is shown for each BPIFBsi.

(E) Titration of DENV and ZIKV by FFU assay for panel E. Students t test were performed to determine statistical significance (*< 0.05, ** < 0.01, *** < 0.001, **** < 0.0001).

2.2.2 BPIFB3 depletion restricts flavivirus infections at an early stage of replication

To define which step(s) of flavivirus replication was facilitated by BPIFB3 expression, we assessed the effects of BPIFB3 silencing on viral RNA (vRNA) replication and membrane rearrangement. To address the effects of BPIFB3 expression on vRNA replication, we performed multi-step growth curves with DENV and ZIKV (MOI of 1) in CONsi- or BPIFB3si-transfected HBMEC, or in HBMEC treated with Bafilomycin A1 to prevent viral entry (**Figure 7A-B**). In CONsi-transfected HBMEC, we detected increased vRNA between 12-24 hours post-infection (h.p.i.). In contrast, levels of vRNA remained very low in BPIFB3si-transfected cells and were comparable to BafA1 treated cells at 24 h.p.i. (**Figure 7A-B**). However, by 48 h.p.i. vRNA in BPIFB3si-transfected cells had a slight increase compared to BafA1. These data suggest that BPIFB3 facilitates flavivirus infection at an early stage after entry, at or prior to genome replication. To confirm this, we utilized HBMEC stably propagating a DENV subgenomic replicon ($HBMEC^{rep}$), that expresses the full seven non-structural proteins, allowing for the replication of replicon RNA in membrane bound replication organelles similar to viral infection (157). We found that silencing of BPIFB3 in $HBMEC^{rep}$ had no effect on replicon RNA levels 48 hours after BPIFB3 depletion (**Figure 7C)**, suggesting that BPIFB3si restriction may occur before replication of the viral genome. This lack of effect on replicon RNA can likely be attributed to $HBMEC^{rep}$ cells having already undergone extensive ER remodeling to establish and maintain replicon expression. This could further suggest that BPIFB3 is required for the initial stages of ER remodeling.

Prior to vRNA replication, flaviviruses induce large scale expansion and remodeling of the endoplasmic reticulum in order to allow for the formation of ROs. To determine if BPIFB3 depletion had an effect on these membrane remodeling stages, we performed transmission electron microscopy (TEM) in CONsi- or BPIFB3si-transfected HBMEC infected with either DENV or ZIKV. Depletion of BPIFB3 prior to DENV or ZIKV infection significantly inhibited the formation of ER bound ROs (**Figure 7D-E**). Additionally, BPIFB3 silencing inhibited other hallmarks of flaviviral membrane manipulation (**Figure 7D**), black arrows indicate signs of viral replication and white arrows indicate ER membranes lacking viral replication), including the formation of convoluted membranes frequently seen adjacent to ROs that serve as sites of lipid synthesis.

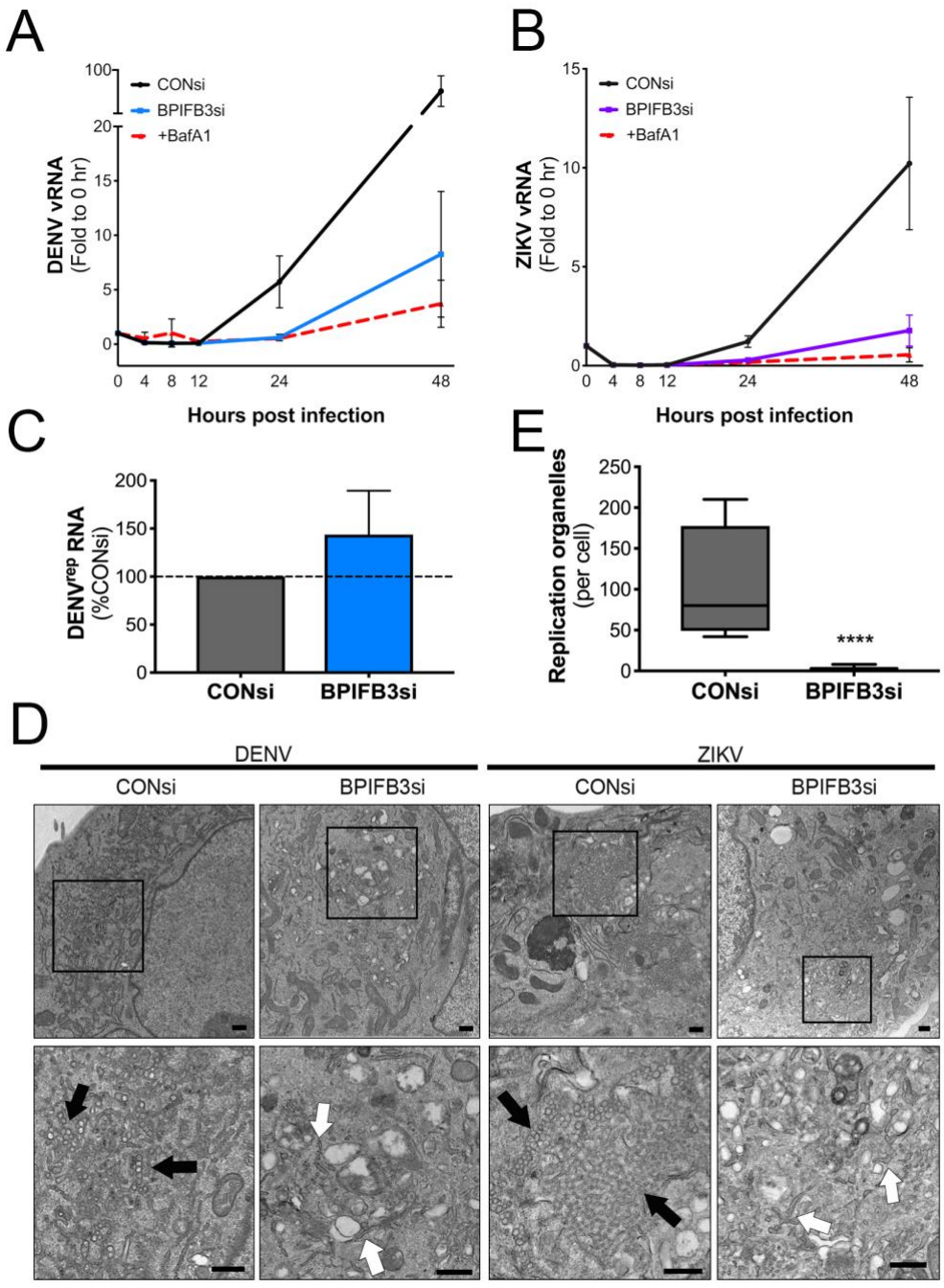

Figure 7 BPIFB3 depletion restricts flavivirus infection prior to genome replication

(A) RT-qPCR of multi-step growth curve for DENV **(A)** and ZIKV **(B)** performed using an MOI of 1. Data are represented as fold change to CONsi at 0-hour timepoint. **(C)** DENV replicon RNA levels determined by RT-qPCR in response to BPIFB3 depletion, presented as percent of CONsi. **(D)** TEM from HBMEC transfected with CONsi or BPIFB3si and infected with DENV or ZIKV. Black arrows indicate viral replication organelles and white arrows

indicate ER membranes lacking signs of viral replication. Top panel scale bar is 2 μm and bottom panel scale bar is 500 nm. **(E)** Quantification of the number of ZIKV replication organelles per cell in TEM images (panel D). Students t test were performed to determine statistical significance (*< 0.05, ** < 0.01, *** < 0.001, **** < 0.0001).

2.2.3 BPIFB3 depletion restricts flavivirus replication independent of innate immune activation and viral binding

To eliminate any impact of BPIFB3 on innate immune signaling, which could inhibit flaviviral replication, we performed whole genome RNASeq on CONsi- and BPIFB3si-transfected HBMEC in mock-, DENV-, or ZIKV-infected cells. Consistent with our RT-qPCR-based approaches, RNASeq confirmed the very low levels of flaviviral vRNA in BPIFB3si-transfected cells, with viral FPKM values significantly lower in BPIFB3 depleted cells (**Figure 8A**). Consistent with this, we did not detect any induction of innate immune signaling, as assessed by no changes in the expression of interferons (IFNs) type I (IFNβ) or type III (IFNλ), or in the induction of interferon stimulated genes (ISGs) (**Figure 8B**). As expected, we observed robust induction of IFNs and ISGs in CONsi-transfected HBMEC infected with both DENV and ZIKV (**Figure 8B**).

We next confirmed that the decreases in flavivirus replication were not due to decreases in cell viability or in the ability of viral particles to bind to the cell surface. We found that there were no differences in the extent of cell viability between CONsi- and BPIFB3si-transfected cells, as assessed by Trypan blue staining (**Figure 8C**). In addition, there were no differences in the levels of viral binding as assessed by RT-qPCR of vRNA bound to cells (**Figure 8D**).

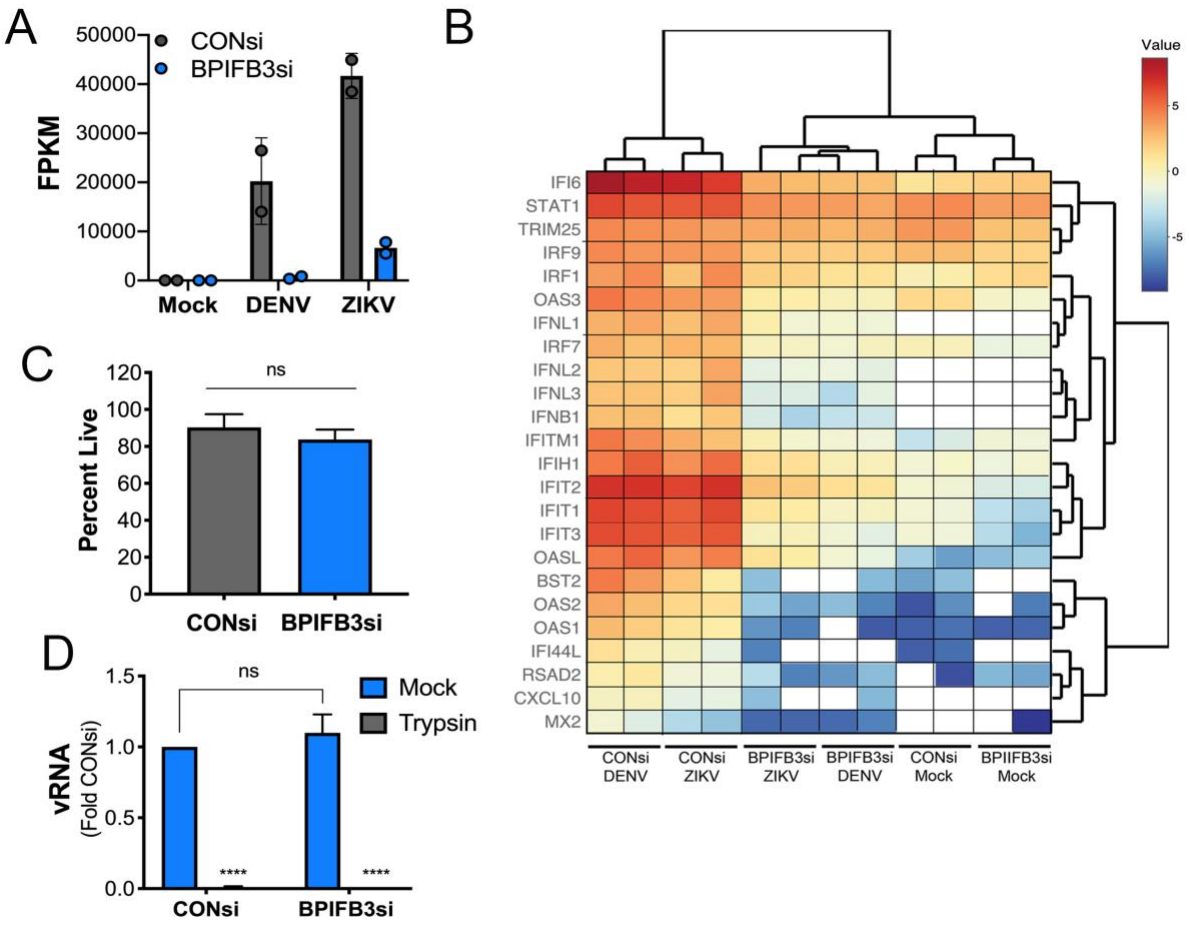

Figure 8 BPIFB3 dependent regulation of flavivirus infection is not caused by enhanced innate immune signaling or impairment of viral binding

(A) RNAseq showing viral FPKM values for DENV and ZIKV infected CONsi or BPIFB3si HBMEC. Mock infected cells for both had zero reads for both DENV and ZIKV. **(B)** RNAseq analysis of mock, DENV, or ZIKV infected CONsi or BPIFB3si HBMEC showing interferon and ISG mRNA levels from ln(RPKM) values, white indicates no reads for the specified sample. **(C)** Trypan blue stain for cell-viability in CONsi and BPIFB3si HBMEC. **(D)** ZIKV binding assay in CONsi and BPIFB3si HBMEC, quantified by RT-qPCR for vRNA. Cells were either incubated in normal media (mock) or Trypsin was added to inhibit ZIKV binding as a control. Data are normalized to mock CONsi.

2.2.4 Flavivirus infection of BPIFB3 depleted cells induces aberrant ER morphology

We next performed transmission electron microscopy (TEM) to determine the impact of BPIFB3 silencing on ER morphology with ultrastructural detail. These studies revealed remarkable effects of BPIFB3 silencing on ER morphology that were exaggerated in cells infected with DENV or ZIKV, including ER "whorls" and stacked membranes (**Figure 9A**), which have been previously associated with microautophagy in yeast, but remain largely uncharacterized in mammalian cells (158, 159). To further characterize these changes in ER morphology, we performed immunofluorescence imaging of HBMEC for the ER sheet marker Climp63 and viral dsRNA to identify infected cells. In uninfected cells, ER sheets originate at the nuclear envelope and extend to the cell periphery in a uniform arrangement; however, during infection with DENV and ZIKV, ER sheets condense around the perimeter of the nucleus where they co-localize with viral dsRNA (**Figure 9B**), designating the location of viral membrane remodeling and replication organelle formation (146). In cases where viral replication was detected by dsRNA staining in BPIFB3 depleted cells, the ER sheet marker, Climp63 showed aberrant rearrangements that did not co-localize with sites of viral replication (**Figure 9B**). To assess how frequent these unique ER structures were during BPIFB3 depletion, we quantified abnormal ER morphology across 50 individual cells from ZIKV infected CONsi or BPIFB3si HBMEC by TEM, as well as scored for visible replication organelles (**Figure 9C**). BPIFB3 depleted cells infected with ZIKV showed significantly higher instances of aberrant ER structures compared to CONsi, which lacked traditional ER localized viral replication organelles.

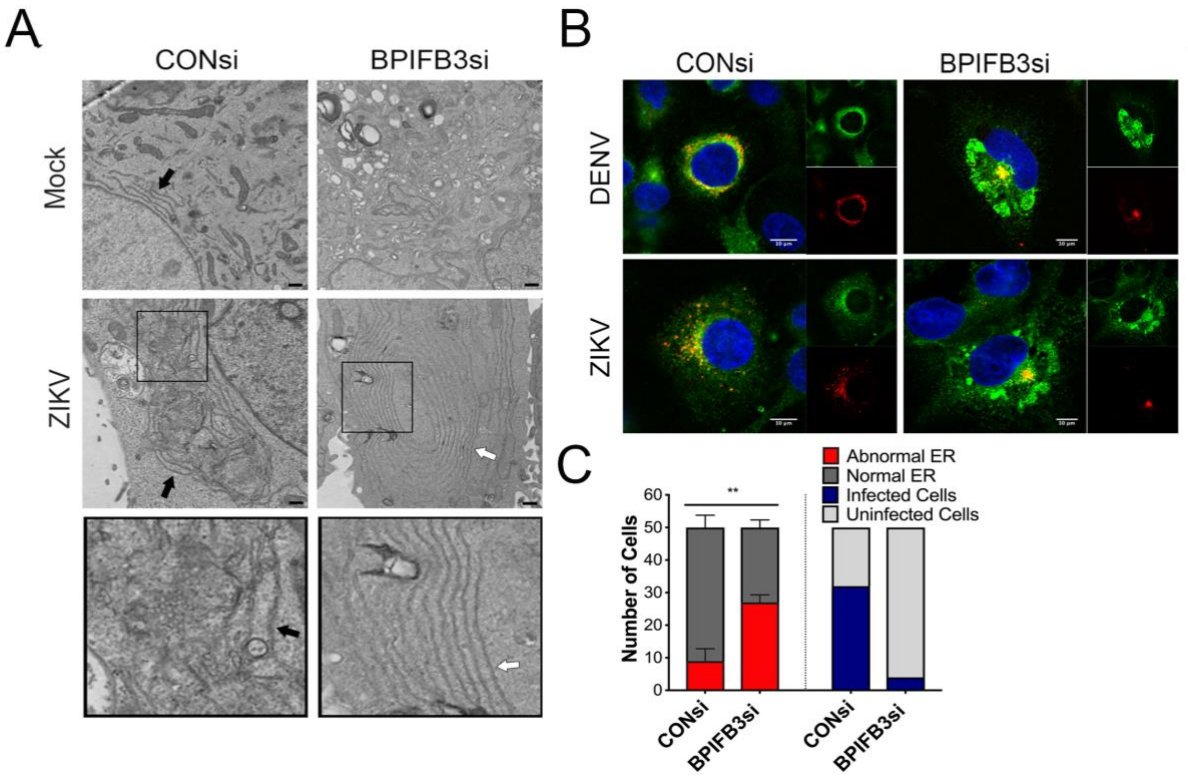

Figure 9 BPIFB3 depletion induces aberrant ER phenotypes in response to flavivirus infection

(A) TEM images from CONsi or BPIFB3si transfected HBMEC infection with ZIKV (or mock infected controls. Scale bars are 2 μm. Black arrows indicated normal ER morphology and white arrows indicate examples of abnormal ER that are quantified in C. **(B)** Confocal microscopy from CONsi or BPIFB3si HBMEC infected with DENV or ZIKV (MOI=1) and stained for dsRNA (red) and Climp63 (green) 48hrs post-infection. Scale bars are 10 μm. **(C)** Quantification of abnormal ER expansion by TEM (A) from 50 cells were scored blindly as either normal/ abnormal. These same cells were assessed for visible viral replication and scored as either infected or uninfected.

2.2.5 RETREG1 silencing restores flavivirus replication in BPIFB3si-transfected cells

DENV and ZIKV are dependent on the availability of ER membranes to replicate and we previously showed that reticulophagy functions as an antiviral pathway that limits the availability of these membranes (146). We next determined whether co-depletion of RETREG1 and/or other

reticulophagy receptors including reticulon 3 (RTN3) and Sec62 restored flavivirus infection in BPIFB3si-transfected cells. We found that co-silencing of RETREG1, but not RTN3 or Sec62, reversed the inhibition of flavivirus infection in BPIFB3si-transfected cells, as determined by both qPCR for vRNA and FFU for viral titers (**Figure 10A-C**). In contrast, silencing of RTN3 or Sec62 had no impact on BPIFB3si-mediated suppression of DENV infection (**Figure 10A**). Knockdown efficiency for all reticulophagy receptors were confirmed by RT-qPCR (**Figure 10A**).

To define the kinetics of RETREG1-mediated restoration of flavivirus infection in BPIFB3si-transfected cells, we examined the production of the DENV nonstructural protein 3 (NS3) by immunoblotting at various times post-infection. Consistent with our findings for vRNA, silencing of BPIFB3 significantly inhibited the production of NS3 at 8, 16, and 24 h.p.i. (**Figure 10D**). Moreover, RETREG1si transfection enhanced the production of NS3 at 16 h.p.i compared to CONsi-transfected cells (**Figure 10D**, middle panel). Co-silencing of RETREG1 with BPIFB3 reversed the inhibition of NS3 production and enhanced the production of NS3 by 16 h.p.i. in BPIFB3si-transfected cells (**Figure 6D**, middle panel). We confirmed these findings by immunofluorescence microscopy for NS3 followed by quantitative image analysis, representative images for NS3 staining are shown for the 48h time point (**Figure 10E-F**).

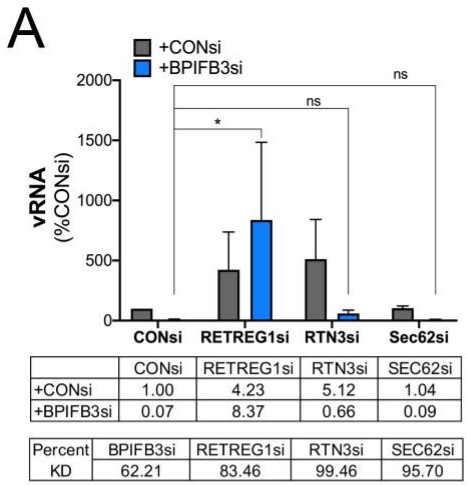

	CONsi	RETREG1si	RTN3si	SEC62si
+CONsi	1.00	4.23	5.12	1.04
+BPIFB3si	0.07	8.37	0.66	0.09

Percent KD	BPIFB3si	RETREG1si	RTN3si	SEC62si
	62.21	83.46	99.46	95.70

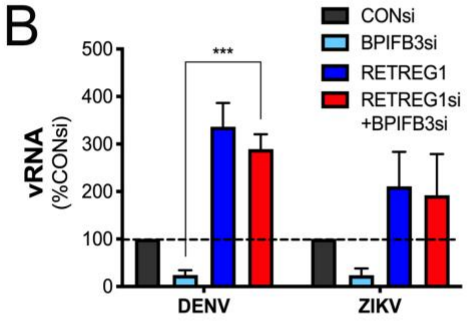

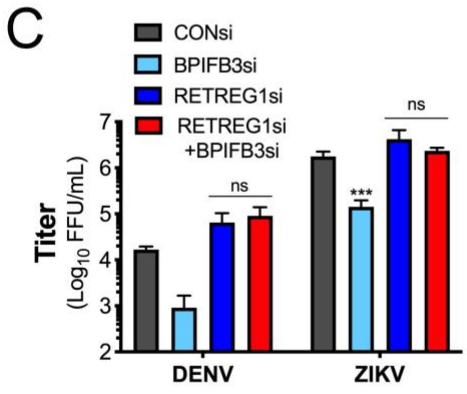

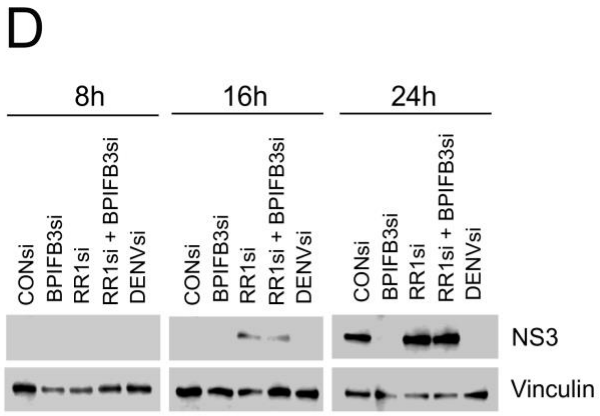

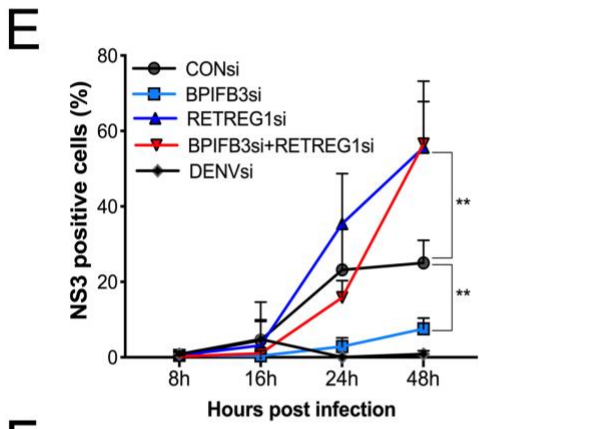

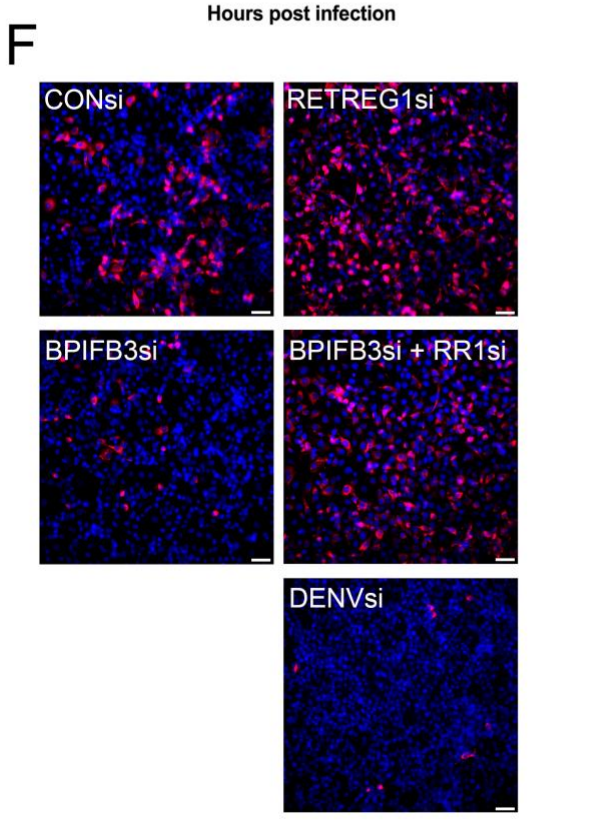

Figure 10 Inhibition of RETREG1 reticulophagy by RNAi restores flavivirus replication

(A) RT-qPCR of DENV infection of BPIFB3 depletion alone or with the reticulophagy receptors RETREG1, RTN3, or Sec62 in HBMEC. Mean fold change to CONsi for each knockdown is shown in table below the graph. Percent KD was determined by RT-qPCR and is shown for each siRNA. **(B)** RT-qPCR for DENV and ZIKV infection levels in cells depleted of BPIFB3 and RETREG1 alone or together. **(C)** Infectious particle production from BPIFB3 and RETREG1 depleted cells determined by FFU assay from panel B. **(D)** Western blot for DENV NS3 at 8, 16 and 24 hours post infection in BPIFB3 and RETREG1 depleted cells. **(E)** siRNA transfected HBMEC infected with DENV were stained and imaged for NS3 at 8, 16, 24, and 48 hours post infection and quantified by automated imaging software to determine the percent of NS3 positive cells per field. **(F)** Representative images from panel E.

2.2.6 BPIFB3 depleted cells exhibit enhanced reticulophagy

To mechanistically determine whether the reversal of flavivirus infection by RETREG1 co-depletion corresponded with a reversal in the autophagy phenotype associated with BPIFB3 depletion, we performed TEM of HBMEC transfected with BPIFB3si or RETREG1si alone or in combination, or with CONsi (**Figure 11A**). Quantification of the number of vesicles in each condition demonstrated that co-depletion of RETREG1 with BPIFB3 inhibited the increase in autophagy observed in BPIFB3si-transfected cells (**Figure 11B**). Given that depletion of RETREG1 reversed the enhancement of autophagy and the inhibition of viral infection associated with BPIFB3 silencing, we determined whether BPIFB3 depleted cells exhibited increases in reticulophagy specifically. To test this, we performed TEM to directly examine the association of the ER with autophagosomes and lysosomes. TEM imaging confirmed that the ER is highly associated with autophagosomes during BPIFB3 depletion (**Figure 11C**, black arrows indicate ER and white arrows indicate closely associated autophagosomes). Lastly, we confirmed that BPIFB3 silencing enhanced overall levels of autophagosome formation by immunoblotting for the

autophagy adapter protein, LC3 by immunoblot. In agreement with our prior studies (1), BPIFB3 depletion increased the autophagy-committed form of LC3 II (**Figure 11D-E**). Taken together, these data suggest that BPIFB3 is required to facilitate flavivirus replication due to its regulation of RETREG1-dependent reticulophagy.

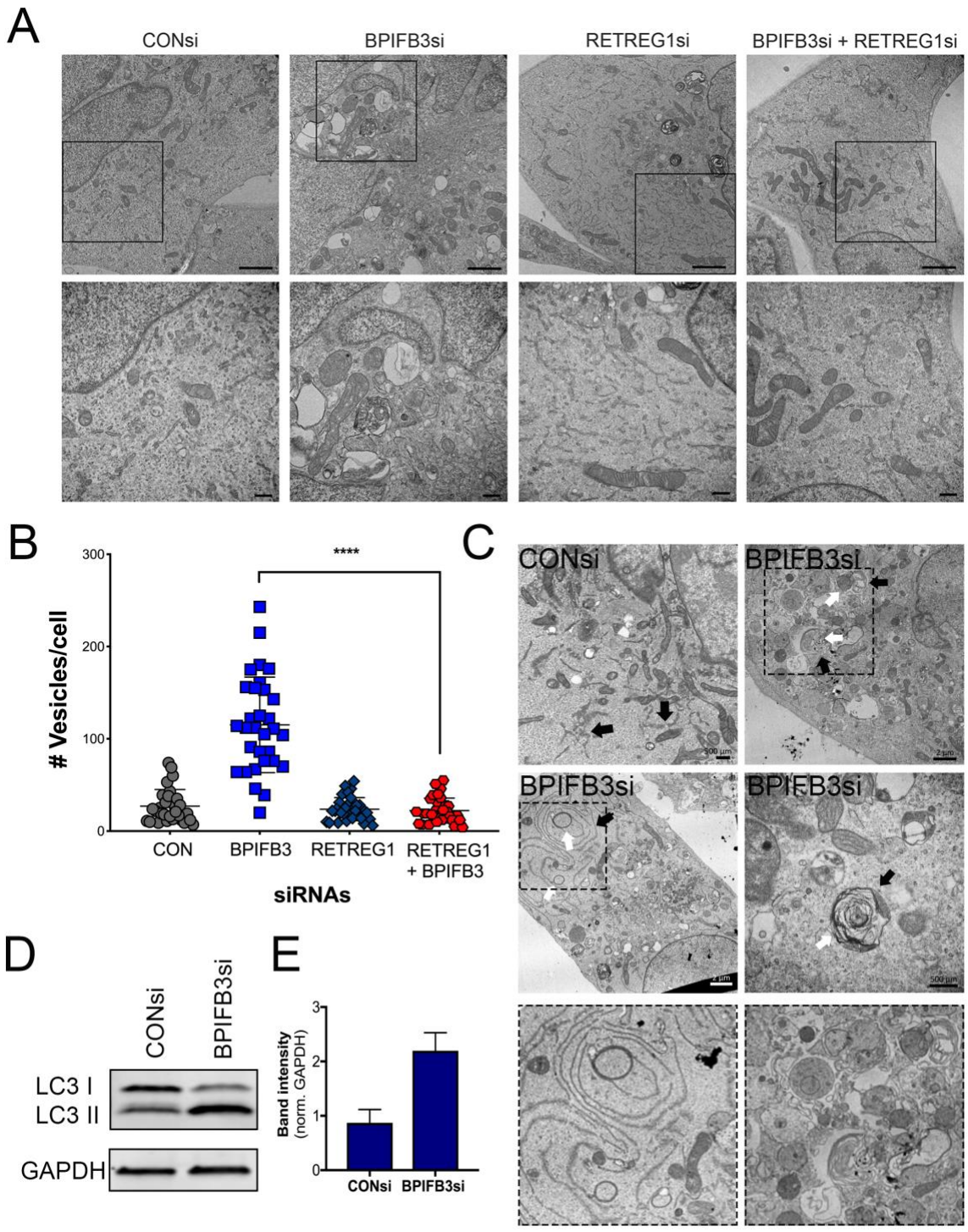

Figure 11 RETREG1 depletion inhibits BPFB3si induced autophagy

(A) TEM of HBMEC depleted of BPIFB3 and RETREG1 alone or together. Top panel shows total cell morphology, scale bars represent 2 μm. Black boxes indicated regions magnified in bottom panel to show ER membrane and vesicle

morphology. **(B)** Quantification of total number of vesicles (autophagosomes, lysosomes, and enlarged endosomes/ amphisomes) per cell from TEM images in panel A. **(C)** TEM images of CONsi or BPIFB3si HBMEC showing ER membranes closely associated with autophagosomes. **(D)** Western blot of siRNA transfected HBMEC for the autophagy protein LC3 and the GAPDH as a loading control, quantified in panel **(E)**.

2.3 Discussion

The success of flavivirus infection depends on the cooperation of numerous cellular organelles and pathways that function to produce progeny virions, specifically relying on host membranes throughout their lifecycles. Here we show that BPIFB3 is required for DENV and ZIKV infection by regulating the availability of ER membranes for viral remodeling of the ER. Our data show that BPIFB3 depletion enhances ER sheet turnover by RETREG1-mediated reticulophagy. These findings not only define the role of specific autophagic pathways in the regulation of flavivirus infection, but also identify BPIFB3 as a novel regulator of RETREG1-specific forms of reticulophagy.

Unlike other RNA viruses, flaviviruses depend solely on ER-derived membranes for their replication. The viral genome is delivered to the rough ER following entry and uncoating, where translation of viral proteins induces expansion of the ER. Of the seven nonstructural proteins, the majority remain associated with the ER throughout the lifecycle, where they function in viral replication, membrane remodeling, and inactivation of reticulophagy and ER stress pathways (13, 38, 142, 146, 150, 160). While it has been suggested that the virally encoded non-structural proteins NS1, NS4A, and NS4B are involved in membrane manipulation during DENV infection, little is known regarding host factors essential for this process. Currently, only three host factors have been implicated in membrane expansion, including fatty acid synthase (FASN), RETREG1,

and reticulon 3.1A (RTN3.1A). FASN is recruited to sites of replication organelle formation by the DENV protease NS3, demonstrating increased lipid synthesis is important for membrane remodeling (155). Additionally, both DENV and ZIKV inhibit ER degradation by cleaving the RETREG1 reticulophagy receptor, allowing for an accumulation of ER membranes (146). Lastly, RTN3.1A localizes to viral replication organelles to facilitate proper membrane curvature, however it does not interact with DENV or ZIKV NS4A during membrane remodeling (161). Our work presented here further confirms that degradation of the ER is an antiviral process and suggests BPIFB3 as a new host cell factor that regulates ER turnover. RNAi mediated silencing of BPIFB3 leads to enhanced levels of reticulophagy, which decreases the availability of ER membranes for flavivirus replication. Concurrent depletion of RETREG1 with BPIFB3 overcomes this defect, demonstrating that the antiviral effects of BPIFB3 depletion are specific to RETREG1-mediated reticulophagy.

One method proposed to promote membrane expansion during flavivirus infection is the induction of autophagy (142). However, our data demonstrate that enhanced levels of reticulophagy, particularly early during infection, inhibit membrane remodeling and replication organelle formation. Recent work has identified a number of ER-specific autophagy pathways that differ by the receptor used to target cargo to autophagosomes (63, 100, 107). However, it remains unclear whether these pathways are regulated by the same machinery that controls canonical macroautophagy. The growing diversity in the various forms of autophagy further complicates our understanding of the relationship between viral infection and this pathway, as certain forms of autophagy may differentially regulate viral replication at various stages of the viral life cycle. The work presented here, in combination with our previous work characterizing BPIFB3 as a negative regulator of CVB infection, demonstrates the unique requirements for autophagy between different

RNA virus families. In contrast to the unclear role for distinct autophagic pathways in flavivirus infection, CVB benefits from autophagy induction, as it uses autophagosomes and other cytoplasmic vesicles for replication organelle formation. Importantly, CVB inhibits fusion of the autophagosome with the lysosome, which enhances the number of cytoplasmic vesicles and prevents the degradation of viral replication machinery (23, 128, 162). Conversely, it has not been demonstrated whether flaviviruses have developed strategies to avoid clearance through the macroautophagy pathway similar to CVB and other enteroviruses. While the induction of autophagy during flavivirus infection has been implicated in enhancing viral replication (141), the precise timing of induction may have distinct effects on the viral lifecycle. Furthermore, the ability to specifically activate one form of autophagy while inhibiting others may be essential for successful flavivirus infection. The distinction between membrane manipulation during CVB infection and flavivirus infection explains the differential effects of BPIFB3 in regulating these unique viruses and further suggests that increased flux through autophagy is detrimental to flavivirus replication.

The BPIFB family of proteins were initially named and identified because of their homology to the bactericidal/permeability-increasing (BPI) protein; a secreted antimicrobial protein that functions through binding to LPS (3, 5, 48). Despite the high degree of predicted structural homology, BPIFB3 localizes to the ER and is not secreted (1). Of the other members of the family, BPIFB2 and BPIFB6 are also ER localized, however neither appear to regulate autophagy (2) or flavivirus infection. BPIFB proteins contain two BPI folds demonstrated to have lipid binding properties. Unlike other BPIFB proteins, the first BPI domain (BPI1) of BPIFB3 lacks the ability to bind lipids, while BPI2 is capable of binding phosphatidic acid, phosphatidylserine, cardiolipin, and other lipid molecules (2). Of the related proteins, BPIFB6 is

the only protein to be characterized, and has been demonstrated to regulate secretory trafficking and Golgi morphology (2). Together with the data presented here, this suggests that a possible unifying function of these proteins is to regulate sites of vesicle trafficking, however the mechanism by which they do so remains unclear. BPIFB3 over expression has been associated with inhibition of autophagy, while here we show that its depletion specifically enhances RETREG1 reticulophagy, but not other reticulophagy pathways universally. In comparison, BPIFB6 depletion results in Golgi dispersal and a disruption of retrograde and anterograde trafficking (2). This alludes to a possible mechanism whereby BPIFB3 and BPIFB6 expression is associated with decreased vesicle trafficking to the autophagic and secretory pathways respectively, while loss of expression leads to enhanced vesicle trafficking originating in the ER. Importantly, expression of BPIFB3 is remarkably low, and we are unable to detect endogenous protein by either western or immunofluorescence. Despite its low expression, depletion of BPIFB3 elicits a dramatic phenotype in cells, suggesting an essential role in regulating the morphology of the cellular membrane network. This is consistent with other ER structural proteins that drastically effect membrane morphology at very low levels of endogenous expression (163). Their potential roles in vesicle trafficking have important implications for the ability of these proteins to impact the trafficking and spread of a variety of viruses. However, further characterization is required to delineate the different methods by which viruses are trafficked during infection.

The relationship between flavivirus infection and the autophagic pathway is likely to be complex. While the initiation of autophagy and lipophagy have been demonstrated as proviral pathways (141, 142, 148, 154), flux through the autophagic pathway and reticulophagy are antiviral (143, 146, 164). Thus, further characterization of the role of specific autophagic pathways

in the regulation of flavivirus infection is needed to understand and develop new mechanisms to control infection.

3.0 BPIFB3 interacts with ARFGAP1 and TMED9 to regulate a non-canonical form of autophagy and positive strand RNA virus infection

Autophagy is a degradative cellular pathway that targets cytoplasmic contents and organelles for turnover by the lysosome. Various autophagy pathways play key roles in the clearance of viral infections, and many families of viruses have developed unique methods for avoiding degradation. Some positive stranded RNA viruses, such as enteroviruses and flaviviruses, usurp the autophagic pathway to promote their own replication. We previously identified the endoplasmic reticulum-localized protein BPIFB3 as an important regulator of non-canonical autophagy that uniquely impacts the replication of enteroviruses and flaviviruses. Here, we find that many components of the canonical autophagy machinery are not required for BPIFB3-regulated autophagy and identify the host factors that facilitate its role in the replication of enteroviruses and flaviviruses. Using proximity-dependent biotinylation (BioID) followed by mass spectrometry, we identify ARFGAP1 and TMED9 as two cellular components that interact with BPIFB3 to regulate autophagy and viral replication. Importantly, our data demonstrate that non-canonical autophagy in mammalian cells can be controlled outside of the traditional pathway regulators and define the role of two proteins in BPIFB3-mediated non-canonical autophagy. The data presented in this chapter have been submitted for publication in the Journal of Cell Science and are currently under revision. This manuscript can also be located on bioRxiv at Evans AS, Lennemann NJ, Coyne CB. 2020. BPIFB3 interacts with ARFGAP1 and TMED9 to regulate non-canonical autophagy and RNA virus infection. bioRxiv 2020.07.16.207035.

3.1 Introduction

Autophagy is a catabolic cellular process that is responsible for the degradation of many cellular proteins, lipids, and excess organelles. Despite the extensive characterization of signaling components involved in the regulation of macroautophagy, the origin of membranes responsible for the formation of nascent autophagosomes remains unclear. Each organelle within the secretory pathway has been implicated as a source of membranes for autophagosome biogenesis in mammalian cells, demonstrating a more complex relationship between membrane supply and autophagosome formation than what has been established in yeast. While it has been widely accepted that the ER plays an essential role in autophagosome formation, many studies have sought to narrow down the subdomain of the ER responsible for autophagosome nucleation. ER exit sites, ER-plasma membrane contact sites, and ER-mitochondria associated membranes have all been described as essential sites for autophagosome formation (64, 75, 173–175). Additional studies have also suggested that sites of COPI vesicle formation within the Golgi may play an important role in early stages of autophagosome formation (176). Despite these efforts to discern the sites and membrane features of autophagosome biogenesis, there still remains much variability and uncertainty surrounding this process. While the site of autophagosome formation likely has a significant impact on the cargo to be degraded, many questions remain. For example, does the site of isolation membrane nucleation also impact the type of autophagy (canonical versus an alternate noncanonical pathway)? These questions become more complex when thinking about the context of autophagy during viral infections, as there can be direct implications for the location of autophagosome formation and the targeted clearance of viral particles or membrane associated viral replication organelles. We previously identified that the specific turnover of ER membranes

by reticulophagy is a highly antiviral pathway for certain viruses (146), however the impact of other specific autophagy pathways on viral replication is less clear.

Our previous characterization of BPIFB3 revealed that its RNAi-mediated silencing resulted in a striking enhancement of autophagy, while it's over expression restricted autophagy (1). This regulation of autophagy has been demonstrated to have important implications in regulating the infection of two distinct families of viruses, enteroviruses and flaviviruses. Depletion of BPIFB3 specifically enhances the replication capacity of the enterovirus CVB, while restricting the replication of the two flaviviruses DENV and ZIKV (1, 7). These disparate effects on replication highlight key replication differences between the two families of viruses and their sensitivity to turnover by BPIFB3-regulated autophagy. Recently, we demonstrated that depletion of BPIFB3 not only impacts autophagic flux, but also disrupts ER integrity, which can be reversed by inhibition of ER turnover via RETREG1-dependent reticulophagy (7), suggesting that the depletion of BPIFB3 broadly affects multiple aspects of autophagy. However, the specific components that interact with BPIFB3 to elicit these effects remain unclear. In this study, we defined the interactome of BPIFB3 and characterized the role of specific interactions on autophagy and RNA virus infection. Using BioID followed by mass spectrometry, we identified two binding partners of BPIFB3, ARFGAP1 and TMED9, which we found regulate BPIFB3-specific autophagy. Our data presented here point to a mechanism whereby BPIFB3 interaction with ARFGAP1 and TMED9 regulates the initiation of a form of non-canonical autophagy.

3.2 Results

3.2.1 BPIFB3 depletion-induced autophagy does not rely on canonical autophagy regulators

Given that BPIFB3 regulates a non-canonical autophagy pathway, we sought to characterize which components of the autophagic initiation machinery were required for the induction of autophagy during BPIFB3 depletion. To do this, we used two distinct viruses, CVB and DENV, as read outs for the reversal of autophagy induction given that our previous studies showed that BPIFB3-induced autophagy increases the replication of CVB, while it restricts DENV infection (1, 7). We tested components associated with three key phases of autophagy induction—autophagosome nucleation (ULK1), isolation membrane formation (the catalytic component of PI3K (PI3KC3), UVRAG1, and BECN1), and processing of LC3 (ATG7). To determine if these factors were essential for the induction of autophagy observed during BPIFB3 knockdown, we depleted each component by RNAi-mediated silencing in human brain microvascular endothelial cells (HBMEC) either alone or during the context of BPIFB3 depletion and infected with CVB or DENV. Consistent with previous findings, BPIFB3 depletion alone resulted in an enhancement of CVB replication (**Figure 12A**) and a restriction of DENV replication (**Figure 12B**). Silencing of the autophagosome nucleation kinase ULK1 independently had minimal effect on both CVB and DENV (**Figure 12A-B**). Consistent with these results, when ULK1 was co-depleted with BPIFB3 there was no change in the effects of BPIFB3 silencing on CVB or DENV replication (**Figure 12A-B**). These data directly indicate that the enhancement of autophagy observed during BPIFB3 depletion is not reversed when ULK1 expression is knocked down. We performed these same analyses for factors associated with isolation membrane formation (**Figure 12C-D**) and LC3

processing (**Figure 12E-F**), using both CVB and DENV infection levels as an indication of the inhibition of autophagy. We found that none of the canonical autophagy components tested were able to inhibit BPIFB3si-induced autophagy. Intriguingly, the co-depletion of BPIFB3 with BECN1 seemed to exaggerate the effect of BPIFB3 depletion alone, suggesting some degree in similarity between the effects of BECN1 and BPIFB3 depletion on CVB and DENV. However, BECN1 depletion was still insufficient to inhibit the enhancement of autophagy observed during BPIFB3 silencing. Knockdown efficiency of the siRNAs was confirmed by RT-qPCR (**Figure 13**). These data provide a clear indication that the regulation of autophagy during BPIFB3 depletion is not dependent on macroautophagy regulatory components.

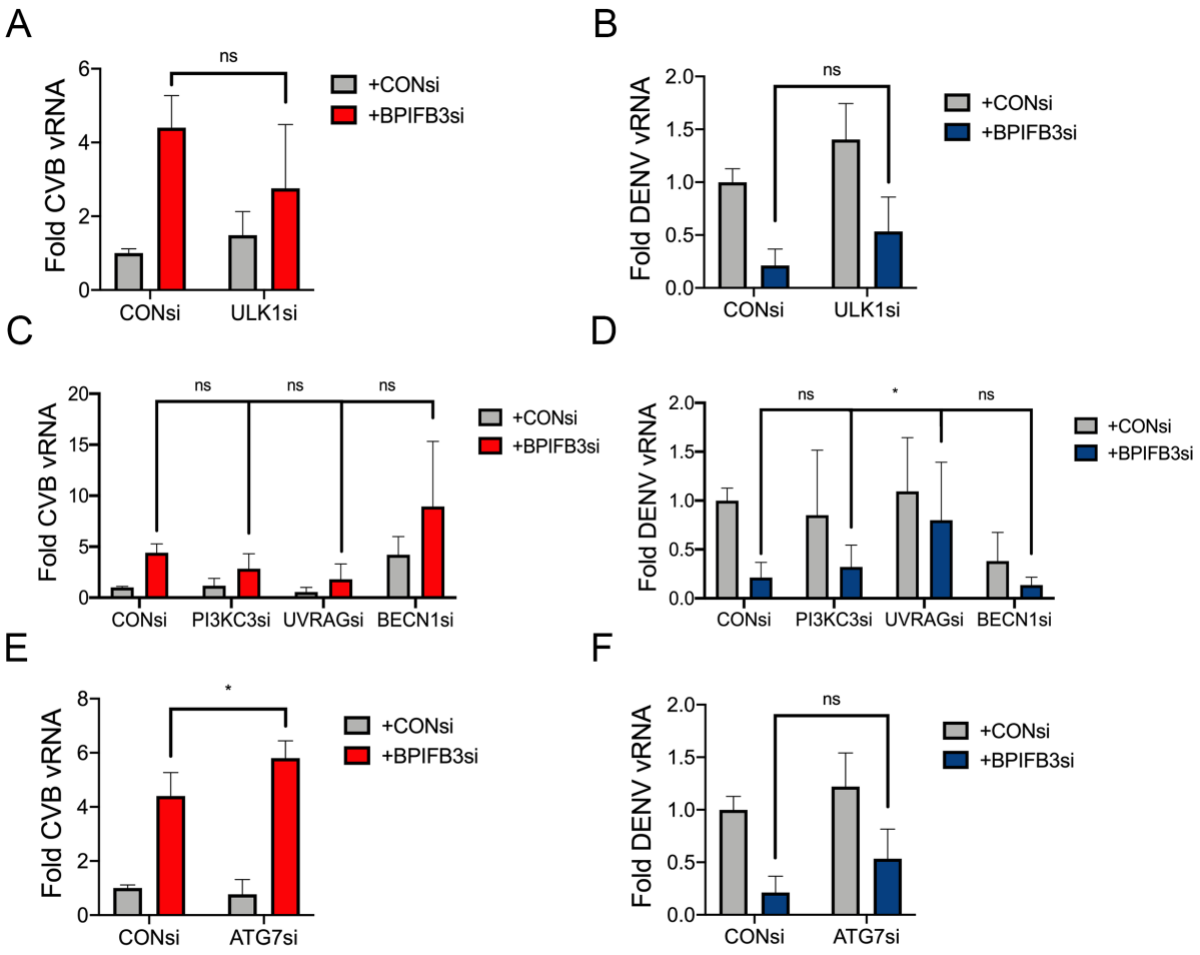

Figure 12 Canonical autophagy components are not required for BPIFB3si induced autophagy

HBMECs were depleted with BPIFB3 alone or in combination with key macroautophagy regulatory components, including factors involved in autophagosome nucleation, ULK1 **(A and B)**; components of the PI3K complex required for isolation membrane formation, PI3KC3, UVRAG, BECN1 **(C and D)**; and ATG7, which is required for LC3 and ATG5-ATG12 formation **(E and F)**. 48 hours post knockdown HBMEC were infected with CVB (16h) and DENV (48h) and viral replication was determined by RT-qPCR. CVB and DENV were used as a readout for BPIFB3si induced autophagy as our prior studies have determined BPIFB3 depletion increases CVB replication and restricts DENV infection. Data were analyzed using a two-way ANOVA, * $P < 0.05$.

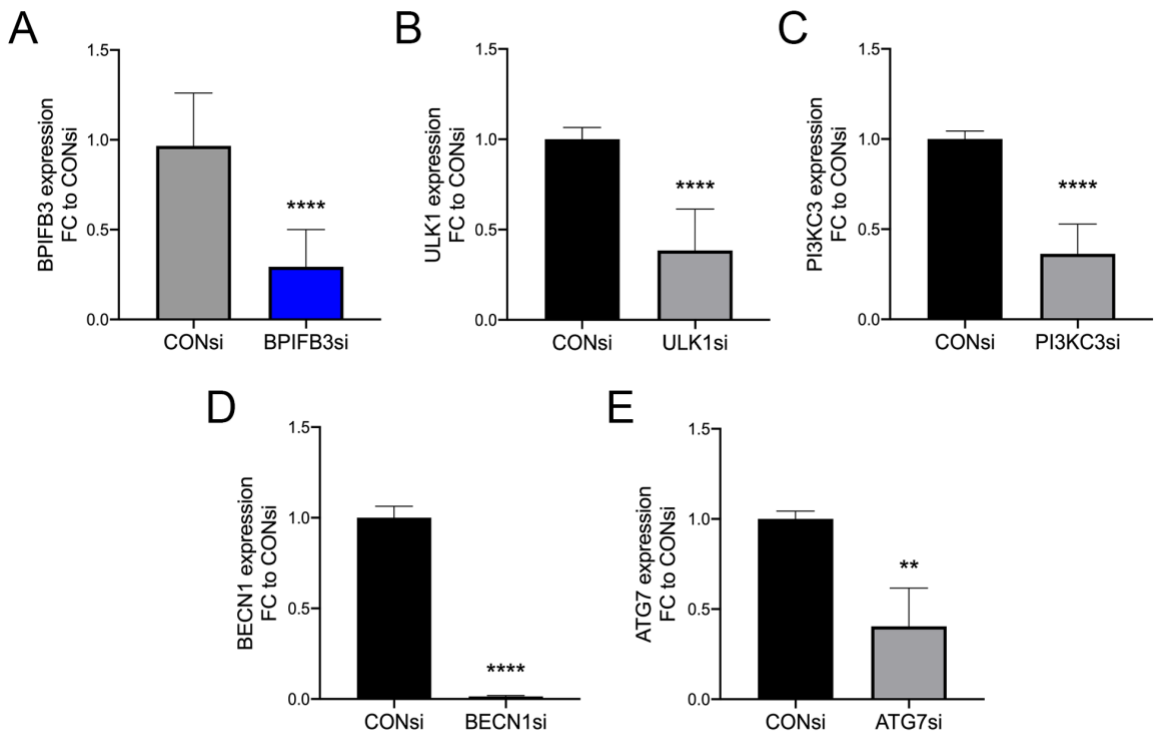

Figure 13 siRNA knockdown efficiency of autophagy regulatory components

The knockdown efficiency for each siRNA targeting BPIFB3 **(A)**, ULK1 **(B)**, PI3KC3 **(C)**, BECN1 **(D)**, and ATG7 **(E)** was determined by qPCR for target mRNA and expressed as fold change to control siRNA transfected cells (CONsi). Data were analyzed using an unpaired t test, ** $P < 0.01$, **** $P < 0.0001$.

3.2.2 BioID mass spectrometry identifies ARFGAP1 and TMED9 as BPIFB3 interacting proteins

In order to identify proteins that interact with BPIFB3 and gain further insights into the mechanism(s) of its non-canonical autophagy regulation, we utilized the improved biotinylation based assay, BioID2 followed by mass spectrometry analysis (177). To achieve this, biotinylated

proteins were isolated from HBMEC expressing BPIFB3-BioID2 or an empty BioID2 control vector. BPIFB3 interacting candidates were selected following mass spectrometry detection by analyzing raw peptide counts (**Figure 14A and 14D**) and percent protein coverage (**Figure 14B, 14C, and 14D**) as fold change to vector control samples. BioID identified a number of potential BPIFB3 interacting partners, including ARFGAP1 and TMED9 which have been previously implicated in the regulation of vesicle trafficking between the ER and Golgi (178–180).

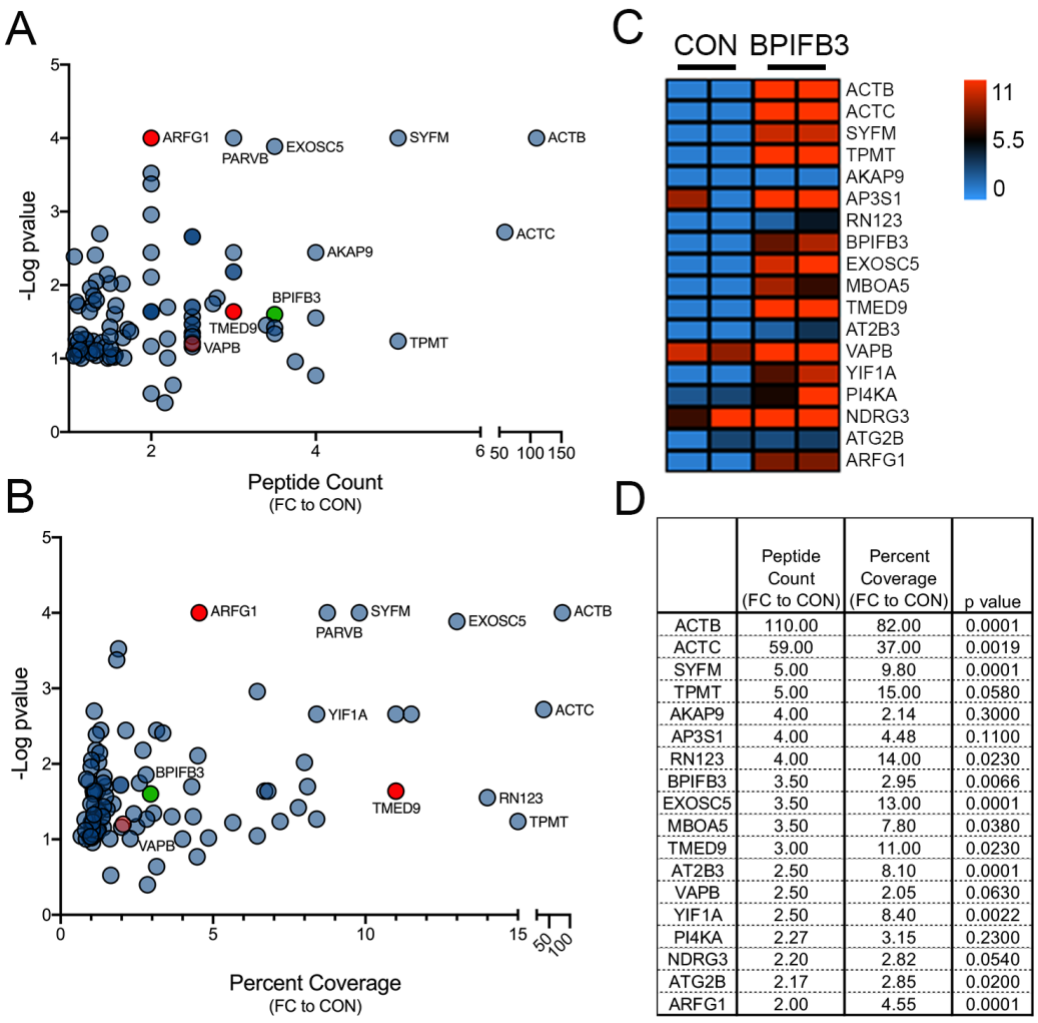

	Peptide Count (FC to CON)	Percent Coverage (FC to CON)	p value
ACTB	110.00	82.00	0.0001
ACTC	59.00	37.00	0.0019
SYFM	5.00	9.80	0.0001
TPMT	5.00	15.00	0.0580
AKAP9	4.00	2.14	0.3000
AP3S1	4.00	4.48	0.1100
RN123	4.00	14.00	0.0230
BPIFB3	3.50	2.95	0.0066
EXOSC5	3.50	13.00	0.0001
MBOA5	3.50	7.80	0.0380
TMED9	3.00	11.00	0.0230
AT2B3	2.50	8.10	0.0001
VAPB	2.50	2.05	0.0630
YIF1A	2.50	8.40	0.0022
PI4KA	2.27	3.15	0.2300
NDRG3	2.20	2.82	0.0540
ATG2B	2.17	2.85	0.0200
ARFG1	2.00	4.55	0.0001

Figure 14 BioID analysis identified BPIFB3 interacting proteins

Mass spectrometry results from BioID tagged BPIFB3 expressed in HBMEC. Data represented as raw peptide counts **(A)** or percent protein coverage **(B)**. **(C)** Heatmap showing individual percent coverage of mass spectrometry results for both vector control (CON) and BPIFB3. Average values for peptide counts, percent coverage, and significance for select candidates are shown in **(D)**.

Validation of the BioID results by immunoprecipitation of BPIFB3 tagged with V5 expressed alone or with GFP-fused ARFGAP1 and TMED9 confirmed their interaction **(Figure 15A**). Interestingly, we also tested the interaction of BPIFB3 with VAPB, which was identified at low levels by the BioID screen (shown in **Figure 14A** and **14B** as the pale red point) and found

that we were not able to validate its association with BPIFB3. These data confirm the specificity of interaction of BPIFB3 with ARFGAP1 and TMED9. We next examined the localization of ARFGAP1 and TMED9 when expressed with an ER marker or with BPIFB3. In agreement with our prior studies, ectopic expression of BPIFB3 with the ER marker KDEL-mCherry (**Figure 15B** top row) confirmed BPIFB3 localizes to the ER in a punctate expression pattern with a high Pearson's correlation coefficient of 0.72 (**Figure 15D**). ARFGAP1 expression was primarily diffuse in the cytoplasm with a small amount of punctate perinuclear expression that is indicative of its known localization with the Golgi complex (181). The punctate expression of ARFGAP1 further co-localized with the KDEL-mCherry marker (Pearson's $r = 0.82$), as it has been previously reported that ARFGAP1 enhances both anterograde and retrograde trafficking between the ER and Golgi (**Figure 15B** middle row) (182, 183). Interestingly, co-expression of ARFGAP1 with BPIFB3 disrupted the punctate Golgi localization of ARFGAP1 (**Figure 15C** top row) however still remained highly co-localized with BPIFB3 (Pearson's $r = 0.72$) (**Figure 15D**). Expression of ARFGAP1 also altered the morphology of BPIFB3 localization, causing BPIFB3 to localize in a more reticular pattern with clusters of aggregated signal (**Figure 15C** top row). Ectopic expression of TMED9 was highly localized to the ER in a reticular pattern (Pearson's $r = 0.93$), which is retained upon co-expression with BPIFB3 (**Figure 15B-C** bottom rows). Likewise, expression of TMED9 does not alter the localization pattern of BPIFB3. These results show that BPIFB3 interacts and colocalizes with ARFGAP1 and TMED9.

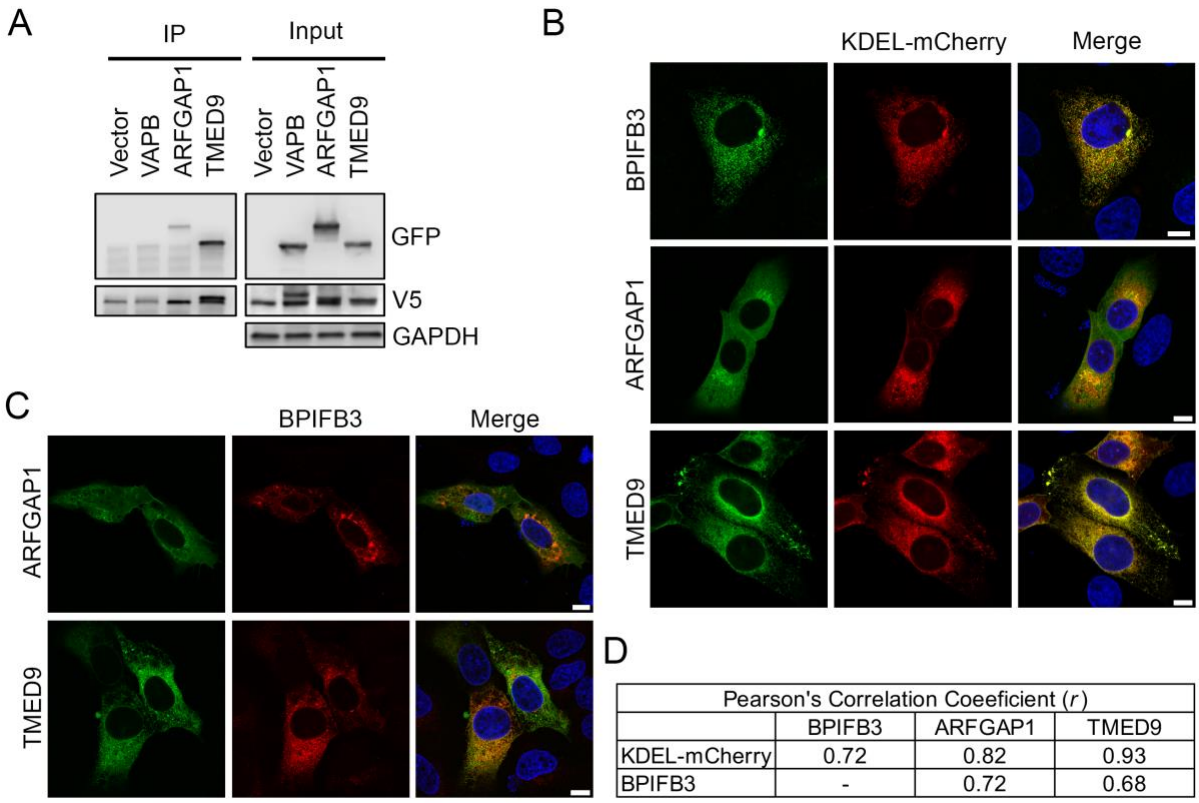

Pearson's Correlation Coeeficient (*r*)			
	BPIFB3	ARFGAP1	TMED9
KDEL-mCherry	0.72	0.82	0.93
BPIFB3	-	0.72	0.68

Figure 15 Validation of BioID results confirms ARFGAP1 and TMED9 interact with BPIFB3

(A) Immunoprecipitation of BPIFB3-V5 with select candidates identified by BioID, VAPB-GFP, ARFGAP1-GFP, and TMED9-GFP. Note that the double band on the V5 input blot is residual VAPB (top band) above BPIFB3 (bottom band) and is not a BPIFB3-V5 doublet. **(B)** Immunofluorescence imaging of U2OS cells expressing BPIFB3, ARFGAP1, and TMED9 (all green) with the ER marker, KDEL-mCherry. Scale bars are 10 μm. **(C)** Co-localization of BPIFB3 (red) was assessed with both ARFGAP1 and TMED9 (green) in U2OS cells by immunofluorescence. Scale bars are 10 μm. **(D)** A Pearson's correlation analysis was used to determine colocalization between ARFGAP1, TMED9, and BPIFB3.

3.2.3 ARFGAP1 and TMED9 expression are required for BPIFB3-mediated autophagy

Given that a hallmark of BPIFB3-silencing is increased levels of autophagy, we next sought to determine whether ARFGAP1 or TMED9 were required for this phenotype. HBMEC

were transfected with a control siRNA (CONsi) or with BPIFB3si alone or in combination with siRNAs against ARFGAP1 and TMED9 (ARFGAP1si or TMED9si). Samples were then infected with CVB, which enhances the levels of BPIFB3si-induced autophagy (1). Consistent with our prior studies, BPIFB3 silencing induced an increase in lipidated LC3 (LC3 II), which can be distinguished from non-lipidated LC3-I by immunoblot (**Figure 16A**). LC3-II levels were further enhanced in BPIFB3si-transfected cells infected with CVB (**Figure 16A**). Depletion of ARFGAP1 and TMED9 independently had minimal effects on LC3 levels during CVB infection (**Figure 16A**). However, co-depletion of ARFGAP1 and TMED9 with BPIFB3 led to a decrease in LC3-II levels compared to BPIFB3si alone, suggesting that the depletion of each inhibited BPIFB3si induced autophagy enhancement. In contrast co-depletion of BPIFB3 with VAPB, did not reverse BPIFB3si induced autophagy (**Figure 16A**).

In order to confirm that ARFGAP1 and TMED9 depletion reversed the enhancement of autophagy in BPIFB3si-transfected cells, we used immunofluorescence-based microscopy to examine autophagy levels on a per cell basis. We performed these experiments in the absence of CVB infection to define the effect of BPIFB3 silencing independent of viral infection**.** LC3 positive autophagosomes and p62 positive vesicles were quantified in HBMEC transfected with CONsi or BPIFB3si alone or in combination with ARFGAP1 and TMED9 siRNAs **(Figure 16B-D**). In agreement with our previous findings (1, 7), BPIFB3 depletion lead to an enhancement of LC3 positive puncta, which corresponds to the increase in lipidated LC3 observed by western blot. Silencing of ARFGAP1 and TMED9 alone had no impact on the number of LC3 positive autophagosomes when compared to control cells (CONsi). In contrast, co-depletion of ARFGAP1 or TMED9 with BPIFB3 inhibited the induction of autophagy induced by BPIFB3si alone (**Figures 16B-D**). Despite the clear changes observed in LC3 levels, it did not correspond with

changes in the number of p62 positive puncta across any conditions, confirming our previously published data that BPIFB3 regulates a non-canonical form of autophagy and not macroautophagy (1, 7).

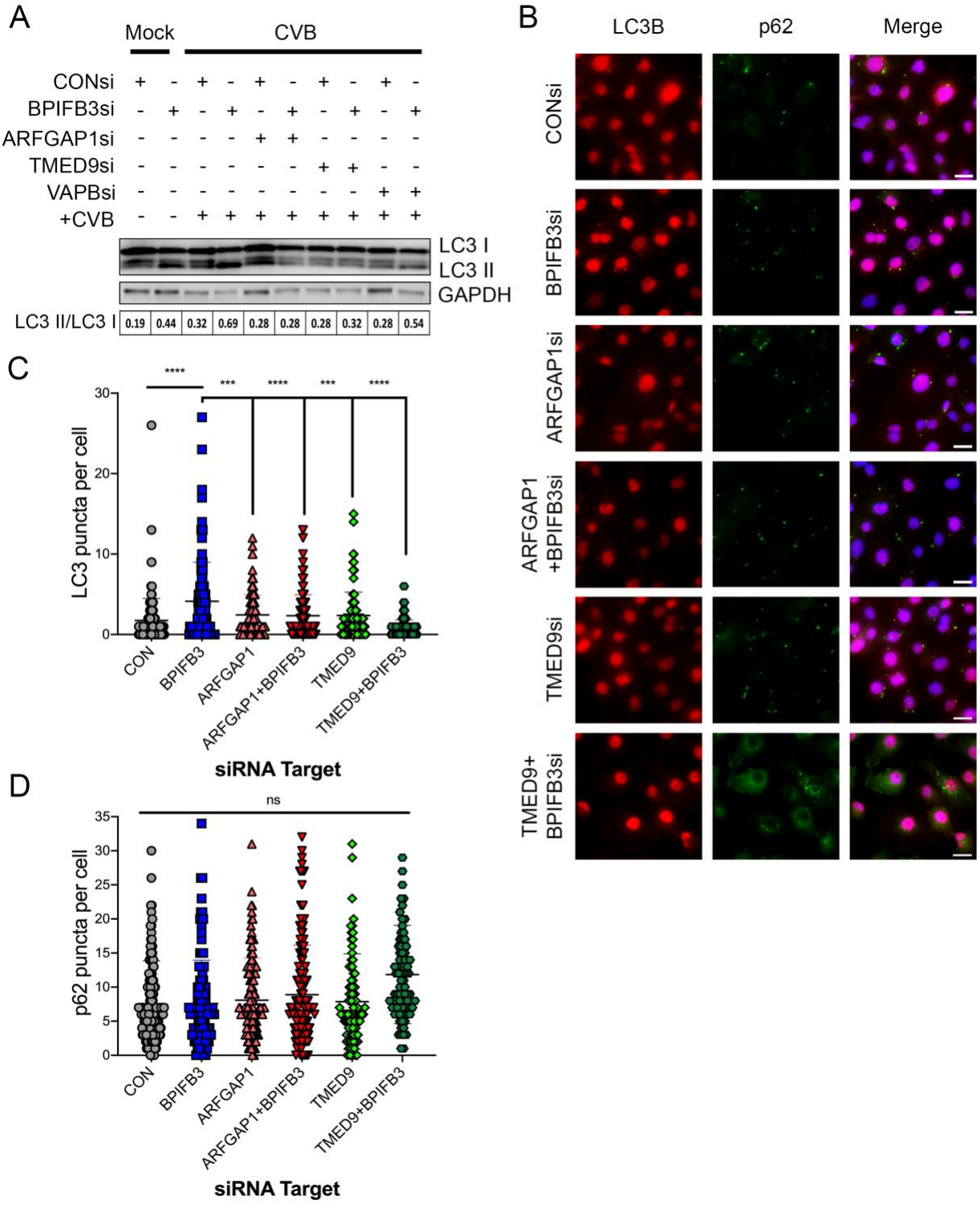

Figure 16 ARFGAP1 and TMED9 are required for BPIFB3si induced autophagy

(A) Western blot for LC3 protein levels from HBMEC transfected with BPIFB3si alone or in combination with ARFGAP1si, TMED9si, or VAPBsi. HBMEC were infected with CVB to exacerbate the effects of BPIFB3si induced autophagy and delineate changes in LC3 protein expression. The ratio of LC3 II/LC3 I shown in the table below, indicates the level of autophagy. **(B)** HBMECs depleted of BPIFB3 alone or in combination with ARFGAP1 or TMED9 were analyzed for level of autophagy by immunofluorescence imaging ot LC3 (red) and p62 (green). Scale bars are 25 μm. Quantification of LC3 and p62 puncta are shown in **(C and D)**. Data were analyzed using a one-way ANOVA, *** P <0.001, **** P < 0.0001.

To further define the impact of ARFGAP1 and TMED9 silencing on BPIFB3-associated autophagy, we performed transmission electron microscopy (TEM). Consistent with our previous work, BPIFB3 depletion increased the number of autophagy-associated vesicles (e.g. double membrane vesicles, amphisomes, and lysosomes) compared to control cells, which was reversed by co-depletion of either ARFGAP1 or TMED9 (**Figure 17A-B**). Depletion of ARFGAP1 alone lead to an increase in the number amphisomes present, indicative of the role that ARFGAP1 plays in both COPI and endocytic vesicle trafficking (180, 184), however there was no observable impact on autophagy levels (**Figure 17B**). The co-depletion of ARFGAP1 with BPIFB3 showed a similar phenotype, with fewer autophagy associated vesicles than BPIFB3si alone (quantified in **Figure 17B**). Additionally, we also observed an increase in the presence of ER membranes throughout the cytoplasm during co-depletion of ARFGAP1 and BPIFB3 that was not apparent in the individual knockdowns. This phenotype shows interesting parallels to the effects of BPIFB3 silencing on ER morphology that we previously showed was rescued by the depletion of the reticulophagy receptor RETREG1 (7). The depletion of TMED9 alone showed no significant effect on the formation of autophagy-associated vesicles but did show modest evidence of changes in ER morphology, with less continuous ER sheet-like membranes (**Figure 17A**). This is likely associated with the role TMED9 (also referred to $p24\alpha_2$) plays in ER exit site formation (185). In

agreement with LC3 immunoblots and immunofluorescence, the co-depletion of TMED9 with BPIFB3 significantly reversed the increase in autophagy observed during BPIFB3 depletion alone (**Figure 17B**). Furthermore, we previously published that the depletion of BPIFB3 directly impacts ER morphology (7), and the TEM data presented here demonstrates not only that co-depletion of ARFGAP1 or TMED9 with BPIFB3 reverses the BPIFB3si-enhanced autophagy, but also further impacts ER morphology during BPIFB3 depletion.

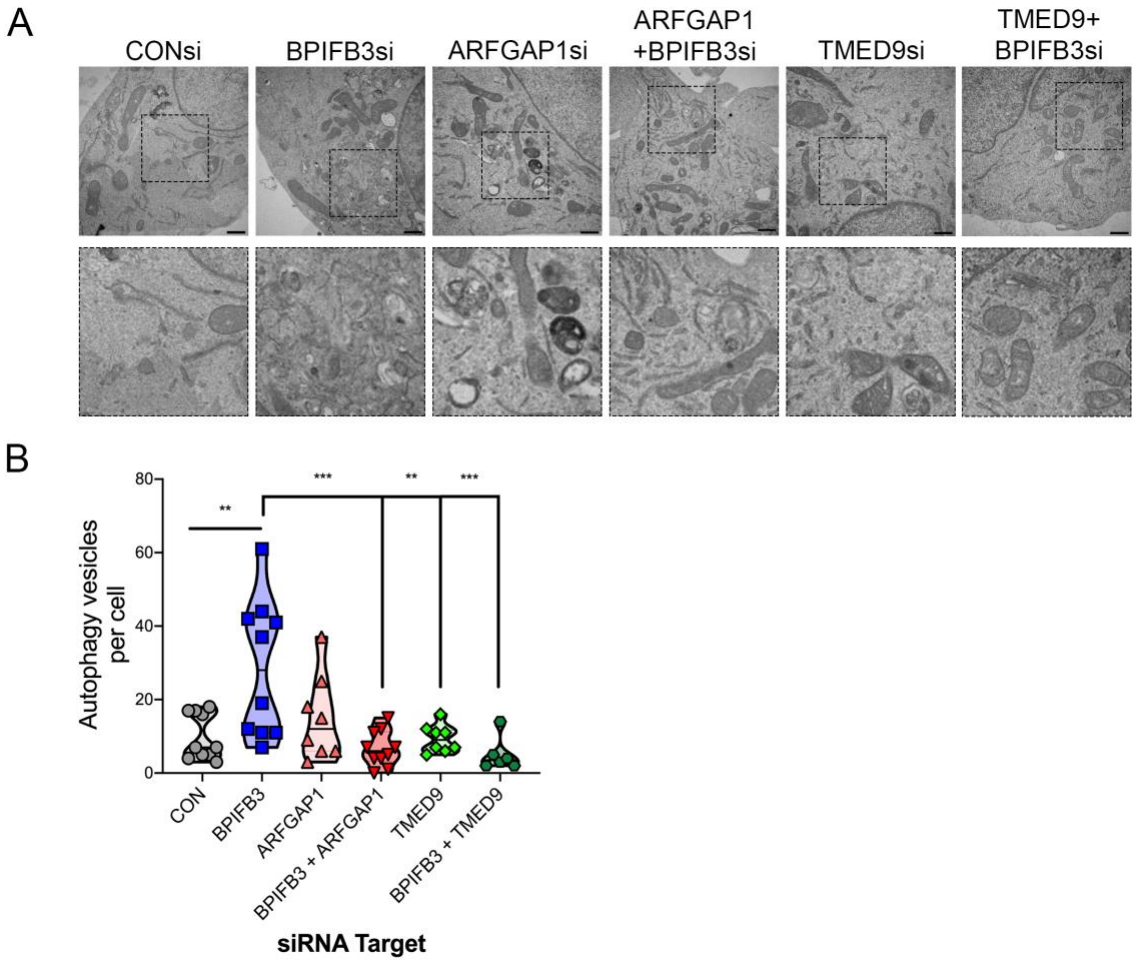

Figure 17 ARFGAP1 and TMED9 depletion reverse BPIFB3si morphology

(A) Transmission electron microscopy of HBMEC transfected with BPIFB3si alone or in combination with the BioID hits, ARFGAP1 and TMED9. Top row depicts large sections of the cytosol with dashed box around the zoomed in region shown in the bottom panel. Scale bars are 800 nm. **(B)** The number of autophagy-associated vesicles (e.g. double membrane vesicles, amphisomes, and lysosomes) were quantified per cell to determine if ARFGAP1 and TMED9 reversed the enhancement in non-canonical autophagy observed by BPIFB3 depletion. Data were analyzed using a one-way ANOVA, ** $P < 0.01$, *** $P < 0.001$.

3.2.4 Characterization of autophagy organelle markers during BPIFB3 depletion

Given that our characterization of key autophagy regulators on BPIFB3si induced autophagy showed no impact on the effects of autophagy induction (**Figure 12**), we performed immunofluorescence imaging of key organelle markers during the co-depletion of BPIFB3 with ARFGAP1 or TMED9. First, we examined lysosomal morphology by immunofluorescence microscopy of the late endosome/ lysosome marker LAMP1 (**Figure 18A**). In addition, samples were co-immunostained with the macroautophagy marker p62 to confirm that the increase in autophagy associated vesicles observed by TEM were not consistent with the macroautophagy pathway. In agreement with previous findings (1, 7) and our TEM data (**Figure 17**), BPIFB3 depletion increased the number of lysosomes, but not p62 positive vesicles (**Figure 18A**) . Intriguingly, depletion of ARFGAP1 and TMED9 independently also increased the numbers of LAMP1 positive late endosomes/ lysosomes, which may correspond to the increased number of amphisomes observed by TEM. Despite this observable increase in LAMP1 vesicles during independent knockdown of each factor, the co-depletion of ARFGAP1 or TMED9 with BPIFB3 resulted in a reduction in the number of LAMP1 lysosomes compared to each of the single siRNA knockdowns (**Figure 18A**). These data confirm our TEM results that the co-depletion of ARFGAP1 and TMED9 with BPIFB3 reduces the number of autophagy associated vesicles beyond the autophagosome marker LC3 alone.

We also examined the morphology of ER exit sites during BPIFB3 depletion alone or with ARFGAP1 and TMED9. ARFGAP1 is a well-known regulator of COPI vesicle trafficking, while TMED9 has also been suggested to impact COPI trafficking (178, 180, 185). However, our previous studies determined that BPIFB3 depletion has no effect on COPI morphology (2). Despite its known role in COPI trafficking, early reports of TMED9 function suggest a role in ER exit site

formation and morphology (185). Therefore, we aimed to determine if the BPIFB3-ARFGAP1/TMED9 axis had a role in maintaining ER exit site morphology. We also sought to determine if ER exit sites served as sites of BPIFB3si-induced autophagosome formation. Immunofluorescence imaging of Sec31A, a component of the COPII coat complex, and LC3B during BPIFB3 depletion alone or with ARFGAP1 and TMED9 (**Figure 18B**), demonstrated no clear association between LC3 puncta and ER exit sites. Despite this, we observed morphological changes of Sec31A during ARFGAP1 and TMED9 depletion (**Figure 18B**). Quantification of Sec31A staining revealed a reduction in the total Sec31A area during ARFGAP1 and TMED9 depletion (**Figure 18C**). This reduction of ER exit site area was maintained during the co-depletion of ARFGAP1 and TMED9 with BPIFB3 but was not seen during BPIFB3 silencing alone. This suggests that ARFGAP1 and TMED9's known role in COPI trafficking may extend to the regulation of ER exit site morphology. While there is no evidence of direct association between ER exit sites and BPIFB3si induced autophagy, these changes observed in ER exit site morphology might have downstream implications for the impact on vesicle trafficking and may explain the reversal autophagy that occurs.

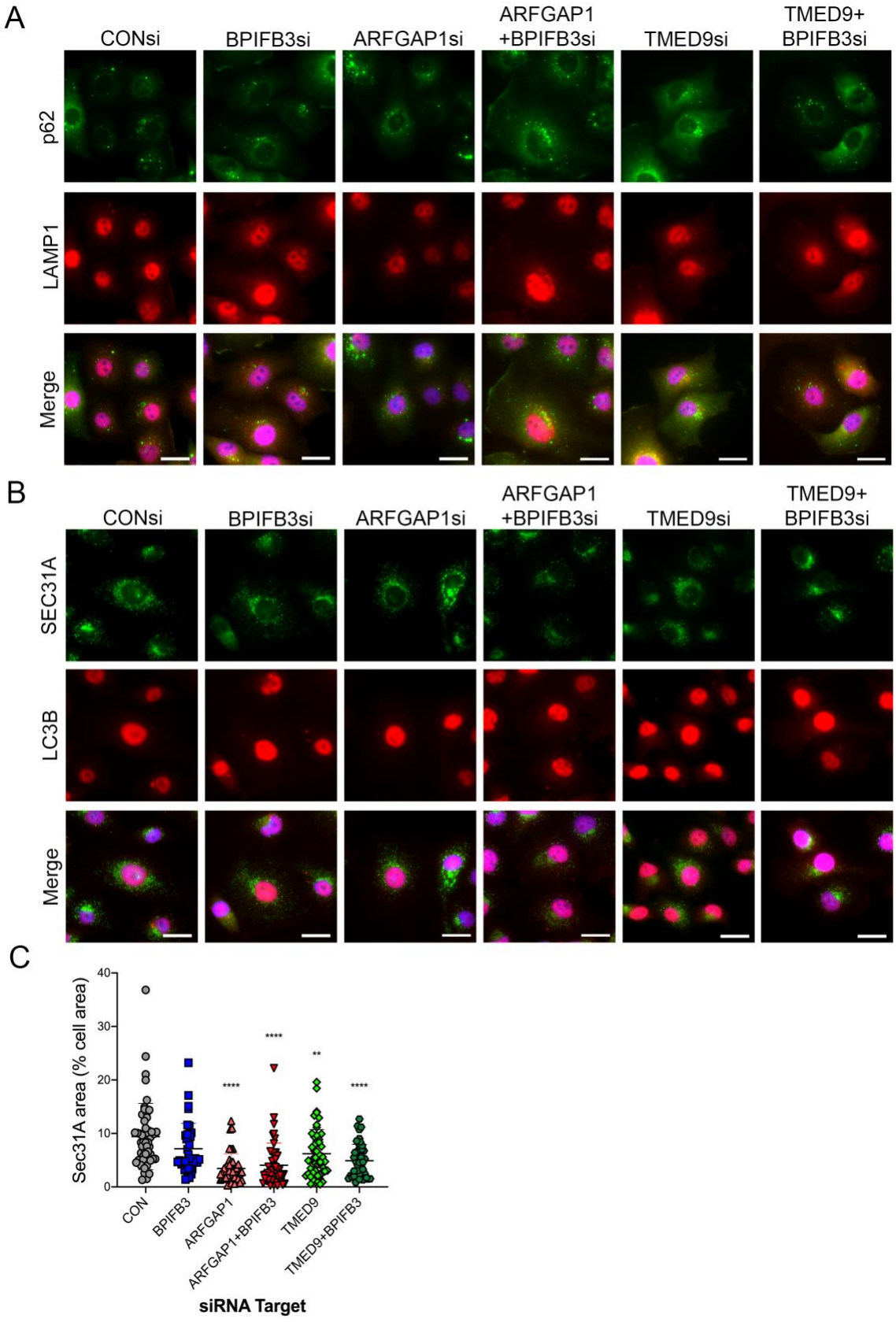
A
CONsi
BPIFB3si
ARFGAP1si
ARFGAP1 +BPIFB3si
TMED9si
TMED9+ BPIFB3si
p62
LAMP1
Merge
B
CONsi
BPIFB3si
ARFGAP1si
ARFGAP1 +BPIFB3si
TMED9si
TMED9+ BPIFB3si
SEC31A
LC3B
Merge
C
Sec31A area (% cell area)
40
30
20
10
0
****
****
**
****
CON
BPIFB3
ARFGAP1
ARFGAP1+BPIFB3
TMED9
TMED9+BPIFB3
siRNA Target

Figure 18 Characterization of autophagy related organelle markers during the co-depletion of BPIFB3 and ARFGAP1 or TMED9

(A) HBMEC transfected with each indicated combination of siRNAs were fixed and stained with antibodies to the macroautophagy receptor p62 and the late endosome/ lysosome marker LAMP1. **(B)** HBMEC transfected with BPIFB3si alone or in combination with ARFGAP1 or TMED9 were fixed and stained for the COPII vesicle coat component, Sec31A, and the autophagy marker, LC3B. Scale bars are 25 μm. **(C)** Quantification of Sec31A positive signal as percent of total cell area by siRNA knockdown conditions. Data were analyzed using a one-way ANOVA of each siRNA condition compared to control (CON), ** P <0.01, *** P < 0.001, **** P < 0.0001.

To further characterize the role of ARFGAP1 and TMED9 during BPIFB3 knockdown, we ectopically expressed GFP-tagged ARFGAP1 or TMED9 in control or BPIFB3 depleted cells. Expression of ARFGAP1 during BPIFB3si conditions showed no changes of localization or morphology (**Figure 19A**). However, the expression of TMED9 during BPIFB3 depletion showed slight changes in distribution of its reticular pattern paired with increased co-localization with ER exit sites marked by Sec31A (**Figure 19B**). Taken together, these data indicate clear alterations in the COPI and COPII trafficking pathways during BPIFB3 depletion that is dependent on the presence of TMED9.

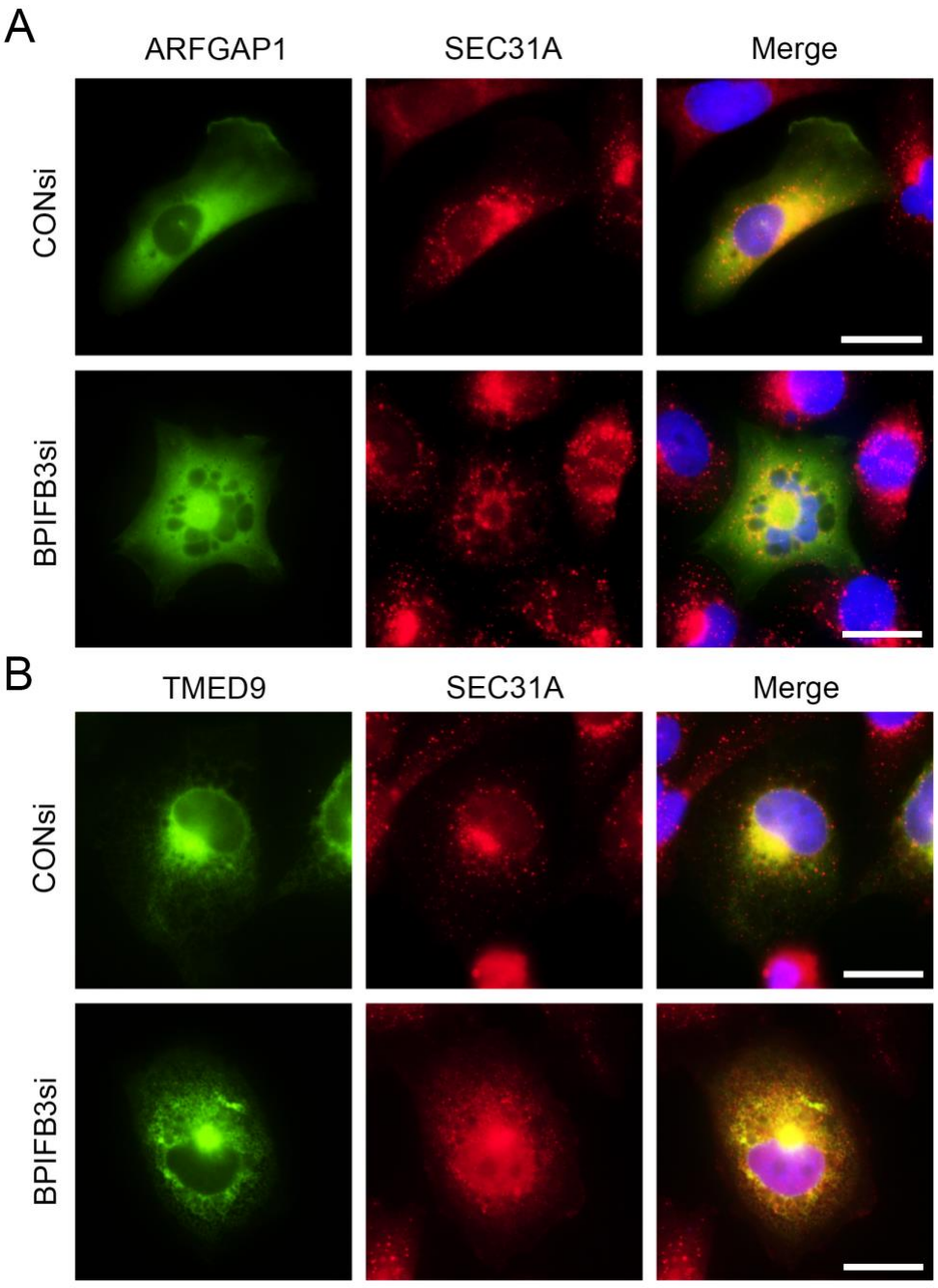

Figure 19 TMED9 expression effects ER exit site morphology during BPIFB3 depletion

CONsi or BPIFB3si HBMEC were transfected with ARFGAP1-GFP **(A)** or TMED9-GFP **(B)** and stained for the Sec31A. Scale bars are 25μm.

3.2.5 ARFGAP1 and TMED9 are required for BPIFB3si modulation of RNA virus infection

Because we found that co-depletion of ARFGAP1 and TMED9 both reversed the effects of BPIFB3si-mediated autophagy, we next determined whether they were required for BPIFB3-mediated regulation of RNA virus infection Analysis of CVB (**Figure 20A**) and DENV (**Figure 20B**) infection upon depletion of ARFGAP1 or TMED9 had no effect on viral replication, whereas co-depletion with BPIFB3 demonstrated a reversal of the effects of BPIFB3 silencing alone. The knockdown efficiency of siRNAs targeting ARFGAP1 and TMED9 was confirmed by RT-qPCR (**Figure 21**). These data are in contrast to our findings with canonical regulators of autophagy (**Figure 12**). Given that ARFGAP1 and TMED9 reverse the phenotypes associated with each virus, confirms our findings that the effects of BPIFB3si are fully reversed.

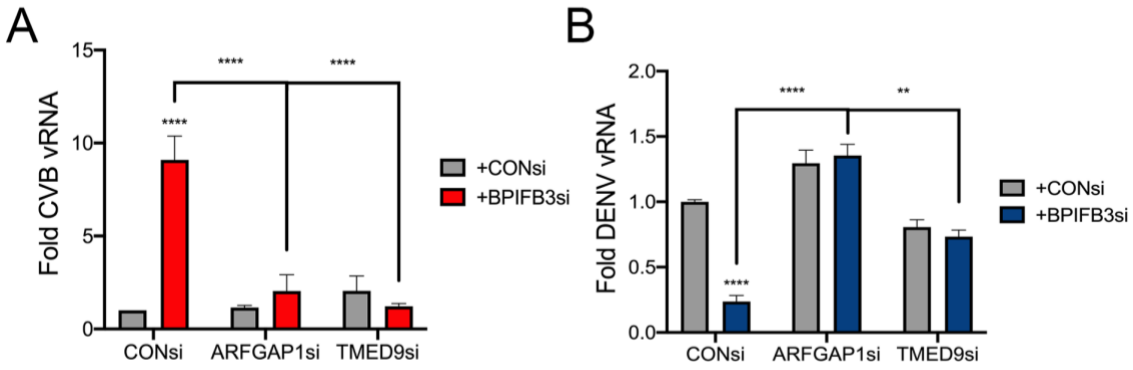

Figure 20 ARFGAP1 and TMED9 reverse the effects of BPIFB3 depletion on viral infection

HBMEC transfected with CONsi or BPIFB3si alone or in combination of ARFGAP1 and TMED9 were infected with CVB **(A)** or DENV **(B)** at a MOI of 1 and analyzed for level of infection by qPCR. Data were analyzed using a two-way ANOVA, ** $P < 0.01$, **** $P < 0.0001$.

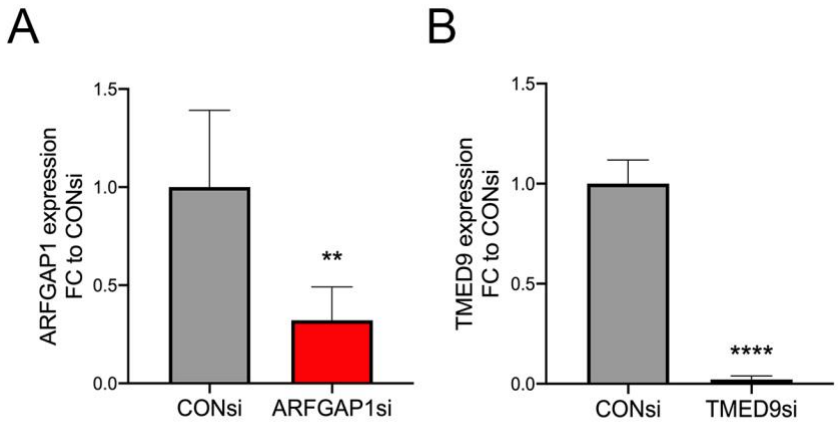

Figure 21 siRNA knockdown efficiency and ARFGAP1 and TMED9

The knockdown efficiency for siRNAs targeting **(A)** ARFGAP1, and **(B)** TMED9 was determined by qPCR for target mRNA and expressed as fold change to control siRNA transfected cells (CONsi). Data were analyzed using an unpaired t test, ** $P < 0.01$, **** $P < 0.0001$.

3.3 Discussion

Here, we define the cellular factors that regulate a noncanonical form of autophagy that occurs in the absence of BPIFB3 expression and which is important for RNA virus replication. The characterization of autophagy pathways in mammalian cells is made more complex than the study of parallel pathways in yeast due to significantly increased variability in the signals that control autophagosome biogenesis, the diversity of membranes used for autophagosome formation, and the increased expansion of the ATG8 protein family (61). This complexity is further complicated by the collection of autophagy pathways in mammalian cells that serve unique functions, such as organelle specific pathways. Traditionally, macroautophagy functions in

response to nutrient stress, specifically amino acid starvation. However, new evidence suggests that changes in lipid content and signals independent from the PI3K complex can play an important role in driving different forms of autophagy (132, 186, 187). The ER localized protein BPIFB3 as a negative regulator of a non-canonical autophagy pathway (1, 7). While our prior work characterized the induction of autophagy observed during BPIFB3 depletion and eluded to a non-canonical pathway, here we focused on defining the factors required for the induction of BPIFB3-regulated autophagy. The work presented here, demonstrates that many of the regulatory components involved in controlling canonical autophagy are not essential to the form of autophagy induced by decreased BPIFB3 expression. Instead, we show that two host cell factors, ARFGAP1 and TMED9, are required for BPIFB3 induced autophagy, and loss of expression is sufficient to negate the induction of autophagy. We further conclude that ARFGAP1 and TMED9 are required for the effects of BPIFB3 depletion on both CVB and DENV replication. These findings indicate that the enhancement observed in CVB replication is due to the increase in autophagosomes and endosomes within the cytoplasm that occurs during BPIFB3 silencing, which may directly enhance viral replication due to more available membranes for viral RO formation. In contrast, the inhibition of DENV replication that occurs during BPIFB3 silencing, is a result of a disruption in ER integrity and enhanced ER turnover (7). Given that these effects are linked to changes in two distinct organelle compartments, our findings support that both ARFGAP1 and TMED9 play essential roles in BPIFB3 function.

BPIFB3 belongs to the BPIFB family of proteins named for their homology to BPI, a secreted antimicrobial protein that functions by binding bacterial lipopolysaccharide (3, 5, 46). Despite the high degree of predicted structural homology, BPIFB3 and other ER localized members of the family, BPIFB2 and BPIFB6, are not secreted and remain associated with the ER

(1, 2). Furthermore, BPIFB proteins are predicted to have a high degree of structural homology to lipid transfer proteins, such as cholesterylester transfer protein (CETP). We previously confirmed that BPIFB3 binds lipids, but have not found direct evidence that it is involved in lipid transfer between membranes like other lipid transfer proteins (2). Despite this, our prior studies have determined that both BPIFB3 and BPIFB6 play important roles in vesicle trafficking, with BPIFB3 impacting autophagy and BPIFB6 disrupting secretory pathway trafficking (1, 2). Recent evidence has demonstrated that the glycolipid transfer protein (GLTP), ceramide-1-phosphate transfer protein (CPTP), plays an essential role in regulating the balance of autophagy induction and apoptosis via direct regulation of Golgi lipid content (186). This mechanism, in agreement with other studies, more broadly implies that the regulation of membrane lipid content alone can directly impact the induction of autophagy or other membrane trafficking events (132, 188). This insight might offer an explanation for how BPIFB3 regulates autophagy independent of each canonical autophagy protein we have tested, and further define how membrane lipid content can directly impact vesicle trafficking events. Beyond the impact of cellular trafficking events, it has been clearly demonstrated that distinct RNA virus families require specific lipid content at sites of RO formation and that virus replication often requires a remodeling of cellular lipids (131, 189–192). Taken together with the role of lipid transfer proteins in autophagy induction, this suggests a mechanism by which lipid trafficking pathways can directly promote or restrict viral replication.

Given that ARFGAP1 and TMED9 are required for BPIFB3 regulated autophagy and their deletion is sufficient to disrupt this pathway, it is necessary to consider what role these proteins have in the regulation of non-canonical autophagy. ARFGAP1 and TMED9 are both important secretory pathway proteins and have been implicated in the regulation of retrograde COPI vesicle formation (179, 180). ARFGAP1 functions as a key GTPase for the well-known secretory pathway

GTP binding protein, ARF1. ARFGAP1 has been demonstrated to have important activity in both regulating COPI vesicle formation as well as vesicle coat disassembly (180). However, outside of COPI vesicle trafficking, ARFGAP1 has been demonstrated to play a key role in regulating clathrin adapter protein-2 (clathrin-AP-2) endocytosis where it is suggested to function in a similar mechanism to its role in COPI trafficking (184), and regulate membrane curvature through its lipid packing sensor (193, 194). In contrast to ARFGAP1's clearly defined role in vesicle trafficking, TMED9 belongs to the p24 family of proteins which have been broadly implicated in secretory pathway trafficking and COPI vesicle formation, however these processes have not been directly linked to TMED9 (178). Beyond their role in COPI trafficking, there is evidence that both ARFGAP1 and TMED9 effect ER exit sites morphology (180, 185), which may be directly tied to their association with BPIFB3 autophagy induction. Many questions remain unanswered, including whether the implicated function of ARFGAP1 and TMED9 within COPI trafficking is related to the role they serve here during BPIFB3si induced autophagy. Our prior studies have shown that loss of BPIFB3 expression has no impact on the localization or morphology of COPI vesicles (2), and the only apparent change we observe are an enhancement of autophagy and disruption of ER integrity (1, 7). The data presented here suggest a role for TMED9 in regulating ER exit site morphology during BPIFB3 silencing, however this is not the case upon TMED9 depletion alone, or for ARFGAP1 silencing.

Considering the predicted role of BPIFB3 as a lipid transfer protein, perhaps BPIFB3 functions in lipid trafficking between the ER and Golgi, with ARFGAP1 and TMED9 serving as key regulators of this pathway. In this scenario, we predict depletion of BPIFB3 disrupts the trafficking of lipids, resulting in enhanced autophagy and increased vesicle trafficking out of the ER and directly impacting the replication of RNA viruses that rely on ER derived membranes.

While this hypothesis might provide some insight into the function of BPIFB3 and an explanation as to why canonical autophagy regulators are unable to reverse this phenotype, testing this is not trivial. Expression of BPIFB proteins is extremely low and we have yet to be able to detect endogenous BPIFB3 protein to date. Therefore, we have relied on RNAi mediated silencing and ectopic expression of BPIFB3 to study its function. Our results presented here, provide further insight into the requirements for BPIFB3 mediated autophagy and clearly demonstrate ARFGAP1 and TMED9 interact with BPIFB3 to facilitate this pathway.

4.0 Materials and Methods

4.1 Cells and viruses

Human brain microvascular endothelial cells (HBMEC) were maintained in RPMI 1640 supplemented with 10% fetal bovine serum (FBS), 10% NuSerum, 1x non-essential amino acids, 1x minimum essential medium vitamins, 1% sodium pyruvate, and 1% antibiotic. Human bone osteosarcoma U2OS (ATCC HTB-96), HEK 293T, and Vero (ATCC CCL-81) cells were grown in DMEM with 10% FBS and 1% antibiotic. Development of DENV replicon HBMECs using constructs provided by Theodore Pierson (NIH/NIAID) was described previously (165). *Aedes albopictus* midgut C6/36 cells were cultured in DMEM supplemented with 10% FBS and 1% antibiotic at 28°C in a 5% CO_2 atmosphere. Cell viability was assessed by trypan-blue staining at a 1:1 ratio and analyzed on a Bio-Rad TC20 Automated Cell Counter.

DENV2 16881 and ZIKV Paraiba/2015 (provided by David Watkins, University of Miami) were propagated in C6/36 or Vero cells, respectively (166). Titers were determined by fluorescent focus assay as previously described, using recombinant anti-double-stranded RNA monoclonal antibody (provided by Abraham Brass, University of Massachusetts) (167). Propagation and titration of CVB3 (RD) has been described previously (168). All experiments measuring infection levels were performed using a multiplicity of infection (MOI) of 1 for 16 hours (CVB) or 48 hours (DENV and ZIKV) unless stated otherwise, and infection was quantified by RT-qPCR or fluorescent focus assay.

4.2 siRNAs, plasmids and transfections

Characterization of siRNAs targeting BPIFB3, BPIFB2, BPIFB6, and RETREG1 (FAM134B) have been described previously (1, 146). siRNAs targeting RTN3 or Sec62 were purchased from Sigma and the sequences are, RTN3: CCACUCAGUCCCAUUCCAUtt, and Sec62: GAAGGAUGAGAAAUCUGAAtt. ON-TARGETplus SMARTpool siRNAs targeting ARFGAP1 and TMED9 were purchased from Dharmacon. Sequences for pooled siRNAs are as follows: ARFGAP1 (GAGAGGAGGAGCUCGGACA, CAGGAUGAGAACAACGUUU, GCCACAGCCUGAACGAGAA, CGUCCAUGGUGCACCGAGU), TMED9 (GGACGCAGCUGUAUGACAA, CGGGCUGGGUAGAGUGAUG, AGUGCUUUAUUGAGGAGAU, ACAUCGGAGAGACGGAGAA). Efficiency of knockdown was determined by RT-qPCR for each siRNA target. siRNAs were reverse transfected at 25 nM in to HBMEC using Dharmafect 1, and cells were either infected or RNA was collected 48 hrs post transfection.

Development of GFP tagged RETREG1 and RETREG1mutLIR have been described elsewhere (146). Development of GFP tagged ARFGAP1 and TMED9 was accomplished according to the manufacturers protocol using the CT-GFP Fusion TOPO™ Expression Kit purchased from ThermoFisher Scientific. VAPB-eGFP was a gift from Dr. Gerry Hammond (University of Pittsburgh). Plasmids were transfected into U2OS and 293T cells using X-tremeGENE™ 9 DNA Transfection Reagent (Sigma) or HBMEC cells using Lipofectamine 3000 (ThermoFisher) according to the manufacturers protocols and fixed for fluorescence microscopy or lysed for immunoprecipitation 48 hrs post transfection.

4.3 RNA extraction, cDNA synthesis, and RT-qPCR

RNA was isolated using the GenElute Total RNA MiniPrep kit from Sigma according to the kit protocol. RNA was reverse transcribed using the iScript cDNA Synthesis kit (Bio-Rad) with 1μg of RNA per sample. RT-qPCR was performed using IQ SYBR green SuperMix (Bio-Rad) in a Bio-Rad CFX96 Touch real-time PCR detection system. A modified threshold cycle (ΔCT) method was used to calculate gene expression using human actin for normalization. Primer sequences for actin, DENV, ZIKV, CVB, BPIFB3, and RETREG1 have been described previously (146, 169). Predesigned KiCqstart qPCR primers for ARFGAP1 (H_ARFGAP1_1) and TMED9 (H_TMED9_1) were purchased from Sigma.

4.4 Virus binding assay

HBMEC were transfected with the indicated siRNA. Approximately 48h post-transfection, cells were washed with PBS and ZIKV (MOI=10) was adsorbed for 1h at 16°C. Following adsorption, cells were washed extensively with PBS and directly lysed for RNA extraction (termed mock) or incubated with Trypsin (3 min), washed with PBS, and lysed for RNA extraction (termed + Trypsin). Following RNA extraction, cDNA synthesis, and qPCR, the data was analyzed using the ΔΔCT method and normalized to mock CONsi.

4.5 RNAseq

Total RNA was isolated as described above, and RNA sequencing was performed as previously described (157). Analysis of RNAseq data sets was performed using CLC Genomics 11 (Qiagen) to process and map sequences to the human genome (hg19) or the appropriate viral genome to calculate viral fragments per kilobase of transcript per million mapped reads (FPKM) values. Differentially expressed genes were identified using the DeSeq2 package in R with a significance cutoff of 0.001 and a fold change cutoff of two (170). Gene set enrichment analysis (GSEA) and manual sorting were used to identify pathways or specific transcripts differentially regulated. Generation of heat maps was done using MeViewer software based on ln(RPKM) values. RNA sequencing files have been deposited to NCBI Sequence Read Archive (SRA) and can be located under the accession number PRJNA606334.

4.6 Antibodies

Mouse monoclonal anti-V5 epitope tag was purchased from Invitrogen (R960-25). Rabbit polyclonal antibody against CKAP4 (16686-1-AP) was purchased from ProteinTech. Rabbit polyclonal antibodies to DENV NS3 (GTX124252) and ZIKV NS4B (GTX133311) were purchased from GeneTex. Recombinant mouse monoclonal anti-dsRNA was provided by Abraham Brass (University of Massachusetts). Rabbit anti-LC3B (ab48394) and mouse anti-p62 (ab56416) were purchased from Abcam. Mouse monoclonal antibody against LAMP1 (H4A3) and rabbit monoclonal antibody against GAPDH (FL-335) were purchased from Santa Cruz

Biotechnology. Mouse monoclonal Sec31A (612350) antibody was purchased from BD Biosciences and Alexa Fluor conjugated secondary antibodies were purchased from Invitrogen.

4.7 Immunofluorescence and electron microscopy

Immunofluorescence microscopy was performed on cells grown in 8-well chamber slides (Millipore Sigma), fixed in 4% paraformaldehyde, and permeabilized with 0.1% Triton. In some cases, cells were fixed in ice cold methanol. Primary antibodies were incubated in PBS with cells for 1 hr, followed by staining with Alexa Fluor conjugated secondary antibodies for 30 min. Slides were mounted with coverslips using VectaShield containing 40-6-diamino-2-phenylindole (DAPI). Imaging was performed on an Olympus IX83 inverted microscope or a Zeiss LSM 710 confocal microscope where specified. All image quantification was performed using ImageJ/FIJI. Pixel intensity measurements were performed using isolated channels on individual cells with the region of interest (ROI) manager. Data are presented as mean pixel intensity, normalized to cell area. Quantification of fluorescent puncta was performed manually. Preparation of samples for TEM were done as previously described, by the Center for Biologic Imaging (University of Pittsburgh) (169). Imaging was performed on a JEOL 1011 transmission electron microscope. Quantification of TEM images was performed manually.

4.8 BioID2 assay

HBMEC were seeded in 2 10 cm dishes and transiently transfected with BPIFB3-BioID2 or MCS-BioID2. 24 hours post transfection, cells were rinsed with PBS and media was replaced containing 50 μM D-Biotin and incubated at 37 C for 24 hours. Media was removed and washed twice with PBS. Cells were lysed using 1X RIPA lysis buffer at pH 7.4 and incubated with monomeric Avidin resin overnight (~16 hours). Purification of biotinylated proteins was performed according to the previously described protocol (177). Purified protein extracts were submitted to MSBioworks for further purification and mass spectrometry analysis.

4.9 Statistical analyses

All analyses were performed using GraphPad Prism. Experiments were performed at least three times. Student's t test, 2way analysis of variance (ANOVA), or one-way ANOVA were used where indicated. Analysis of fluorescent microscopy data was done using a non-parametric Kruskal-Wallis test. Data are presented as mean ± standard deviation, with specific p-values detailed in the figure legends.

5.0 Discussion and model of BPIFB3 function

Mammalian BPIFB proteins are predicted lipid transport proteins within the larger BPI-like family (3). This protein family broadly includes important innate immune regulators, as well as factors that play essential roles in circulating lipid transport (44). In contrast to the extracellular function that has been attributed to other members of the BPI-like protein family, our work clearly defines an important function for BPIFB3 in intracellular trafficking of autophagy related vesicles (1, 7). Given that the effects on vesicle trafficking extends to BPIFB6 (2), it suggests that the BPIFB proteins may play an important role in controlling membrane lipid content as a means in regulating cellular trafficking events. In line with this predicted function, perhaps BPIFB proteins play an essential role in controlling the transport of specific lipids at membrane contact sites, and depletion of these proteins disrupts membrane lipid content. Given that vesicle trafficking is one of the primary means to transport lipids intracellularly, the increase in vesicle trafficking that occurs in response to BPIFB3 and BPIFB6 depletion could in fact be a cellular mechanism to try to compensate for the disruption in lipid homeostasis. Although the role in autophagy regulation is unique to BPIFB3 and not other members of the BPIFB protein family, we can extrapolate key conclusions from these studies to guide our understanding of the larger BPIFB family.

The relationship between lipid metabolism and autophagy has been well documented, as autophagy remains to be one of the primary mechanisms to mobilize lipids from adipocytes and degrade lipids from intracellular lipid droplets into their fatty acid components during increased energy demand (147, 195–197). However only recently has the relationship between membrane lipid content and autophagy began to be understood. It is well established that different membrane sources within the cell are composed of distinct lipids, for example the plasma membrane contains

a high percentage of cholesterol and sphingolipids, where the ER has a significantly smaller fraction of each. Likewise, the mitochondrial membrane has high levels of cardiolipin compared to other membranous organelles (198). However, the impact this lipid content has on downstream processes like cellular trafficking events has remained poorly understood. To address this phenomenon in the context of autophagy, one research group treated cells with individual saturated (SFA) or unsaturated fatty acids (UFA) (123). They found that treating cells with oleate and other UFAs distinctly caused an increase in non-canonical autophagy that functioned independent of canonical autophagy regulators such as ULK1, BECN1, and PI3KC3. They also found that this non-canonical autophagy pathway showed a specific dependence on Golgi membranes, that was not seen in canonical macroautophagy. In contrast, treating cells with SFA, led to an enhancement of canonical autophagy that was dependent on the macroautophagy regulator components (123). This has been the first and only report to distinctly associate specific lipid treatment to the induction of non-canonical autophagy. Intriguingly, the non-canonical pathway stimulated by UFA treatment has a number of similarities to BPIFB3 depletion-induced autophagy, which also functions independent of ULK1, BECN1, and PI3KC3.

A more recent study identified a novel lipid transfer protein that controls autophagy activation through its lipid transfer abilities. Ceramide-1-phosphate transfer protein (CPTP) depletion by RNAi led to the accumulation of ceramide-1-phosphate (C1P) in the Golgi where it is synthesized, resulting in increased autophagy levels (186). Both of these studies point to a new mechanism of autophagy control that draws similar parallels to what we know about BPIFB3. Depletion of BPIFB3 is able to induce autophagy, similar to CPTP silencing. However, unlike CPTP, BPIFB3 depletion specifically controls a non-canonical autophagy pathway that is similar to what was observed during UFA treatment. These studies combined with the results presented

here, suggest a mechanism where BPIFB3 is responsible for trafficking lipids between the ER and other organelles, perhaps at membrane contact sites. And the subsequent loss of BPIFB3 expression by RNAi disrupts membrane lipid content, perhaps increasing the proportion of UFA in Golgi membranes that is directly responsible for the enhanced level of non-canonical autophagy observed (**Figure 20**). Importantly, our prior characterization of BPIFB3's lipid binding ability did not show a strong preference for saturated versus unsaturated fatty acids (2). Therefore, the effects of BPIFB3 depletion may be attributed to the mis-trafficking of a specific lipid and not a broad disruption of multiple lipids, however this remains to be determined.

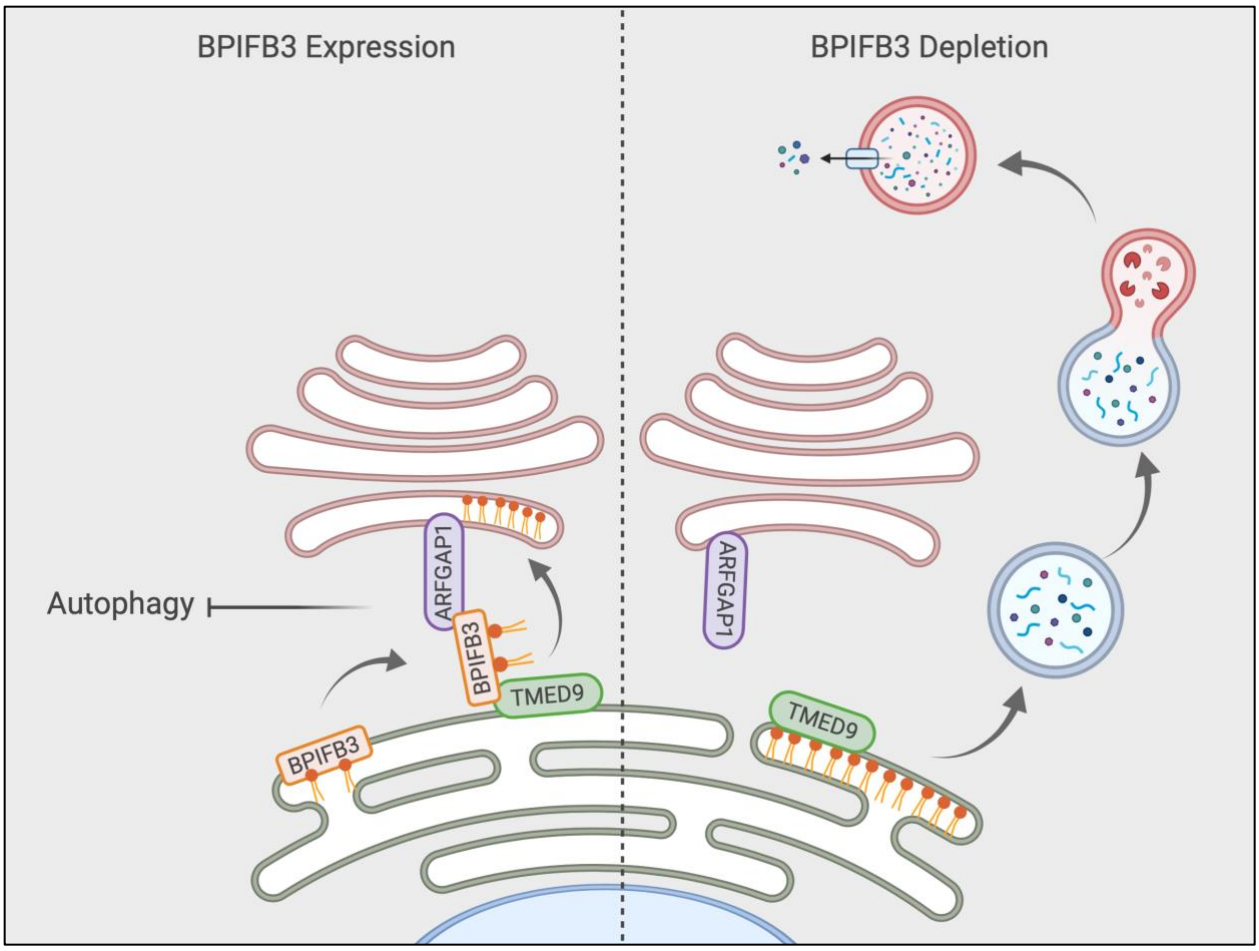

Figure 22 Proposed model of BPIFB3 function

Given that BPIFB3 is predicted to be a lipid transfer protein, we propose a model where BPIFB3 functions to traffic lipids from the ER, which is serves as a major site for cellular lipid synthesis, to the Golgi. We propose that ARFGAP1 and TMED9 serve as key regulators of this pathway based on their interaction with BPIFB3 and role in regulating BPIFB3 depletion dependant autophagy. When BPIFB3 expression is reduced, either by RNAi treatment or the undetermined cellular mechanisms used to regulate its expression, lipid trafficking is disrupted, which specifically increases the level of autophagy and vesicle trafficking out of the ER. Created with BioRender.com.

This possible model for BPIFB3 function would also provide additional insight into the requirement for membrane composition during positive strand RNA virus RO formation. As it has been well established that individual viruses have distinct preference for membrane lipid content

(22, 131, 191, 199). Perhaps the restriction of flavivirus infection and enhancement in CVB replication observed during BPIFB3 depletion is more complex than differences in the sensitivity to level of autophagy by each virus. Instead the distinction could also tied to the lipid preference of the virus. If this were the case, it would suggest that BPIFB3 depletion, alters the ER membrane composition to be unfavorable during flavivirus infection, and instead further enhances the lipid content preferred by CVB. This, however, does not change the requirement in expression observed for each virus, as the presence of BPIFB3 is still beneficial to flavivirus infection while it restricts CVB (**Figure 21**). Intriguingly, prior reports have demonstrated that there are unique differences between the lipid requirements for flavivirus and enterovirus ROs. Enteroviruses, like CVB specifically require PI(4)P and hijack this lipid homeostasis pathway to establish RO formation (22). While flavivirus RO formation appears to be largely independent of PI(4)P, but significantly more linked to cellular cholesterol homeostasis (131). This distinction might provide an important clue for the mechanism behind BPIFB3 regulation of both autophagy and positive strand RNA viral infection.

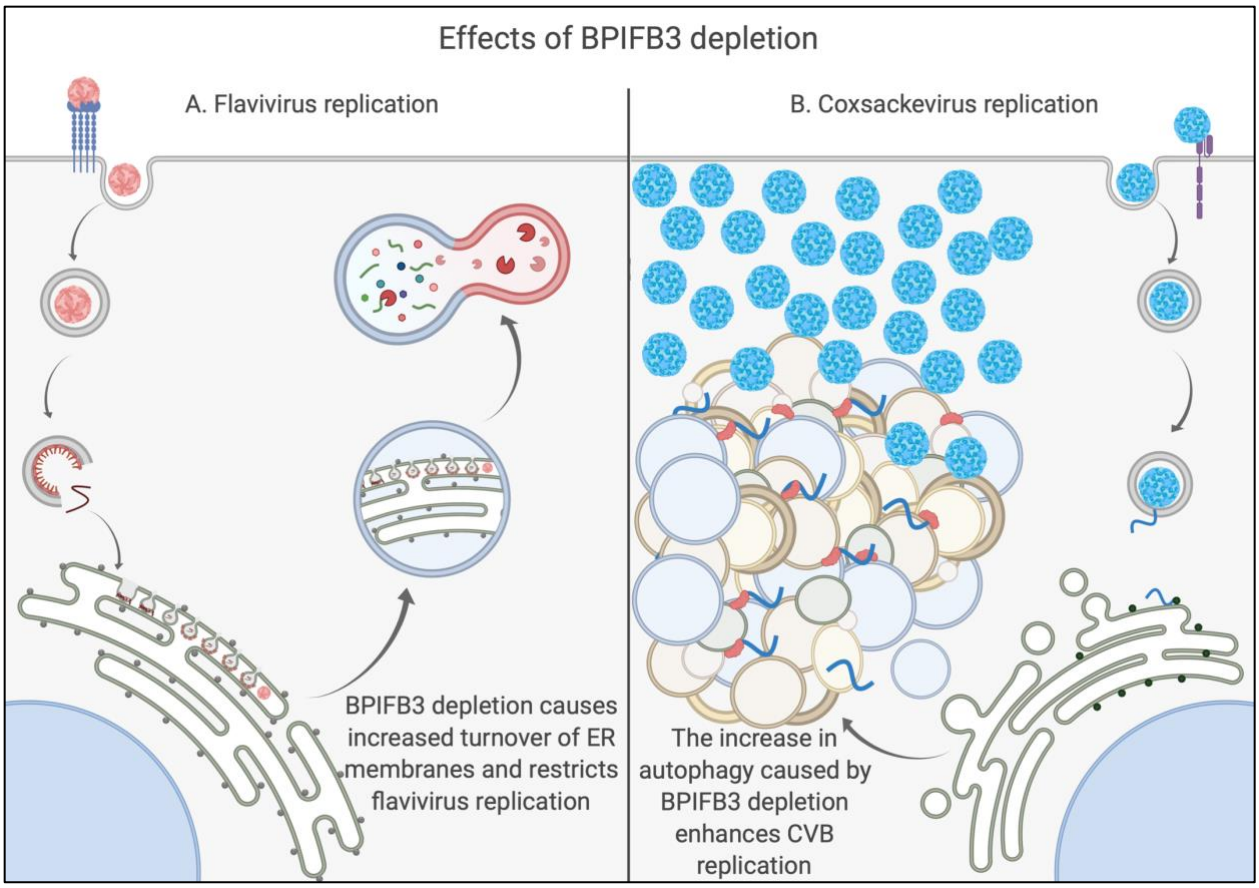

Figure 23 Effects of BPIFB3 depletion on flavivirus infection and CVB replication

(A) In cases of BPIFB3 depletion, flaviviruses bind their cognate receptor and are internalized into the cell. However the increase in ER turnover that occurs in response to reduced BPIFB3 expression prevents flaviviruses, including DENV and ZIKV, from forming replication organelles and initiating early stages of their lifecycle. **(B)** In contrast, CVB infection is enhanced due to the increase in autophagy that occurs during loss of BPIFB3 expression. This increase in autophagy allows CVB to ramp up viral replication as the increased number of autophagosomes and other cytoplasmic vesicles are used for the formation of additional CVB replication organelles. Created with BioRender.com.

Based on this potential cellular function of BPIFB3, future studies focused on characterizing the mechanism of action should investigate changes in membrane lipid composition in response to BPIFB3 depletion or expression. Furthermore, if we extrapolate this proposed

molecular function to other members of the BPIFB family, perhaps the reason why BPIFB6 depletion restricts CVB but has no significant impact on DENV infection is related to the reliance of CVB ROs on Golgi derived PI(4)P lipids. This is a logical hypothesis given that we have previously shown that BPIFB6 silencing disrupts Golgi morphology, a major source of PI(4)P for enterovirus RO formation. The role of BPIFB6 is further intriguing, because its depletion has no impact on DENV, but significantly restricts ZIKV replication. Perhaps this is due to distinct differences related to membrane lipid preference between these two viruses that remains to be characterized. This is further compelling, given the high degree of similarity between DENV and ZIKV RO morphology when observed by TEM.

While very little is known about other members of the BPIB protein family, it is feasible that they elicit similar cellular functions but regulate distinct lipid trafficking pathways. BPIFB2, is also an ER localized protein, but we have observed no distinct differences related to ER, autophagy, or Golgi morphology. In contrast, BPIFB4 localizes to the nucleus where it may function to regulate lipid trafficking with the nuclear envelop. The studies presented here are the first extensive characterization of a BPIFB protein and provide key observations that will be invaluable in guiding the future studies of proteins within the BPIFB family. Particularly due to the fact that the studies of BPIFB proteins by our research group are the first reports of intracellular activity for members of the BPI-like family.

Bibliography

1. Delorme-Axford E, Morosky S, Bomberger J, Stolz DB, Jackson WT, Coyne CB. 2014. BPIFB3 regulates autophagy and coxsackievirus B replication through a noncanonical pathway independent of the core initiation machinery. MBio 5:e02147.

2. Morosky S, Lennemann NJ, Coyne CB. 2016. BPIFB6 Regulates Secretory Pathway Trafficking and Enterovirus Replication 90:5098–5107.

3. Bingle CD, Craven CJ. 2002. PLUNC: a novel family of candidate host defence proteins expressed in the upper airways and nasopharynx. Hum Mol Genet 11:937–943.

4. Bingle L, Bingle CD. 2011. Distribution of human PLUNC/BPI fold-containing (BPIF) proteins. Biochem Soc Trans 39:1023–1027.

5. Bingle CD, LeClair EE, Havard S, Bingle L, Gillingham P, Craven CJ. 2004. Phylogenetic and evolutionary analysis of the PLUNC gene family. Protein Sci 13:422–30.

6. Musa M, Wilson K, Sun L, Mulay A, Bingle L, Marriott HM, LeClair EE, Bingle CD. 2012. Differential localisation of BPIFA1 (SPLUNC1) and BPIFB1 (LPLUNC1) in the nasal and oral cavities of mice. Cell Tissue Res 350:455–464.

7. Evans AS, Lennemann NJ, Coyne CB. 2020. BPIFB3 Regulates Endoplasmic Reticulum Morphology to Facillitate Flavivirus Replication. J Virol 94:1–13.

8. Evans AS, Lennemann NJ, Coyne CB. 2020. BPIFB3 interacts with ARFGAP1 and TMED9 to regulate non-canonical autophagy and RNA virus infection. bioRxiv 2020.07.16.207035.

9. N. H. Acheson. 2011. Fundamentals of Molecular Virology. Wiley.

10. Flint SJ, Racaniello VR, Rall GF, Skalka AM, Enquist LW. 2015. Principles of Virology. Wiley.

11. Sasvari Z, Nagy PD. 2010. Making of viral replication organelles by remodeling interior membranes. Viruses 2:2436–2442.

12. Hsu NY, Ilnytska O, Belov G, Santiana M, Chen YH, Takvorian PM, Pau C, van der Schaar H, Kaushik-Basu N, Balla T, Cameron CE, Ehrenfeld E, van Kuppeveld FJM, Altan-Bonnet N. 2010. Viral reorganization of the secretory pathway generates distinct organelles for RNA replication. Cell 141:799–811.

13. Paul D, Bartenschlager R. 2015. Flaviviridae Replication Organelles: Oh, What a Tangled Web We Weave. Annu Rev Virol 2:289–310.

14. Reid CR, Airo AM, Hobman TC. 2015. The virus-host interplay: Biogenesis of +RNA replication complexes. Viruses 7:4385–4413.

15. Welsch S, Miller S, Romero-Brey I, Merz A, Bleck CKE, Walther P, Fuller SD, Antony C, Krijnse-Locker J, Bartenschlager R. 2009. Composition and Three-Dimensional Architecture of the Dengue Virus Replication and Assembly Sites. Cell Host Microbe 5:365–375.

16. Cortese M, Goellner S, Acosta EG, Neufeldt CJ, Oleksiuk O, Lampe M, Haselmann U, Funaya C, Schieber N, Ronchi P, Schorb M, Pruunsild P, Schwab Y, Chatel-Chaix L, Ruggieri A, Bartenschlager R. 2017. Ultrastructural Characterization of Zika Virus Replication Factories. Cell Rep 18:2113–2123.

17. Corona AK, Saulsbery HM, Corona Velazquez AF, Jackson WT. 2018. Enteroviruses Remodel Autophagic Trafficking through Regulation of Host SNARE Proteins to Promote Virus Replication and Cell Exit. Cell Rep 22:3304–3314.

18. Lennemann NJ, Coyne CB. 2015. Catch Me If You Can: The Link between Autophagy and Viruses. PLoS Pathog 11:1–6.

19. Wells AI, Coyne CB. 2019. Enteroviruses: A gut-wrenching game of entry, detection, and evasion. Viruses 11:1–20.

20. Pons-Salort M, Parker EPK, Grassly NC. 2015. The epidemiology of non-polio enteroviruses: Recent advances and outstanding questions. Curr Opin Infect Dis 28:479–487.

21. Baggen J, Thibaut HJ, Strating JRPM, Van Kuppeveld FJM. 2018. The life cycle of non-polio enteroviruses and how to target it. Nat Rev Microbiol 16:368–381.

22. van der Schaar HM, Dorobantu CM, Albulescu L, Strating JRPM, van Kuppeveld FJM. 2016. Fat(al) attraction: Picornaviruses Usurp Lipid Transfer at Membrane Contact Sites to Create Replication Organelles. Trends Microbiol 24:535–546.

23. Wu H, Zhai X, Chen Y, Wang R, Lin L, Chen S, Wang T, Zhong X, Wu X, Wang Y, Zhang F, Zhao W, Zhong Z. 2016. Protein 2B of coxsackievirus B3 induces autophagy relying on its transmembrane hydrophobic sequences. Viruses 8:1–11.

24. Suhy DA, Giddings TH, Kirkegaard K. 2000. Remodeling the Endoplasmic Reticulum by Poliovirus Infection and by Individual Viral Proteins: an Autophagy-Like Origin for Virus-Induced Vesicles. J Virol 74:8953–8965.

25. Albulescu L, Bigay J, Biswas B, Weber-Boyvat M, Dorobantu CM, Delang L, van der Schaar HM, Jung YS, Neyts J, Olkkonen VM, van Kuppeveld FJM, Strating JRPM. 2017. Uncovering oxysterol-binding protein (OSBP) as a target of the anti-enteroviral compound TTP-8307. Antiviral Res 140:37–44.

26. Centers for Disease Control and Prevention, National Center for Emerging and Zoonotic

Infectious Diseases (NCEZID), Division of High-Consequence Pathogens and Pathology (DHCPP) VSPB (VSPB). 2013. Flaviviridae. Web Page.

27. Pierson TC, Diamond MS. 2020. The continued threat of emerging flaviviruses. Nat Microbiol 5:796–812.

28. Diamond MS, Pierson TC. 2015. Molecular Insight into Dengue Virus Pathogenesis and Its Implications for Disease Control. Cell 162:488–492.

29. Dejnirattisai W, Supasa P, Wongwiwat W, Rouvinski A, Barba-Spaeth G, Duangchinda T, Sakuntabhai A, Cao-Lormeau V-M, Malasit P, Rey FA, Mongkolsapaya J, Screaton GR. 2016. Dengue virus sero-cross-reactivity drives antibody-dependent enhancement of infection with zika virus. Nat Immunol 17:1102–1108.

30. Arora N, Sadovsky Y, Dermody TS, Coyne CB. 2017. Microbial Vertical Transmission during Human Pregnancy. Cell Host Microbe 21:561–567.

31. Zhang Q, Sun K, Chinazzi M, Pastore y Piontti A, Dean NE, Rojas DP, Merler S, Mistry D, Poletti P, Rossi L, Bray M, Halloran ME, Longini IM, Vespignani A. 2017. Spread of Zika virus in the Americas. Proc Natl Acad Sci 201620161.

32. Tang H, Hammack C, Ogden SC, Wen Z, Qian X, Li Y, Yao B, Shin J, Zhang F, Lee EM, Christian KM, Didier RA, Jin P, Song H, Ming GL. 2016. Zika virus infects human cortical neural progenitors and attenuates their growth. Cell Stem Cell 18:587–590.

33. Miner JJ, Sene A, Richner JM, Smith AM, Santeford A, Ban N, Weger-Lucarelli J, Manzella F, Rückert C, Govero J, Noguchi KK, Ebel GD, Diamond MS, Apte RS. 2016. Zika Virus Infection in Mice Causes Panuveitis with Shedding of Virus in Tears. Cell Rep 16:3208–3218.

34. Brasil P, Pereira JP, Moreira ME, Nogueira RMR, Damasceno L, Wakimoto M, Rabello RS, Valderramos SG, Halai UA, Salles TS, Zin AA, Horovitz D, Daltro P, Boechat M, Gabaglia CR, De Sequeira PC, Pilotto JH, Medialdea-Carrera R, Da Cunha DC, De Carvalho LMA, Pone M, Siqueira AM, Calvet GA, Baiao AER, Neves ES, De Carvalho PRN, Hasue RH, Marschik PB, Einspieler C, Janzen C, Cherry JD, De Filippis AMB, Nielsen-Saines K. 2016. Zika virus infection in pregnant women in rio de janeiro. N Engl J Med 375:2321–2334.

35. De Fatima Vasco Aragao M, Van Der Linden V, Brainer-Lima AM, Coeli RR, Rocha MA, Da Silva PS, Gomes MDC, De Carvalho, Van Der Linden A, De Holanda AC, Valenca MM. 2016. Clinical features and neuroimaging (CT and MRI) findings in presumed Zika virus related congenital infection and microcephaly: Retrospective case series study. BMJ 353:1–10.

36. Van Der Schaar HM, Rust MJ, Chen, Van Der Ende-Metselaar H, Wilschut J, Zhuang X, Smit JM. 2008. Dissecting the cell entry pathway of dengue virus by single-particle tracking in living cells. PLoS Pathog 4.

37. Panyasrivanit M, Khakpoor A, Wikan N, Smith DR. 2009. Linking dengue virus entry and translation/replication through amphisomes. Autophagy 5:434–435.

38. Peña J, Harris E. 2012. Early dengue virus protein synthesis induces extensive rearrangement of the endoplasmic reticulum independent of the UPR and SREBP-2 pathway. PLoS One 7:1–15.

39. Youn S, Li T, McCune BT, Edeling MA, Fremont DH, Cristea IM, Diamond MS. 2012. Evidence for a Genetic and Physical Interaction between Nonstructural Proteins NS1 and NS4B That Modulates Replication of West Nile Virus. J Virol 86:7360–7371.

40. Youn S, Ambrose RL, Mackenzie JM, Diamond MS. 2013. Non-structural protein-1 is required for West Nile virus replication complex formation and viral RNA synthesis. Virol J 10:339.

41. Miller S, Kastner S, Krijnse-Locker J, Bühler S, Bartenschlager R. 2007. The non-structural protein 4A of dengue virus is an integral membrane protein inducing membrane alterations in a 2K-regulated manner. J Biol Chem 282:8873–8882.

42. Neufeldt CJ, Cortese M, Acosta EG, Bartenschlager R. 2018. Rewiring cellular networks by members of the Flaviviridae family. Nat Rev Microbiol 16:125–142.

43. Stolp ZD, Smurthwaite CA, Reed C, Williams W, Dharmawan A, Djaballah H, Wolkowicz R. 2015. A multiplexed cell-based assay for the identification of modulators of pre-membrane processing as a target against dengue virus. J Biomol Screen 20:616–626.

44. Alva V, Lupas AN. 2016. The TULIP superfamily of eukaryotic lipid-binding proteins as a mediator of lipid sensing and transport. Biochim Biophys Acta - Mol Cell Biol Lipids 1861:913–923.

45. Kopec KO, Alva V, Lupas AN. 2011. Bioinformatics of the TULIP domain superfamily. Biochem Soc Trans 39:1033–1038.

46. Wong LH, Levine TP. 2017. Tubular lipid binding proteins (TULIPs) growing everywhere. Biochim Biophys Acta - Mol Cell Res 1864:1439–1449.

47. Toulmay A, Prinz WA. 2012. A conserved membrane-binding domain targets proteins to organelle contact sites. J Cell Sci 125:49–58.

48. Bingle CD, Seal RL, Craven CJ. 2011. Systematic nomenclature for the PLUNC/PSP/BSP30/SMGB proteins as a subfamily of the BPI fold-containing superfamily. Biochem Soc Trans 39:977–83.

49. Balakrishnan A, Marathe SA, Joglekar M, Chakravortty D. 2013. Bactericidal/permeability increasing protein: A multifaceted protein with functions beyond LPS neutralization. Innate Immun 19:339–347.

50. Zhang M, Zhai X, Li J, Albers JJ, Vuletic S, Ren G. 2018. Structural basis of the lipid

transfer mechanism of phospholipid transfer protein (PLTP). Biochim Biophys Acta - Mol Cell Biol Lipids 1863:1082–1094.

51. Chirasani VR, Revanasiddappa PD, Senapati S. 2016. Structural plasticity of cholesteryl ester transfer protein assists the lipid transfer activity. J Biol Chem 291:19462–19473.

52. Schicht M, Rausch F, Beron M, Jacobi C, Garreis F, Hartjen N, Beileke S, Kruse F, Bräuer L, Paulsen F. 2015. Palate lung nasal clone (PLUNC), a novel protein of the tear film: Three-dimensional structure, immune activation, and Involvement in dry eye disease (DED). Investig Ophthalmol Vis Sci 56:7312–7323.

53. Liu Y, Bartlett JA, Di ME, Bomberger JM, Chan YR, Gakhar L, Mallampalli RK, McCray PB, Di YP. 2013. SPLUNC1/BPIFA1 contributes to pulmonary host defense against klebsiella pneumoniae respiratory infection. Am J Pathol 182:1519–1531.

54. Prokopovic V, Popovic M, Andjelkovic U, Marsavelski A, Raskovic B, Gavrovic-Jankulovic M, Polovic N. 2014. Isolation, biochemical characterization and anti-bacterial activity of BPIFA2 protein. Arch Oral Biol 59:302–309.

55. Bartlett J, Gakhar L, Penterman J, Singh P, Mallampalli RK, Porter E, McCray PB. 2011. PLUNC: A multifunctional surfactant of the airways. Biochem Soc Trans 39:1012–1016.

56. Bingle CD, Craven CJ. PLUNC: A novel family of candidate host defence proteins expressed in the upper airways and nasopharynx.

57. Bingle CD, Bingle L, Craven CJ. 2011. Distant cousins: Genomic and sequence diversity within the BPI fold-containing (BPIF)/PLUNC protein family. Biochem Soc Trans 39:961–965.

58. Yang J, Yan R, Roy A, Xu D, Poisson J, Zhang Y. 2014. The I-TASSER suite: Protein structure and function prediction. Nat Methods 12:7–8.

59. Roy A, Kucukural A, Zhang Y. 2010. I-TASSER: A unified platform for automated protein structure and function prediction. Nat Protoc 5:725–738.

60. Yang J, Zhang Y. 2015. I-TASSER server: New development for protein structure and function predictions. Nucleic Acids Res 43:W174–W181.

61. Bento CF, Renna M, Ghislat G, Puri C, Ashkenazi A, Vicinanza M, Menzies FM, Rubinsztein DC. 2016. Mammalian Autophagy: How Does It Work? Annu Rev Biochem 85:685–713.

62. Moretti J, Roy S, Bozec D, Martinez J, Chapman JR, Ueberheide B, Lamming DW, Chen ZJ, Horng T, Yeretssian G, Green DR, Blander JM. 2017. STING Senses Microbial Viability to Orchestrate Stress-Mediated Autophagy of the Endoplasmic Reticulum. Cell 171:809-823.e13.

63. Fumagalli F, Noack J, Bergmann TJ, Presmanes EC, Pisoni GB, Fasana E, Fregno I, Galli

C, Loi M, Soldà T, D'Antuono R, Raimondi A, Jung M, Melnyk A, Schorr S, Schreiber A, Simonelli L, Varani L, Wilson-Zbinden C, Zerbe O, Hofmann K, Peter M, Quadroni M, Zimmermann R, Molinari M. 2016. Translocon component Sec62 acts in endoplasmic reticulum turnover during stress recovery. Nat Cell Biol 18:1173–1184.

64. Omari S, Makareeva E, Roberts-Pilgrim A, Mirigian L, Jarnik M, Ott C, Lippincott-Schwartz J, Leikin S. 2018. Noncanonical autophagy at ER exit sites regulates procollagen turnover. Proc Natl Acad Sci 115:E10099–E10108.

65. Anding AL, Baehrecke EH. 2017. Cleaning House: Selective Autophagy of Organelles. Dev Cell. Cell Press.

66. Li WW, Li J, Bao JK. 2012. Microautophagy: Lesser-known self-eating. Cell Mol Life Sci 69:1125–1136.

67. Kaushik S, Cuervo AM. 2018. The coming of age of chaperone-mediated autophagy. Nat Rev Mol Cell Biol 19:365–381.

68. Kim J, Kundu M, Viollet B, Guan KL. 2011. AMPK and mTOR regulate autophagy through direct phosphorylation of Ulk1. Nat Cell Biol 13:132–141.

69. Park JM, Jung CH, Seo M, Otto NM, Grunwald D, Kim KH, Moriarity B, Kim YM, Starker C, Nho RS, Voytas D, Kim DH. 2016. The ULK1 complex mediates MTORC1 signaling to the autophagy initiation machinery via binding and phosphorylating ATG14. Autophagy 12:547–564.

70. Nazio F, Strappazzon F, Antonioli M, Bielli P, Cianfanelli V, Bordi M, Gretzmeier C, Dengjel J, Piacentini M, Fimia GM, Cecconi F. 2013. mTOR inhibits autophagy by controlling ULK1 ubiquitylation, self-association and function through AMBRA1 and TRAF6. Nat Cell Biol 15:406–416.

71. Shibutani ST, Yoshimori T. 2014. A current perspective of autophagosome biogenesis. Cell Res 24:58–68.

72. Russell RC, Tian Y, Yuan H, Park HW, Chang Y-Y, Kim J, Kim H, Neufeld TP, Dillin A, Guan K-L. 2013. ULK1 induces autophagy by phosphorylating Beclin-1 and activating VPS34 lipid kinase. Nat Cell Biol 15:741–750.

73. Su H, Yang F, Wang Q, Shen Q, Huang J, Peng C, Zhang Y, Wan W, Wong CCL, Sun Q, Wang F, Zhou T, Liu W. 2017. VPS34 Acetylation Controls Its Lipid Kinase Activity and the Initiation of Canonical and Non-canonical Autophagy. Mol Cell 67:907-921.e7.

74. Gómez-Sánchez R, Rose J, Guimarães R, Mari M, Papinski D, Rieter E, Geerts WJ, Hardenberg R, Kraft C, Ungermann C, Reggiori F. 2018. Atg9 establishes Atg2-dependent contact sites between the endoplasmic reticulum and phagophores. J Cell Biol 217:2743–2763.

75. Carlsson SR, Simonsen A. 2015. Membrane dynamics in autophagosome biogenesis. J Cell

Sci 1–13.

76. Axe EL, Walker SA, Manifava M, Chandra P, Roderick HL, Habermann A, Griffiths G, Ktistakis NT. 2008. Autophagosome formation from membrane compartments enriched in phosphatidylinositol 3-phosphate and dynamically connected to the endoplasmic reticulum. J Cell Biol 182:685–701.

77. Nascimbeni AC, Codogno P, Morel E. 2017. Local detection of PtdIns3P at autophagosome biogenesis membrane platforms. Autophagy 8627:1–11.

78. Dooley HC, Razi M, Polson HEJ, Girardin SE, Wilson MI, Tooze SA. 2014. WIPI2 Links LC3 Conjugation with PI3P, Autophagosome Formation, and Pathogen Clearance by Recruiting Atg12-5-16L1. Mol Cell 55:238–252.

79. Polson HEJ, De Lartigue J, Rigden DJ, Reedijk M, Urb?? S, Clague MJ, Tooze SA. 2010. Mammalian Atg18 (WIPI2) localizes to omegasome-anchored phagophores and positively regulates LC3 lipidation. Autophagy 6:506–522.

80. Tanida I, Ueno T, Kominami E. 2004. LC3 conjugation system in mammalian autophagy. Int J Biochem Cell Biol 36:2503–2518.

81. Romanov J, Walczak M, Ibiricu I, Schüchner S, Ogris E, Kraft C, Martens S. 2012. Mechanism and functions of membrane binding by the Atg5-Atg12/Atg16 complex during autophagosome formation. EMBO J 31:4304–4317.

82. Zhang L, Li J, Ouyang L, Liu B, Cheng Y. 2016. Unraveling the roles of Atg4 proteases from autophagy modulation to targeted cancer therapy. Cancer Lett 373:19–26.

83. Pengo N, Agrotis A, Prak K, Jones J, Ketteler R. 2017. A reversible phospho-switch mediated by ULK1 regulates the activity of autophagy protease ATG4B. Nat Commun 8:294.

84. Nath S, Dancourt J, Shteyn V, Puente G, Fong WM, Nag S, Bewersdorf J, Yamamoto A, Antonny B, Melia TJ. 2014. Lipidation of the LC3/GABARAP family of autophagy proteins relies on a membrane-curvature-sensing domain in Atg3. Nat Cell Biol 16:415–424.

85. Dooley HC, Wilson MI, Tooze SA. 2015. WIPI2B links ptdins3P to LC3 lipidation through binding ATG16L1. Autophagy 11:190–191.

86. Lystad AH, Carlsson SR, de la Ballina LR, Kauffman KJ, Nag S, Yoshimori T, Melia TJ, Simonsen A. 2019. Distinct functions of ATG16L1 isoforms in membrane binding and LC3B lipidation in autophagy-related processes. Nat Cell Biol 21:372–383.

87. Lystad AH, Carlsson SR, Simonsen A. 2019. Toward the function of mammalian ATG12–ATG5-ATG16L1 complex in autophagy and related processes. Autophagy 15:1485–1486.

88. Mauvezin C, Nagy P, Juhász G, Neufeld TP. 2015. Autophagosome–lysosome fusion is

independent of V-ATPase-mediated acidification. Nat Commun 6:7007.

89. Zhao YG, Chen Y, Miao G, Zhao H, Qu W, Li D, Wang Z, Liu N, Li L, Chen S, Liu P, Feng D, Zhang H. 2017. The ER-Localized Transmembrane Protein EPG-3/VMP1 Regulates SERCA Activity to Control ER-Isolation Membrane Contacts for Autophagosome Formation. Mol Cell 1–16.

90. Ganley IG, Wong PM, Gammoh N, Jiang X. 2011. Distinct Autophagosomal-Lysosomal Fusion Mechanism Revealed by Thapsigargin-Induced Autophagy Arrest. Mol Cell 42:731–743.

91. Johansen T, Lamark T. 2011. Selective autophagy mediated by autophagic adapter proteins. Autophagy 7:279–296.

92. Cho DH, Kim YS, Jo DS, Choe SK, Jo EK. 2018. Pexophagy: Molecular mechanisms and implications for health and diseases. Mol Cells. Korean Society for Molecular and Cellular Biology.

93. Mijaljica D, Devenish RJ. 2013. Nucleophagy at a glance. J Cell Sci 126:4325–4330.

94. Mochida K, Oikawa Y, Kimura Y, Kirisako H, Hirano H, Ohsumi Y, Nakatogawa H. 2015. Receptor-mediated selective autophagy degrades the endoplasmic reticulum and the nucleus. Nature 522:359–362.

95. Wei H, Liu L, Chen Q. 2015. Selective removal of mitochondria via mitophagy: Distinct pathways for different mitochondrial stresses. Biochim Biophys Acta - Mol Cell Res. Elsevier.

96. Burnett SF, Farré JC, Nazarko TY, Subramani S. 2015. Peroxisomal Pex3 activates selective autophagy of peroxisomes via interaction with the pexophagy receptor Atg30. J Biol Chem 290:8623–8631.

97. Delorme-Axford E, Popelka H, Klionsky DJ. 2019. TEX264 is a major receptor for mammalian reticulophagy. Autophagy 15:1677–1681.

98. Chen Q, Teng J, Chen J. 2019. ATL3, a cargo receptor for reticulophagy. Autophagy 15:1465–1466.

99. An H, Ordureau A, Paulo JA, Shoemaker CJ, Denic V, Harper JW. 2019. TEX264 Is an Endoplasmic Reticulum-Resident ATG8-Interacting Protein Critical for ER Remodeling during Nutrient Stress. Mol Cell 74:891-908.e10.

100. Khaminets A, Heinrich T, Mari M, Grumati P, Huebner AK, Akutsu M, Liebmann L, Stolz A, Nietzsche S, Koch N, Mauthe M, Katona I, Qualmann B, Weis J, Reggiori F, Kurth I, Hübner CA, Dikic I. 2015. Regulation of endoplasmic reticulum turnover by selective autophagy. Nature 522:354–358.

101. Smith MD, Harley ME, Kemp AJ, Wills J, Lee M, Arends M, von Kriegsheim A, Behrends

C, Wilkinson S. 2018. CCPG1 Is a Non-canonical Autophagy Cargo Receptor Essential for ER-Phagy and Pancreatic ER Proteostasis. Dev Cell 44:217-232.e11.

102. Ham SJ, Lee D, Yoo H, Jun K, Shin H, Chung J. 2020. Decision between mitophagy and apoptosis by Parkin via VDAC1 ubiquitination. Proc Natl Acad Sci U S A 117:4281–4291.

103. Xiao B, Goh JY, Xiao L, Xian H, Lim KL, Liou YC. 2017. Reactive oxygen species trigger Parkin/PINK1 pathway–dependent mitophagy by inducing mitochondrial recruitment of Parkin. J Biol Chem 292:16697–16708.

104. Zhang J, Tripathi DN, Jing J, Alexander A, Kim J, Powell RT, Dere R, Tait-Mulder J, Lee JH, Paull TT, Pandita RK, Charaka VK, Pandita TK, Kastan MB, Walker CL. 2015. ATM functions at the peroxisome to induce pexophagy in response to ROS. Nat Cell Biol 17:1259–1269.

105. Schuck S, Gallagher CM, Walter P. 2014. ER-phagy mediates selective degradation of endoplasmic reticulum independently of the core autophagy machinery. J Cell Sci 127:4078–4088.

106. Schäfer JA, Schessner JP, Bircham PW, Tsuji T, Funaya C, Pajonk O, Schaeff K, Ruffini G, Papagiannidis D, Knop M, Fujimoto T, Schuck S. 2020. ESCRT machinery mediates selective microautophagy of endoplasmic reticulum in yeast . EMBO J 39:1–20.

107. Zhang H, Grumati P, Morozzi G, Hö Lper S, Mari M, Harwardt M-LI, Yan R, Mü Ller S, Reggiori F, Heilemann M, Dikic I. Full length RTN3 regulates turnover of tubular endoplasmic reticulum via selective autophagy.

108. Chen Q, Xiao Y, Chai P, Zheng P, Teng J, Chen J. 2019. ATL3 Is a Tubular ER-Phagy Receptor for GABARAP-Mediated Selective Autophagy. Curr Biol 29:846-855.e6.

109. Chino H, Hatta T, Natsume T, Mizushima N. 2019. Intrinsically Disordered Protein TEX264 Mediates ER-phagy. Mol Cell 74:909-921.e6.

110. Santambrogio L, Cuervo AM. 2011. Chasing the elusive mammalian microautophagy. Autophagy 7:652–654.

111. Olsvik HL, Svenning S, Abudu YP, Brech A, Stenmark H, Johansen T, Mejlvang J. 2019. Endosomal microautophagy is an integrated part of the autophagic response to amino acid starvation. Autophagy. Taylor and Francis Inc.

112. Sahu R, Kaushik S, Clement CC, Cannizzo ES, Scharf B, Follenzi A, Potolicchio I, Nieves E, Cuervo AM, Santambrogio L. 2011. Microautophagy of Cytosolic Proteins by Late Endosomes. Dev Cell 20:131–139.

113. Krick R, Muehe † Y, Prick † T, Bremer † S, Schlotterhose P, Eskelinen E-L, Millen J, Goldfarb DS, Thumm M. 2008. Piecemeal Microautophagy of the Nucleus Requires the Core Macroautophagy Genes. Mol Biol Cell 19:4492–4505.

114. Schäfer JA, Schuck S. 2020. ESCRTing endoplasmic reticulum to microautophagic degradation. Autophagy 16:763–764.

115. Chiang HL, Terlecky SR, Plant CP, Dice JF. 1989. A role for a 70-kilodalton heat shock protein in lysosomal degradation of intracellular proteins. Science 246:382–385.

116. Fred Dice J. 1990. Peptide sequences that target cytosolic proteins for lysosomal proteolysis. Trends Biochem Sci 15:305–309.

117. Bandyopadhyay U, Kaushik S, Varticovski L, Cuervo AM. 2008. The Chaperone-Mediated Autophagy Receptor Organizes in Dynamic Protein Complexes at the Lysosomal Membrane. Mol Cell Biol 28:5747–5763.

118. Pajares M, Rojo AI, Arias E, Díaz-Carretero A, Cuervo AM, Cuadrado A. 2018. Transcription factor NFE2L2/NRF2 modulates chaperone-mediated autophagy through the regulation of LAMP2A. Autophagy 14:1310–1322.

119. Tekirdag K, Cuervo AM. 2018. Chaperone-mediated autophagy and endosomal microautophagy: Joint by a chaperone. J Biol Chem 293:5414–5424.

120. Arias E, Koga H, Diaz A, Mocholi E, Patel B, Cuervo AM. 2015. Lysosomal mTORC2/PHLPP1/Akt Regulate Chaperone-Mediated Autophagy. Mol Cell 59:270–284.

121. Fletcher K, Ulferts R, Jacquin E, Veith T, Gammoh N, Arasteh JM, Mayer U, Carding SR, Wileman T, Beale R, Florey O. 2018. The WD 40 domain of ATG 16L1 is required for its non-canonical role in lipidation of LC 3 at single membranes . EMBO J 37:1–17.

122. De Faveri F, Chvanov M, Voronina S, Moore D, Pollock L, Haynes L, Awais M, Beckett AJ, Mayer U, Sutton R, Criddle DN, Prior IA, Wileman T, Tepikin A V. 2019. LAP-like non-canonical autophagy and evolution of endocytic vacuoles in pancreatic acinar cells. Autophagy 00:1–18.

123. Niso-Santano M, Malik SA, Pietrocola F, Bravo-San Pedro JM, Mariño G, Cianfanelli V, Ben-Younès A, Troncoso R, Markaki M, Sica V, Izzo V, Chaba K, Bauvy C, Dupont N, Kepp O, Rockenfeller P, Wolinski H, Madeo F, Lavandero S, Codogno P, Harper F, Pierron G, Tavernarakis N, Cecconi F, Maiuri MC, Galluzzi L, Kroemer G. 2015. Unsaturated fatty acids induce non-canonical autophagy. EMBO J 34:1025–1041.

124. Lai JKF, Sam IC, Chan YF. 2016. The autophagic machinery in Enterovirus infection. Viruses 8.

125. Alirezaei M, Flynn CT, Wood MR, Harkins S, Whitton JL. 2015. Coxsackievirus can exploit LC3 in both autophagy-dependent and -independent manners in vivo. Autophagy 11:1389–1407.

126. Robinson SM, Tsueng G, Sin J, Mangale V, Rahawi S, McIntyre LL, Williams W, Kha N, Cruz C, Hancock BM, Nguyen DP, Sayen MR, Hilton BJ, Doran KS, Segall AM, Wolkowicz R, Cornell CT, Whitton JL, Gottlieb RA, Feuer R. 2014. Coxsackievirus B Exits

the Host Cell in Shed Microvesicles Displaying Autophagosomal Markers. PLoS Pathog 10.

127. Kemball CC, Alirezaei M, Flynn CT, Wood MR, Harkins S, Kiosses WB, Whitton JL. 2010. Coxsackievirus Infection Induces Autophagy-Like Vesicles and Megaphagosomes in Pancreatic Acinar Cells In Vivo. J Virol 84:12110–12124.

128. Wong J, Zhang J, Si X, Gao G, Mao I, McManus BM, Luo H. 2008. Autophagosome Supports Coxsackievirus B3 Replication in Host Cells. J Virol 82:9143–9153.

129. Richards AL, Jackson WT. 2012. Intracellular Vesicle Acidification Promotes Maturation of Infectious Poliovirus Particles. PLoS Pathog 8.

130. Yan B, Zou Z, Chu H, Chan G, Tsang JOL, Lai PM, Yuan S, Yip CCY, Yin F, Kao RYT, Sze KH, Lau SKP, Chan JFW, Yuen KY. 2019. Lipidomic profiling reveals significant perturbations of intracellular lipid homeostasis in enterovirus-infected cells. Int J Mol Sci 20.

131. Strating JR, van Kuppeveld FJ. 2017. Viral rewiring of cellular lipid metabolism to create membranous replication compartments. Curr Opin Cell Biol 47:24–33.

132. Wang H, Sun HQ, Zhu X, Zhang L, Albanesi J, Levine B, Yin H. 2015. GABARAPs regulate PI4P-dependent autophagosome: Lysosome fusion. Proc Natl Acad Sci U S A 112:7015–7020.

133. Van Der Schaar HM, Leyssen P, Thibaut HJ, De Palma A, Van Der Linden L, Lanke KHW, Lacroix C, Verbeken E, Conrath K, MacLeod AM, Mitchell DR, Palmer NJ, Van De Poël H, Andrews M, Neyts J, Van Kuppeveld FJM. 2013. A Novel, Broad-Spectrum Inhibitor of Enterovirus Replication That Targets Host Cell Factor Phosphatidylinositol 4-Kinase IIIβ. Antimicrob Agents Chemother 57:4971–4981.

134. Sin J, McIntyre L, Stotland A, Feuer R, Gottlieb RA. 2017. Coxsackievirus B Escapes the Infected Cell in Ejected Mitophagosomes 91:1–16.

135. Bird SW, Maynard ND, Covert MW, Kirkegaard K. 2014. Nonlytic viral spread enhanced by autophagy components. Proc Natl Acad Sci U S A 111:13081–13086.

136. Jackson WT. 2014. Poliovirus-induced changes in cellular membranes throughout infection. Curr Opin Virol 9:67–73.

137. Lee YR, Wang PS, Wang JR, Liu HS. 2014. Enterovirus 71-induced autophagy increases viral replication and pathogenesis in a suckling mouse model. J Biomed Sci 21:1–11.

138. Kim C, Bergelson JM. 2014. Echovirus 7 Entry into Polarized Caco-2 Intestinal Epithelial Cells Involves Core Components of the Autophagy Machinery. J Virol 88:434–443.

139. Wu Q, van Dyk LF, Jiang D, Dakhama A, Li L, White SR, Gross A, Chu HW. 2013. Interleukin-1 receptor-associated kinase M (IRAK-M) promotes human rhinovirus infection

in lung epithelial cells via the autophagic pathway. Virology 446:199–206.

140. Huang S-C, Chang C-L, Wang P-S, Liu H-S. 2009. Enterovirus 71-Induced Autophagy Detected In Vitro and In Vivo Promotes Viral Replication. J Med Virol 81:1241– 1252.

141. Mateo R, Nagamine CM, Spagnolo J, Mendez E, Rahe M, Gale M, Yuan J, Kirkegaard K. 2013. Inhibition of Cellular Autophagy Deranges Dengue Virion Maturation. J Virol 87:1312–1321.

142. Datan E, Roy SG, Germain G, Zali N, McLean JE, Golshan G, Harbajan S, Lockshin R a, Zakeri Z. 2016. Dengue-induced autophagy, virus replication and protection from cell death require ER stress (PERK) pathway activation. Cell Death Dis 7:e2127.

143. Metz P, Chiramel A, Chatel-Chaix L, Alvisi G, Bankhead P, Mora-Rodríguez R, Long G, Hamacher-Brady A, Brady NR, Bartenschlager R. 2015. Dengue Virus Inhibition of Autophagic Flux and Dependency of Viral Replication on Proteasomal Degradation of the Autophagy Receptor p62. J Virol 89:8026–8041.

144. Sharma M, Bhattacharyya S, Nain M, Kaur M, Sood V, Gupta V, Khasa R, Abdin MZ, Vrati S, Kalia M. 2014. Japanese encephalitis virus replication is negatively regulated by autophagy and occurs on LC3-I- and EDEM1-containing membranes. Autophagy 10:1637–1651.

145. Abernathy E, Mateo R, Majzoub K, van Buuren N, Bird SW, Carette JE, Kirkegaard K. 2019. Differential and convergent utilization of autophagy components by positive-strand RNA viruses. PLoS Biol 17:1–28.

146. Lennemann NJ, Coyne CB. 2017. Dengue and Zika viruses subvert reticulophagy by NS2B3-mediated cleavage of FAM134B. Http://DxDoiOrg/101080/1554862720161265192 13:322–332.

147. Heaton NS, Randall G. 2010. Dengue virus-induced autophagy regulates lipid metabolism. Cell Host Microbe 8:422–432.

148. Jordan TX, Randall G. 2017. Dengue Virus Activates the AMP Kinase-mTOR Axis To Stimulate a Proviral Lipophagy. J Virol 91:e02020-16.

149. Kaufusi PH, Kelley JF, Yanagihara R, Nerurkar VR. 2014. Induction of endoplasmic reticulum-derived replication-competent membrane structures by West Nile virus non-structural protein 4B. PLoS One 9.

150. Gillespie LK, Hoenen A, Morgan G, Mackenzie JM. 2010. The Endoplasmic Reticulum Provides the Membrane Platform for Biogenesis of the Flavivirus Replication Complex. J Virol 84:10438–10447.

151. Kirkegaard K. 2009. Subversion of the cellular autophagy pathway by viruses. Curr Top Microbiol Immunol.

152. Levine B, Mizushima N, Virgin HW. 2011. Autophagy in immunity and inflammation. Nature 469:323–335.

153. Stolz A, Grumati P. 2019. The various shades of ER-phagy. FEBS J 1–8.

154. Liang Q, Luo Z, Zeng J, Chen W, Foo SS, Lee SA, Ge J, Wang S, Goldman SA, Zlokovic B V., Zhao Z, Jung JU. 2016. Zika Virus NS4A and NS4B Proteins Deregulate Akt-mTOR Signaling in Human Fetal Neural Stem Cells to Inhibit Neurogenesis and Induce Autophagy. Cell Stem Cell 19:663–671.

155. Heaton NS, Perera R, Berger KL, Khadka S, LaCount DJ, Kuhn RJ, Randall G. 2010. Dengue virus nonstructural protein 3 redistributes fatty acid synthase to sites of viral replication and increases cellular fatty acid synthesis. Proc Natl Acad Sci 107:17345–17350.

156. Stins MF, Badger J, Sik Kim K. 2001. Bacterial invasion and transcytosis in transfected human brain microvascular endothelial cells. Microb Pathog 30:19–28.

157. Bayer A, Lennemann NJ, Ouyang Y, Bramley JC, Morosky S, Marques ETDA, Cherry S, Sadovsky Y, Coyne CB. 2016. Type III Interferons Produced by Human Placental Trophoblasts Confer Protection against Zika Virus Infection. Cell Host Microbe 19:705–712.

158. Schuck S, Gallagher CM, Walter P. 2014. ER-phagy mediates selective degradation of endoplasmic reticulum independently of the core autophagy machinery. J Cell Sci 127:4078–4088.

159. Dykstra KM, Pokusa JE, Suhan J, Lee TH. 2010. Yip1A Structures the Mammalian Endoplasmic Reticulum. Mol Biol Cell 21:1556–1568.

160. Yu C-Y, Hsu Y-W, Liao C-L, Lin Y-L. 2006. Flavivirus Infection Activates the XBP1 Pathway of the Unfolded Protein Response To Cope with Endoplasmic Reticulum Stress. J Virol 80:11868–11880.

161. Aktepe TE, Liebscher S, Prier JE, Simmons CP, Mackenzie JM. 2017. The Host Protein Reticulon 3.1A Is Utilized by Flaviviruses to Facilitate Membrane Remodelling. Cell Rep 21:1639–1654.

162. Harris KG, Morosky SA, Drummond CG, Patel M, Kim C, Stolz DB, Bergelson JM, Cherry S, Coyne CB. 2015. RIP3 regulates autophagy and promotes coxsackievirus B3 infection of intestinal epithelial cells. Cell Host Microbe 18:221–232.

163. Wang S, Tukachinsky H, Romano FB, Rapoport TA. 2016. Cooperation of the ER-shaping proteins atlastin, lunapark, and reticulons to generate a tubular membrane network. Elife 5:1–29.

164. Fang YT, Wan SW, Lu YT, Yao JH, Lin CF, Hsu LJ, Brown MG, Marshall JS, Anderson R, Lin YS. 2014. Autophagy facilitates antibody-enhanced dengue virus infection in human pre-basophil/mast cells. PLoS One 9:1–10.

165. Bramley JC, Drummond CG, Lennemann NJ, Good CA, Kim KS, Coyne CB. 2017. A Three-Dime1. Bramley JC, Drummond CG, Lennemann NJ, Good CA, Kim KS, Coyne CB. A Three-Dimensional Cell Culture System To Model RNA Virus Infections at the Blood-Brain Barrier. mSphere. 2017;2(3):e00206-17. doi:10.1128/mSphere.00206-17.nsional Cell Cult. mSphere 2:e00206-17.

166. Medina F, Medina JF, Colon C, Vergne E, Santiago GA, Munoz-Jordan JL. 2012. Dengue virus: Isolation, propagation, quantification, and storage. Curr Protoc Microbiol 1–24.

167. Payne AF, Binduga-Gajewska I, Kauffman EB, Kramer LD. 2006. Quantitation of flaviviruses by fluorescent focus assay. J Virol Methods 134:183–189.

168. Coyne CB, Bergelson JM. 2006. Virus-induced Abl and Fyn kinase signals permit coxsackievirus entry through epithelial tight junctions. Cell 124:119–131.

169. Delorme-Axford E, Donker RB, Mouillet J-F, Chu T, Bayer A, Ouyang Y, Wang T, Stolz DB, Sarkar SN, Morelli AE, Sadovsky Y, Coyne CB. 2013. Human placental trophoblasts confer viral resistance to recipient cells. Proc Natl Acad Sci 110:12048–12053.

170. Love MI, Huber W, Anders S. 2014. Moderated estimation of fold change and dispersion for RNA-seq data with DESeq2. Genome Biol 15:550.

171. Glick D, Barth S, Macleod KF. 2010. Autophagy : cellular and molecular mechanisms. J Pathol 221:3–12.

172. Reggiori F, Ungermann C. 2017. Autophagosome Maturation and Fusion. J Mol Biol 429:486–496.

173. Graef M, Friedman JR, Graham C, Babu M, Nunnari J. 2013. ER exit sites are physical and functional core autophagosome biogenesis components. Mol Biol Cell 24:2918–2931.

174. Biazik J, Ylä-Anttila P, Vihinen H, Jokitalo E, Eskelinen EL. 2015. Ultrastructural relationship of the phagophore with surrounding organelles. Autophagy 11:439–451.

175. Ge L, Zhang M, Kenny SJ, Liu D, Maeda M, Saito K, Mathur A, Xu K, Schekman R. 2017. Remodeling of ER -exit sites initiates a membrane supply pathway for autophagosome biogenesis . EMBO Rep 18:1586–1603.

176. Razi M, Chan EYW, Tooze SA. 2009. Early endosomes and endosomal coatomer are required for Autophagy. J Cell Biol 185:305–321.

177. Kim DI, Jensen SC, Noble KA, Kc B, Roux KH, Motamedchaboki K, Roux KJ. 2016. An improved smaller biotin ligase for BioID proximity labeling. Mol Biol Cell 27:1188–1196.

178. Pastor-Cantizano N, Montesinos JC, Bernat-Silvestre C, Marcote MJ, Aniento F. 2016. P24 Family Proteins: Key Players in the Regulation of Trafficking Along the Secretory Pathway. Protoplasma 253:967–985.

179. Strating JRPM, Martens GJM. 2009. The p24 family and selective transport processes at the ER-Golgi interface. Biol Cell 101:495–509.

180. Beck R, Adolf F, Weimer C, Bruegger B, Wieland FT. 2009. ArfGAP1 activity and COPI vesicle biogenesis. Traffic 10:307–315.

181. Parnis A, Rawet M, Regev L, Barkan B, Rotman M, Gaitner M, Cassel D. 2006. Golgi localization determinants in ArfGAP1 and in new tissue-specific ArfGAP1 isoforms. J Biol Chem 281:3785–3792.

182. Dong C, Zhang X, Zhou F, Dou H, Duvernay MT, Zhang P, Wu G. 2010. ADP-ribosylation factors modulate the cell surface transport of G protein-coupled receptors. J Pharmacol Exp Ther 333:174–183.

183. Shiba Y, Luo R, Hinshaw JE, Szul T, Hayashi R, Sztul E, Nagashima K, Baxa U, Randazzo PA. 2011. ArfGAP1 promotes COPI vesicle formation by facilitating coatomer polymerization. Cell Logist 1:139–154.

184. Bai M, Gad H, Turacchio G, Cocucci E, Yang JS, Li J, Beznoussenko G V., Nie Z, Luo R, Fu L, Collawn JF, Kirchhausen T, Luini A, Hsu VW. 2011. ARFGAP1 promotes AP-2-dependent endocytosis. Nat Cell Biol 13:559–567.

185. Lavoie C, Paiement J, Dominguez M, Roy L, Dahan S, Gushue JN, Bergeron JJM. 1999. Roles for α2p24 and COPI in endoplasmic reticulum cargo exit site formation. J Cell Biol 146:285–299.

186. Mishra SK, Gao YG, Deng Y, Chalfant CE, Hinchcliffe EH, Brown RE. 2018. CPTP: A sphingolipid transfer protein that regulates autophagy and inflammasome activation†. Autophagy 14:862–879.

187. Vicinanza M, Korolchuk VI, Ashkenazi A, Puri C, Menzies FM, Clarke JH, Rubinsztein DC. 2015. PI(5)P regulates autophagosome biogenesis. Mol Cell 57:219–234.

188. Chiapparino A, Maeda K, Turei D, Saez-Rodriguez J, Gavin AC. 2016. The orchestra of lipid-transfer proteins at the crossroads between metabolism and signaling. Prog Lipid Res 61:30–39.

189. Albulescu L, Wubbolts R, van Kuppeveld FJM, Strating JRPM. 2015. Cholesterol shuttling is important for RNA replication of coxsackievirus B3 and encephalomyocarditis virus. Cell Microbiol 17:1144–1156.

190. Zhanga J, Zhang Z, Chukkapalli V, Nchoutmboube JA, Li J, Randall G, Belov GA, Wang X. 2016. Positive-strand RNA viruses stimulate host phosphatidylcholine synthesis at viral replication sites. Proc Natl Acad Sci U S A 113:E1064–E1073.

191. Chotiwan N, Andre BG, Sanchez-Vargas I, Islam MN, Grabowski JM, Hopf-Jannasch A, Gough E, Nakayasu E, Blair CD, Belisle JT, Hill CA, Kuhn RJ, Perera R. 2018. Dynamic remodeling of lipids coincides with dengue virus replication in the midgut of Aedes aegypti

mosquitoesPLoS Pathogens.

192. Cotton BT, Hyde JL, Sarvestani ST, Sosnovtsev S V, Green KY, White PA, Mackenzie JM. 2017. The Norovirus NS3 Protein Is a Dynamic Lipid- and Microtubule-Associated Protein Involved in Viral RNA Replication. J Virol 91:1–19.

193. Spang A, Shiba Y, Randazzo PA. 2010. Arf GAPs: Gatekeepers of vesicle generation. FEBS Lett 584:2646–2651.

194. Ambroggio E, Sorre B, Bassereau P, Goud B, Manneville JB, Antonny B. 2010. ArfGAP1 generates an Arf1 gradient on continuous lipid membranes displaying flat and curved regions. EMBO J 29:292–303.

195. Moretti F, Bergman P, Dodgson S, Marcellin D, Claerr I, Goodwin JM, DeJesus R, Kang Z, Antczak C, Begue D, Bonenfant D, Graff A, Genoud C, Reece-Hoyes JS, Russ C, Yang Z, Hoffman GR, Mueller M, Murphy LO, Xavier RJ, Nyfeler B. 2018. TMEM 41B is a novel regulator of autophagy and lipid mobilization. EMBO Rep 19:1–14.

196. Xie Y, Li J, Kang R, Tang D. 2020. Interplay Between Lipid Metabolism and Autophagy. Front Cell Dev Biol 8.

197. Saito T, Kuma A, Sugiura Y, Ichimura Y, Obata M, Kitamura H, Okuda S, Lee HC, Ikeda K, Kanegae Y, Saito I, Auwerx J, Motohashi H, Suematsu M, Soga T, Yokomizo T, Waguri S, Mizushima N, Komatsu M. 2019. Autophagy regulates lipid metabolism through selective turnover of NCoR1. Nat Commun 10.

198. Harayama T, Riezman H. 2018. Understanding the diversity of membrane lipid composition. Nat Rev Mol Cell Biol 19:281–296.

199. Banerjee S, Aponte-Diaz D, Yeager C, Sharma SD, Ning G, Oh HS, Han Q, Umeda M, Hara Y, Wang RYL, Cameron CE. 2018. Hijacking of multiple phospholipid biosynthetic pathways and induction of membrane biogenesis by a picornaviral 3CD proteinPLoS Pathogens.